Fisheries

Stock assessment of
Australian Sardine (*Sardinops sagax*)
off South Australia 2023

Grammer, G. L., Bailleul, F., and Ivey, A.

Government
of South Australia

Department of Primary
Industries and Regions

SARDI

SOUTH AUSTRALIAN
RESEARCH AND
DEVELOPMENT
INSTITUTE

Stock assessment of
Australian Sardine (*Sardinops sagax*)
off South Australia 2023

Report to PIRSA Fisheries and Aquaculture

Grammer, G. L., Bailleul, F., and Ivey, A.

January 2024

Front Cover Image: SASIA

TABLE OF CONTENTS

LIST OF FIGURES

LIST OF TABLES

ACKNOWLEDGEMENTS

EXECUTIVE SUMMARY

This report assesses the status of the Southern stock of Australian Sardine (*Sardinops sagax)*. It informs management of the South Australian Sardine Fishery (SASF), which is Australia's largest fishery by weight. The SASF was established in 1991. It is a purse-seine fishery with limited entry. The primary management tool is the Total Allowable Commercial Catch (TACC). The key performance indicator is the estimate of spawning biomass obtained using the Daily Egg Production Method (DEPM).

Stock status is linked prescriptively to reference points specified for the spawning biomass within the harvest strategy in the Management Plan for the fishery (PIRSA 2023). A TACC is set by applying exploitation rates of 12.5 to 27.5%, based on decision rules relating to the size of the spawning biomass and the level of research and monitoring undertaken (i.e. frequency of application of the DEPM, population modelling and ecosystem assessment).

Spatial management was introduced into the SASF in 2010. From 2014 to 2019, the SASF was divided into two main zones: Gulfs Zone and Outside Zone. Since 2020, a third zone has been in place that separates the Gulf Saint Vincent (GSV) Zone from the Spencer Gulf (SG) Zone at the line 137°10'E. In this report, all data have been retrospectively allocated into the three zones. There is a cap on the annual catch from both Gulf Zones, determined by the mean fork length (FL) of Sardine taken in the Zone during the previous year.

In February-April 1995, the spawning biomass (DEPM) of Sardine off South Australia was estimated to be approximately 320,000 t. Mass mortality events in late 1995 and 1998, that mainly effected adults, reduced the spawning biomass to less than 100,000 t in both 1996 and 1999. The stock recovered relatively quickly and, since 2006, the adult stock has been above ~200,000 t. In 2022, the estimate of spawning biomass (95% CI) for Sardine off South Australia obtained using the DEPM was 355,075 t (299,956–410,193) (Grammer and Ivey 2022). In 2023, the estimate of spawning biomass (95% CI) was 307,881 t (260,468–412,113) (Grammer and Ivey 2023).

The total annual catch recorded in Catch Disposal Records (CDR) remained below 8,000 t up to 2001. Catches increased rapidly after 2002 to reach 42,475 t in 2005. From 2006 to 2016, the annual catch ranged from ~26,000 t to ~38,000 t. In 2017 and 2018, the total catch was ~42,500 t, then dipped slightly to ~39,200 t, ~40,800 t and ~38,600 t in 2019, 2020 and 2021 respectively. The total catch rose to ~47,400 t in 2022.

The catch from the SG Zone was capped at 30,000 t from 2016 to 2019. The quota for this zone was reduced to 27,000 t in 2020 after the mean size dropped below the reference size in 2019; it was increased to 30,000 t in 2021. The catch from the Outside Zone increased from 1,460 t in 2010 to ~12,300 t in 2017, reduced to ~5,700 t in 2021, then increased to ~11,100 t in 2022. The quantity of catch from the GSV Zone has been small and has varied historically, reaching ~1,300–2,500 t in 2005, 2006, 2010 and 2016 but remaining below 1,000 t in all other years prior to 2020. The catch in 2020, 2021 and 2022 from the GSV Zone was ~5,600 t, 3,300 t and 5,300 t, respectively. Sardine taken from the Gulf Zones are usually younger and smaller than those taken from the Outside Zone.

The SardEst integrated assessment model was fitted to annual estimates of spawning biomass (DEPM) and age-composition. The model results provide information on key management quantities that include modelled spawning biomass, annual recruitment, annual harvest fraction, total biomass and relative depletion. SardEst generally fitted well to estimates of spawning biomass and age-composition. The unfished equilibrium total biomass (i.e. including juveniles) was estimated to be 645,000 t (± 108,000 t). In 1996, the total biomass was estimated to be 229,000 t (± 20,000 t), equating to a depletion level of 36%. Model estimated spawning biomass in 2022 was 344,000 t (± 20,000 t), indicating an exploitation rate of 18%. The model estimate of spawning biomass for 2023 was 305,000 t (± 20,000 t), indicating an exploitation rate of 21%.

The estimate of spawning biomass obtained using the 2023 DEPM (307,881 t) and from the SardEst integrated population model (305,000 t) were similar and above the target reference point of 200,000 t identified in the Management Plan (PIRSA 2023). Consistent with other recent assessments of the SASF (e.g. Grammer et al. 2021, Piddocke et al. 2021), the Southern stock of Australian Sardine is classified as **Sustainable.**

Statistic	2023	2022	2021	2020	2019
TACC	50,000 t	45,000 t	42,750 t	42,750 t	42,750 t
Spawning Biomass (DEPM)	307,881 t	355,075 t		377,267 t	233,600 t
Spawning Biomass (Model)	305,000 t	344,000 t	366,000 t	342,000 t	281,000 t
Status	**Sustainable**	**Sustainable**	**Sustainable**	**Sustainable**	**Sustainable**

Keywords: Daily Egg Production Method, spawning biomass, pelagic fishes, spawning fraction, egg production, SardEst.

1.   INTRODUCTION

1.1   Overview

Stock assessment reports on the South Australian Sardine Fishery (SASF) have been published annually or biennially since 1999 (Ward and McLeay 1999). Since 2005, the reports have used age-structure models to integrate fishery-dependent and fishery-independent data (Ward et al. 2005). The aims of this report are to: 1) summarise relevant scientific information on Sardine (*Sardinops sagax)* and describe the history of the SASF (Chapter 1); 2) summarise catch and effort data (Chapter 2); 3) present age structure and reproductive information (Chapter 3); 4) present the revised time series of fishery-independent estimates of spawning biomass from 1995 to 2023 based on the recommendations of Ward et al. (2021) and incorporate data from the 2022 and 2023 DEPM surveys (Grammer and Ivey 2022, 2023) (Chapter 4); 5) apply SardEst, a stock assessment model developed specifically for the SASF, to integrate fishery- independent and -dependent data (Chapter 5); and 6) assess the status of the stock, and identify future research needs (Chapter 6).

1.2   Sardine fisheries, abundance fluctuations and stock structure

Sardine, *Sardinops sagax* (Jenyns 1842), occurs off the west coasts of North and South America, off southern Africa, around Japan and off the southern coasts Australia and New Zealand (Parrish et al. 1989, Grant and Leslie 1996, Grant et al. 1998). The Standard Fish Names List for Australia specifies that the common name for *Sardinops sagax* is Australian Sardine. In this report we use the term Sardine to refer to *S. sagax* in Australia and elsewhere*.*

Sardine has historically supported important commercial fisheries throughout its global range; biomasses and catches have fluctuated dramatically over multi-decadal scales (e.g. Schwartzlose et al. 1999). For example, the sardine biomass off California peaked at just over four million tonnes in the 1930s and declined to <3,000 tonnes in the 1970s (Schwartzlose et al. 1999). Similarly, the Japanese catch peaked at 5.43 million tonnes in 1988 but declined to 0.3 million tonnes in 1996 (Schwartzlose et al. 1999). Currently, the biomass and catches of Sardine off the west coasts of North America (Kuriyama et al. 2022) and southern Africa (https://sapfia.org.za/tac/) are relatively low.

Fluctuations in the abundance and catches of Sardine in the Benguela, Californian and Humboldt Current systems off the west coasts of southern Africa and North and South America, respectively, have occurred synchronously (Schwartzlose et al. 1999, Tourre et al. 2007). During periods of low Sardine abundance, the local species of Anchovy (*Engraulis* spp.) has replaced Sardine as the

dominant species of small pelagic fish (Schwartzlose et al. 1999). 'Global synchrony' in the fluctuations in the relative abundance of Sardine and Anchovy appear to have been driven by multi-decadal changes in global ocean conditions (Schwartzlose et al. 1999, Tourre et al. 2007, Checkley et al. 2017).

The multi-decadal fluctuations in the relative abundance of Sardine and Anchovy that have been recorded elsewhere have not been observed off southern Australia (Schwartzlose et al. 1999, Ward et al. 2001a, Grammer and Ivey 2023). Sardine is the dominant clupeoid in this region, occurring throughout coastal and shelf waters. In contrast, Anchovy (*Engraulis australis*) is confined mainly to inshore waters (Schwartzlose et al. 1999, Ward et al. 2001a, Dimmlich et al. 2004, 2009, Dimmlich and Ward 2006). The abundance of Sardine off southern Australia was reduced by mass mortality events that occurred in 1995 and 1998/99, which each killed more fish over a larger area than any other recorded fish-kill (Jones et al. 1997, Ward et al. 2001a, 2001b). After the two Sardine mortality events, which each killed more than 50% of the adult population, the distribution of Anchovy expanded into shelf waters usually dominated by Sardine (Ward et al. 2001a, 2001b). This finding suggests that the fluctuations in relative abundance of Sardine and Anchovy observed globally may also be possible in Australian waters (Ward et al. 2001a, 2001b).

The rapid spread of the 1995 and 1998/99 mortality events across southern Australia (caused by a herpesvirus; Whittington et al. 2008) demonstrated the connectivity of Sardine across this entire geographical range (Whittington et al. 2008). Despite this connectivity, Sardine off southern Australia are considered to be a meta-population (Whittington et al. 2008) comprised of four biological stocks (Izzo et al. 2017, Sexton et al. 2019, Ward et al. 2023). The south-western stock occurs off Western Australia, the southern stock off South Australia; the south-eastern stock off Victoria, Tasmania and southern NSW; and the eastern stock off central New South Wales and southern Queensland. There is some evidence to suggest that the south-western and eastern stocks each include two separate sub-components (Gaughan et al. 2002, Izzo et al. 2017, Sexton et al. 2019).

Commercial fishing for Sardine has been conducted off southern Australia since the 1800s (Kailola et al. 1993), but combined national catches did not exceed 1,000 t until the 1970s. Catches off eastern Australia remained below 500 t up until 2003/04, before reaching a peak of almost 5,000 t in 2008/09 and then declining to <1,000 per annum from 2011/12 onwards (SAFS 2023). Several fisheries for Sardine developed off south-western Australia during the late 1970s (Newman et al. 2023). The total annual catch for Western Australia peaked at ~8,000 t in 1990 and has not exceeded 3,000 t since the mid-2000s, when the stock recovered from the mass mortality events of the 1990s (Newman et al. 2023, Ward et al. 2001b). The SASF was established in 1991 (Ward and Staunton-

Smith 2002). It grew rapidly, and the total annual catch has exceeded 38,000 t since 2017 (Grammer et al. 2021). Catch and effort data for the SASF are presented in Chapter 2 of this report.

1.3 Biology and ecological importance

Sardines have been studied intensively in Australia and elsewhere. Sardine are short-lived (<10 years), fast-growing and highly fecund fish (e.g. Ganias et al. 2012). Growth increments in sagittal otoliths (ear bones) have been widely used to estimate age (Butler et al. 1996, Fletcher and Blight 1996, Rogers et al. 2003). Despite difficulties associated with interpreting and counting opaque and translucent zones (Butler et al. 1996, Fletcher and Blight 1996, Rogers and Ward 2007), it is clear that Sardine grow faster and reach larger sizes in the productive boundary currents off Africa and North America than they do in the less productive waters off southern Australia (e.g. Fletcher and Blight 1996, Ward et al. 2006). Size, age and growth information for Sardine off South Australia are presented in Chapters 2 and 3 of this report.

Sardine are serial spawners with asynchronous oocyte development and indeterminate fecundity (e.g. Ganias et al. 2012). Females release numerous batches of pelagic eggs throughout a spawning season that typically extends for several months (Lasker 1985). Approximately 10-12% of females spawn each night during the peak spawning season (Ganias et al. 2012). The number of eggs in a batch, i.e. batch fecundity, is correlated with female size (Lasker 1985). In Australia, Sardine usually spawn in shelf waters (Blackburn 1950, Fletcher and Tregonning 1992, Fletcher et al. 1994). The timing of spawning varies between locations; off South Australia the peak spawning season occurs during January to April (Ward et al. 2001a, 2001b, Ward and Staunton-Smith 2002). Information on the reproductive biology of Sardine off South Australia is provided in Chapters 3 and 4 of this report.

Sardine are planktivores (Espinoza et al. 2009). They have two feeding modes: filter-feeding on micro-zooplankton and phytoplankton and particulate-feeding on macro-zooplankton. Sardine switch between these two modes depending on relative prey density (van der Lingen 1994, 2002, Louw et al. 1998). Off South Australia, Sardine appear to feed mainly on crustaceans, fish eggs and larvae and gelatinous zooplankton (Daly 2007).

Sardines are an important food source for many predatory fishes, squid, seabirds and marine mammals (e.g. Pikitch et al. 2012). However, the reliance of predators on Sardine and other small pelagic fishes varies among ecosystems and species (e.g. Smith et al. 2011, Hilborne et al. 2017). The trophic role of Sardines is particularly important in 'wasp-waisted' ecosystems, such as those found in the productive California, Humboldt and Benguela Current systems where one or two species usually dominate the pelagic fish biomass (e.g. Cury et al. 2000). In contrast, several studies

have shown that Australia's less productive pelagic ecosystems support a wide range of small- to medium-sized planktivores, and that few predators are highly dependent on a single prey species (Bulman et al. 2011, Smith et al. 2015). Off South Australia, marine predators feed opportunistically on a wide range of prey species (Goldsworthy et al. 2013). While, no predators have been shown to be solely dependent on Sardine as a food source, crested terns rely on them as a major food source during the breeding season (McLeay et al. 2009a, 2009b, Goldsworthy et al. 2013).

1.4   The South Australian Sardine Fishery

The SASF is managed by the *Fisheries Management (Sardine Fishery) Regulations 2021* and *Fisheries Management Act 2007*. Management goals for the SASF are consistent with the objectives of the *Fisheries Management Act 2007* and are outlined in the current Management Plan (PIRSA 2023). Management measures include entry limitations, gear restrictions and individual transferable quotas. Purse-seine nets must not exceed 1,000 m in length or 200 m depth. There are 14 licences with several companies operating multiple licences. The costs of the policy, compliance and research programs that are needed to manage the SASF are recovered through licence fees collected by PIRSA Fisheries and Aquaculture.

The Total Allowable Commercial Catch (TACC) was set at 1,000 t in 1992 (calendar year) and increased to 3,500 t during 1993–1997 (Figure 1–1). In 1998, the TACC was set at 12,500 t, but was reduced to 3,500 t after the mass mortality event in late 1998 and to 3,800 t in both 1999 and 2000. The stock recovered rapidly, and the TACC increased to 51,100 t in 2005. From 2007 to 2017, the TACC increased from 30,000 t to 42,750 t. The TACC was 42,750 t from 2017 to 2021. The TACC increased to 45,000 t in 2022 and to 50,000 t in 2023. From 2010, onwards, there has been a cap on the catch taken from Spencer Gulf (Figures 1–1 and 1–2). In 2022, under-catch and over-catch quota arrangements were implemented in the SASF, where, if under-catch occurred, up to 10% of total quota entitlements on a licence could be carried over into the subsequent fishing season (PIRSA 2021).

From 2014 to 2019, the SASF was divided into two main zones: Gulfs Zone (Spencer Gulf and Gulf St Vincent) and Outside Zone (Figure 1–2). From 2020 to 2022, the Gulfs Zone was temporarily split into two zones: the Spencer Gulf (SG) Zone and Gulf Saint Vincent (GSV) Zone at the line 137°10'E, (PIRSA 2020; Figure 1–2). The management arrangement for the SG Zone remained the same as for the previous Gulfs Zone but up to 6,000 t from the Outside Zone could be taken from the GSV Zone (PIRSA 2020). In 2023, the spatial management arrangement of three zones (SG Zone, GSV Zone, Outside Zone) was formally implemented in the current Management Plan (PIRSA 2023).

The TACC for 2022 of 45,000 t included up to 30,000 t from the SG Zone and 15,000 t from the Outside Zone, of which a maximum of 6,000 t could come from the GSV Zone. The TACC for 2023 is 50,000 t, with an increase to 20,000 t that can be taken from the Outside Zone (6,000 t of this from the GSV Zone; Figures 1–1 and 1–2; Table 1–2).
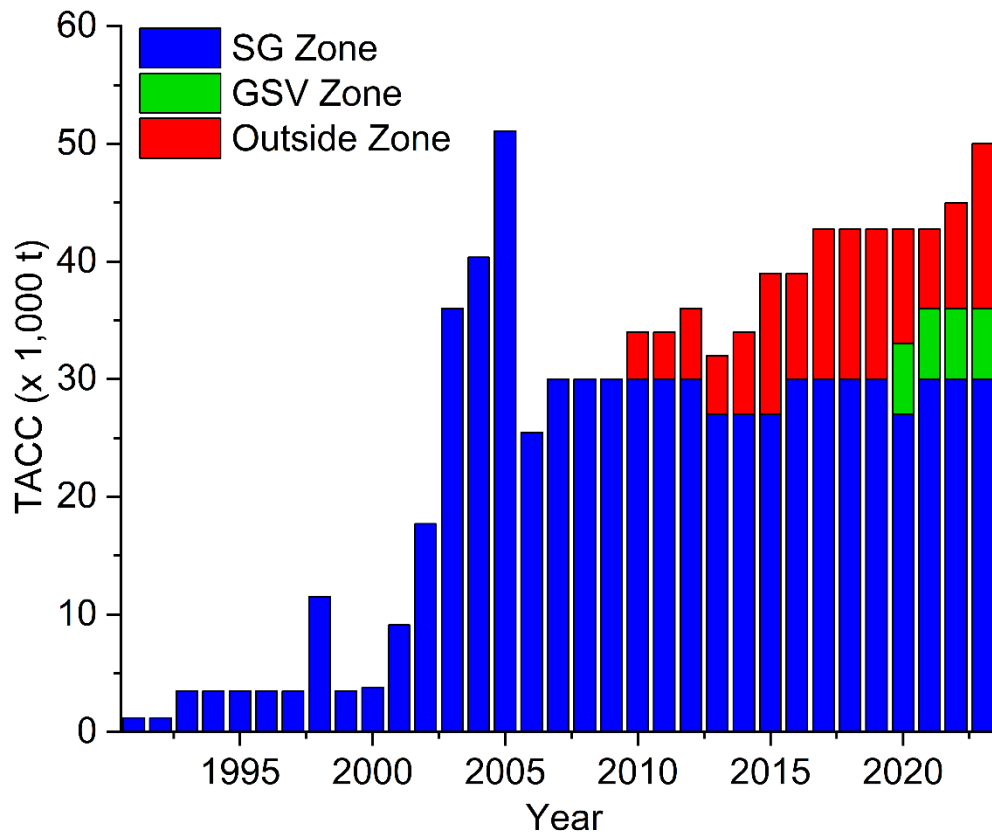
Figure 1-1. Total Allowable Commercial Catch (TACC) for the South Australian Sardine Fishery (SASF) between 1991 and 2023 for Spencer Gulf (SG) Zone, Outside Zone, and Gulf Saint Vincent (GSV) Zone (see Figure 1–2).
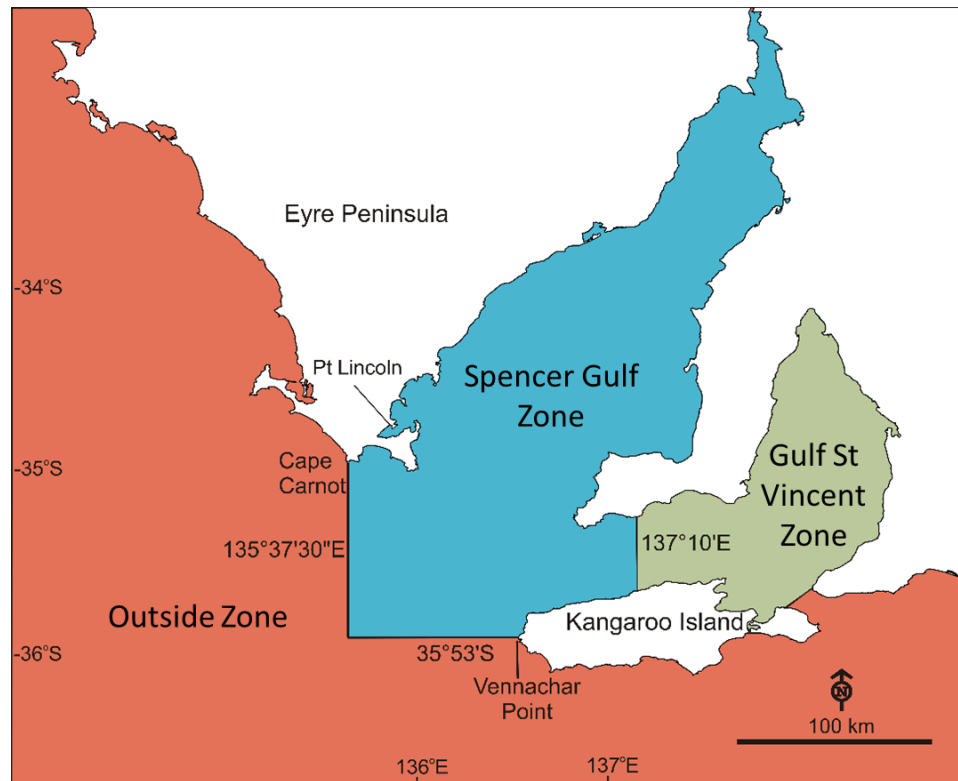
Figure 1-2. The three spatial management zones defined in the Harvest Strategy for the SASF (source PIRSA 2023).

Since 1998, the key biological performance indicator for the SASF has been the estimate of spawning biomass obtained using the DEPM. From 1997 to 2006, the TACC for the following calendar year was set as a proportion of the spawning biomass (i.e. 10.0–17.5%, depending on the size of the spawning biomass). From 2007 to 2009, the indicative TACC was set at 30,000 t (PIRSA 2007), while the estimate of spawning biomass obtained using the DEPM remained between 150,000 and 300,000 t. In 2014 (revised in 2023), a tiered Harvest Strategy (Figure 1–3) was established that sets the TACC based on the size of the spawning biomass and level of monitoring and assessment (Table 1–1). At Tier 3, DEPM and stock assessments are done in alternate years, and the maximum TACC is 45,000 t. At Tier 1, the maximum TACC is 55,000 t, and DEPM and stock assessments are both undertaken annually. At Tier 2, the maximum TACC is 50,000 t, and the DEPM is undertaken annually with a stock assessment done biennially. At all Tiers, an ecosystem assessment is required every four years and would replace a stock assessment in that year if both were set to occur at the same time (PIRSA 2023). Lower TACCs are set at each Tier if the spawning biomass is below 200,000 t. The SASF was managed at Tier 3 in 2015, 2016 and 2022, and at Tier 2 from 2017 to 2021 and in 2023.
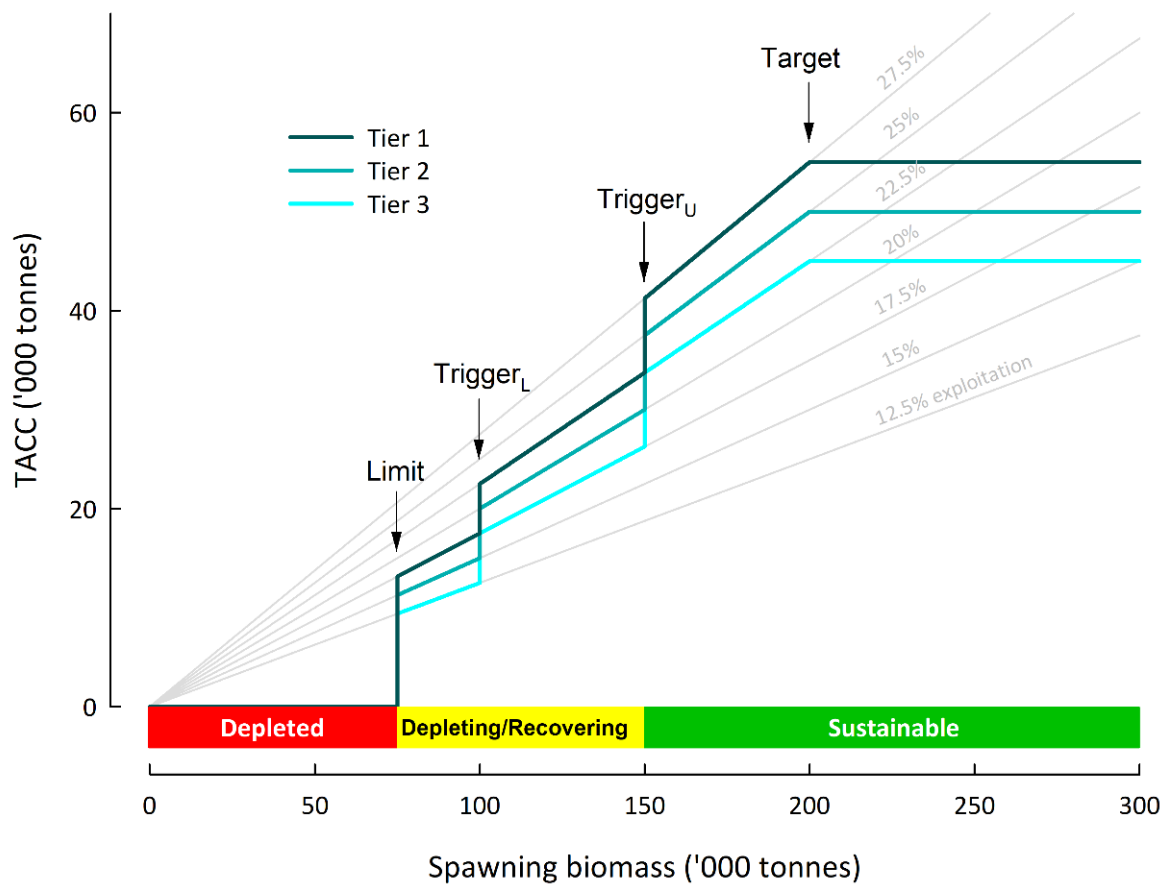
Figure 1-3. The relationship between spawning biomass, stock status and level of exploitation (or TACC) of the Sardine Harvest Strategy for each Tier. Reference Range: Limit (75,000 t), Trigger$_L$ (lower; 100,000 t), Trigger$_U$ (upper; 150,000 t), Target (200,000 t). Source: PIRSA 2023.

Table 1-1. Decision making rules for the tiered Harvest Strategy. Abbreviations: *SpB*: spawning biomass; *B^0*: initial biomass; TACC: total allowable commercial catch; ER: exploitation rate. Source: PIRSA 2023.

Reference Range	SpB (t)	% B^0	Tier 1		Tier 2		Tier 3	
			TACC (t)	Max ER	TACC (t)	Max ER	TACC (t)	Max ER
Upper Target	≥200,000	>67%	55,000	27.5%	50,000	25%	45,000	22.5%
Lower Target	<200,000 to ≥150,000	50-67%	41,250-55,000	27.5%	37,500-50,000	25%	33,750-45,000	22.5%
Upper Trigger	<150,000 to ≥100,000	33-50%	22,500-33,750	22.5%	20,000-30,000	20%	17,500-26,250	17.5%
Lower Trigger	<100,000 to ≥75,000	25-33%	13,125-17,500	17.5%	11,250-15,000	15%	9,375 – 12,500	12.5%
Limit	<75,000	<25%	0	0	0	0	0	0

Spatial management was established in the SASF in 2010, formalised in 2014 (two Zones: Gulfs and Outside; PIRSA 2014), and revised in 2023 (three Zones; Figure 1–2; PIRSA 2023). Since 2020, the spatial management arrangements for the SASF have been based on three Zones (PIRSA 2020, 2023). The catch that can be taken from the SG Zone and GSV Zone is determined from the mean size (mm Fork Length, FL) of Sardine taken in catches from that zone in the previous year (Table 1–2; Figure 1–2). If the mean size is above 142 mm FL, up to 30,000 t can be taken from the SG Zone (GSV Zone: 6,000 t) whereas if it is below 135 mm FL, the maximum catch is 24,000 t (GSV Zone: 2,000 t). If the mean size is between 135 and 142 mm, the maximum catch from the SG Zone is 27,000 t (GSV Zone: 4,000 t) (Table 1–2).

Table 1-2. Catch allocation decision table for the harvest strategy of the SASF to guide the maximum TACC allowed from the Spencer Gulf Zone (SGZ) and Gulf St Vincent Zone (GSVZ) (PIRSA 2023).

Mean size of Sardines (MSS, mm Fork Length)	Maximum catch limits	
	SGZ	GSVZ
>142 mm	30,000 t	6,000 t
>135 mm to ≤ 142 mm	27,000 t	4,000 t
≤ 135 mm	24,000 t	2,000 t

1.5   Stock status classification

A national stock status classification system, Status of Australian Fish Stocks (SAFS), has been developed to assess key Australian fish stocks (Table 1-3; Piddocke et al. 2021). The classification system combines information on current stock size and the level of fishing pressure to assess 'stock status' (Piddocke et al. 2021). Each stock is classified as: 'sustainable', 'depleting', 'recovering', 'depleted', 'undefined' or 'negligible' as outlined in Table 1–3. The SASF targets the Southern Australian stock, which occurs off South Australia and eastern Western Australian (Izzo et al. 2017, Sexton et al. 2019, Ward et al. 2023). The Southern Australian stock was assessed as being sustainable in the most recent Status of Key Australian Fish Stocks (SAFS 2021).

Table 1-3. Stock status terminology (Piddocke et al. 2021).

	Stock status	Description	Potential implications for management of the stock
	Sustainable	Stock for which biomass (or biomass proxy) is at a level sufficient to ensure that, on average, future levels of recruitment are adequate (*i.e.* recruitment is not impaired) and for which fishing mortality (or proxy) is adequately controlled to avoid the stock becoming recruitment impaired	Appropriate management is in place
	Depleting	Biomass (or proxy) is not yet depleted and recruitment is not yet impaired, but fishing mortality (or proxy) is too high (overfishing is occurring) and moving the stock in the direction of becoming recruitment impaired	Management is needed to reduce fishing pressure and ensure that the biomass does not become depleted
	Recovering	Biomass (or proxy) is depleted and recruitment is impaired, but management measures are in place to promote stock recovery, and recovery is occurring	Appropriate management is in place, and there is evidence that the biomass is recovering
	Depleted	Biomass (or proxy) has been reduced through catch and/or non-fishing effects, such that recruitment is impaired. Current management is not adequate to recover the stock, or adequate management measures have been put in place but have not yet resulted in measurable improvements	Management is needed to recover this stock; if adequate management measures are already in place, more time may be required for them to take effect
	Undefined	Not enough information exists to determine stock status	Data required to assess stock status are needed
	Negligible	Catches are so low as to be considered negligible and inadequate information exists to determine stock status	Assessment will not be conducted unless catches and information increase

2.   FISHERY INFORMATION

2.1 Introduction

This chapter presents catch, effort, size composition data and catch-per-unit-effort (CPUE) for the SASF from 1 January 1991 to 31 December 2022. This information is used to describe the main spatial and temporal patterns in the fishery and provides key inputs to the stock assessment model (Chapter 5).

2.2 Methods

2.2.1   Data collection

Catch and effort data were collated from commercial fishing logbooks. Prior to 2001, catch and effort were reported according to the pre-existing South Australian Marine Fishing Areas (MFAs). Following the implementation of SASF logbooks in 1998, catch and effort were reported by latitude and longitude for each purse-seine net-set. Estimated catches presented by month and year are aggregated from daily catches recorded in logbooks. CPUE estimates are based on these aggregated catches and corresponding effort data. Actual total annual catches were determined from the Catch Disposal Records (CDRs) collated from landings reported by PIRSA Fisheries and Aquaculture.

2.2.2   Commercial catch sampling

Between 1995 and 2022, commercial catch samples were collected under a range of sampling protocols; since 2008, independent observers present on about 10% of fishing trips have taken a sample of around 30 fish from each observed net-set. The observer program was stopped in April 2020 due to the COVID-19 lockdown; the program resumed in 2021. Therefore, few catch samples were collected for the 2020 season. In 2019, only length and otolith data were collected due to a freezer breakdown preventing other morphometric data from being taken.

 Size frequencies were constructed from caudal fork lengths (FL) aggregated into 10 mm length classes for all samples. Age determination methods are described in Chapter 3. Catch weightings were applied to size and age frequency data collected since 2010. Prior to 2010, all catch samples were not able to be linked to the corresponding net-nets. Length and age-frequencies were weighted by the total amount of catch taken in the corresponding net-set. Applying catch weightings (since 2010) has resulted in slight adjustments to the mean size of Sardine over this period, which are more representative of the mean size of fish caught by the SASF compared to previous reports. Sex ratio

was calculated as the proportion of female sardines in commercial catch samples. Sex was not recorded for commercial samples obtained in 2007.

Kernal density distributions were used to plot the spatial trends in the mean size of Sardine (mm FL) from 2010 to 2022 in commercial catch samples to meet requirements of data confidentiality (≥ 5 licences reporting catch). Data were plotted as a 2D kernel density estimation ('ked2d' function using MASS R package; Venables and Ripley 2002) on spatial locations grouped by categories of fish length: ≤135; 135-142; 142-155; >155 mm FL. Density estimation makes inferences about the underlying probability density function everywhere, including where no data are observed. Aggregating the individually smoothed contributions gives an overall picture of the structure of the data and its density function, while obscuring the identity and locale of each individual data points.

2.3 Results

2.3.1 Effort, catch and CPUE

Annual patterns

The SASF expanded quickly after its inception in 1991, with total effort and catches increasing from 5 boat-nights and 7 t in 1991 to 736 boat-nights and 3,241 t in 1994 (Figure 2–1). Total effort and catch were reduced in 1995 following the first mass mortality event (Ward et al. 2001b) but increased to 530 boat-nights and 5,973 t in 1998. In 1999, after the second mass mortality event in late 1998 (Ward et al. 2001b), effort declined to 353 boat-nights with 2,760 t of catch.

Since the second mortality event, the fishery expanded rapidly, with total effort reaching 1,266 net-sets across 1,224 boat-nights in 2005, with an estimated total catch (logbooks) of 39,809 t (Figure 2–1). In 2006, total effort dropped to 834 net-sets and 704 boat-nights (estimated catch: 23,507 t). Between 2007 and 2021, total effort was relatively stable at 760–1100 net-sets over 630–900 boat-nights with estimated catches of 27,500–40,600 t. In 2021, estimated catch was 36,279 t. In 2022, estimated catch (logbooks) was 43,947 t, and effort was 1000 net-sets over 730 nights.

Total annual catches recorded in CDRs exceeded catches estimated in logbooks in most years but followed similar trends. Catches from CDRs increased from 2,597 t in 1995 to 42,475 t in 2005 and fell to 25,137 t in 2006 (Figure 2–1). Between 2007 and 2021, catches in CDRs have ranged from 29,854 t in 2009 to 42,511 t in 2017. The total catch was 38,568 t in 2021 and 47,354 t in 2022.

Mean annual CPUE$_{boat-night}$ increased from 1.3 t.boat-night^{-1} in 1991 to 11.3 t.boat-night^{-1} in 1998 and reached a high of 60.2 t.boat-night^{-1} in 2022. From 1999 to 2004, mean CPUE$_{boat-night}$ rose rapidly from 8.5 t.boat-night^{-1} to 36.4 t.boat-night^{-1}, continued to increased to 54.7 t.boat-night^{-1} in 2016 and then dropped to 44.9 t.boat-night^{-1} in 2017 (Figure 2–1). Since 2018, mean CPUE$_{boat-night}$ has been greater than 50 t.boat-night^{-1}.

Mean annual CPUE$_{net-set}$ increased from 7.4 t.net-set^{-1} in 2000 to 32.6 t.net-set^{-1} in 2004, remained between 28.2–33.5 t.net-set^{-1} until 2012, and then increased to 40.1 t.net-set^{-1} in 2013. Since then, mean CPUE$_{net-set}$ has ranged between 36.9–44.4 t.net-set^{-1}. Mean CPUE$_{net-set}$ was 42.4 t.net-set^{-1} in 2021 and 44.1 t.net-set^{-1} in 2022.

Intra-annual patterns

The intra-annual pattern in fishing effort has been reasonably consistent over the last 20 years (Figure 2–2). Relatively little fishing occurs from August to October. Effort and catches typically increase in November–December. Catches continue to increase during January–February and usually peak in March–April. The peak fishing season reflects the generally calm weather between April and June and the high demand for tuna feed during this period. The months where large catches have been taken from the Outside, SG, and GSV Zones have varied among years (Figure 2–2).

Spatial patterns

From 1991 until the second mortality event in 1998, most Sardine were taken from Spencer Gulf (Figure 2–3). From 1999 onwards, a small proportion of the catch has usually been taken from the Outside Zone, mainly off Coffin Bay (Figures 2–3; 2–4a, b). In 2002 and 2003, the fishery expanded northwards in Spencer Gulf (Figure 2–4a). From 2003 to 2012, significant catches were also taken from Investigator Strait in most years. Since 2010, when additional quota was allocated outside Spencer Gulf, an increasing proportion of the total catch has been taken from the eastern Great Australian Bight.

More than 6,500 t have been taken per year from the Outside Zone since 2014 (Figure 2–3). In 2017, the TACC from the Outside Zone was increased to 12,750 t and catches increased accordingly. Substantial catches have been taken southeast of Kangaroo Island since 2017 (Figure 2–4b). In 2020, 6,000 t of TACC from the Outside Zone was allocated to the temporary GSV Zone, which was subsequently incorporated into the current Management Plan (PIRSA 2023). Since then, the catch taken from Gulf Saint Vincent has increased considerably (Figure 2–4b). The catch from

Gulf Saint Vincent has been small and varied historically, reaching ~1,300–2,500 t in 2005, 2006, 2010 and 2016 but remaining below 1,000 t in all other years up to 2020 (Figure 2–3). In 2020, the annual catch (CDR) from the GSV Zone rose to 5,555 t, dropped to 3,236 t in 2021, and was 5,336 t in 2022.
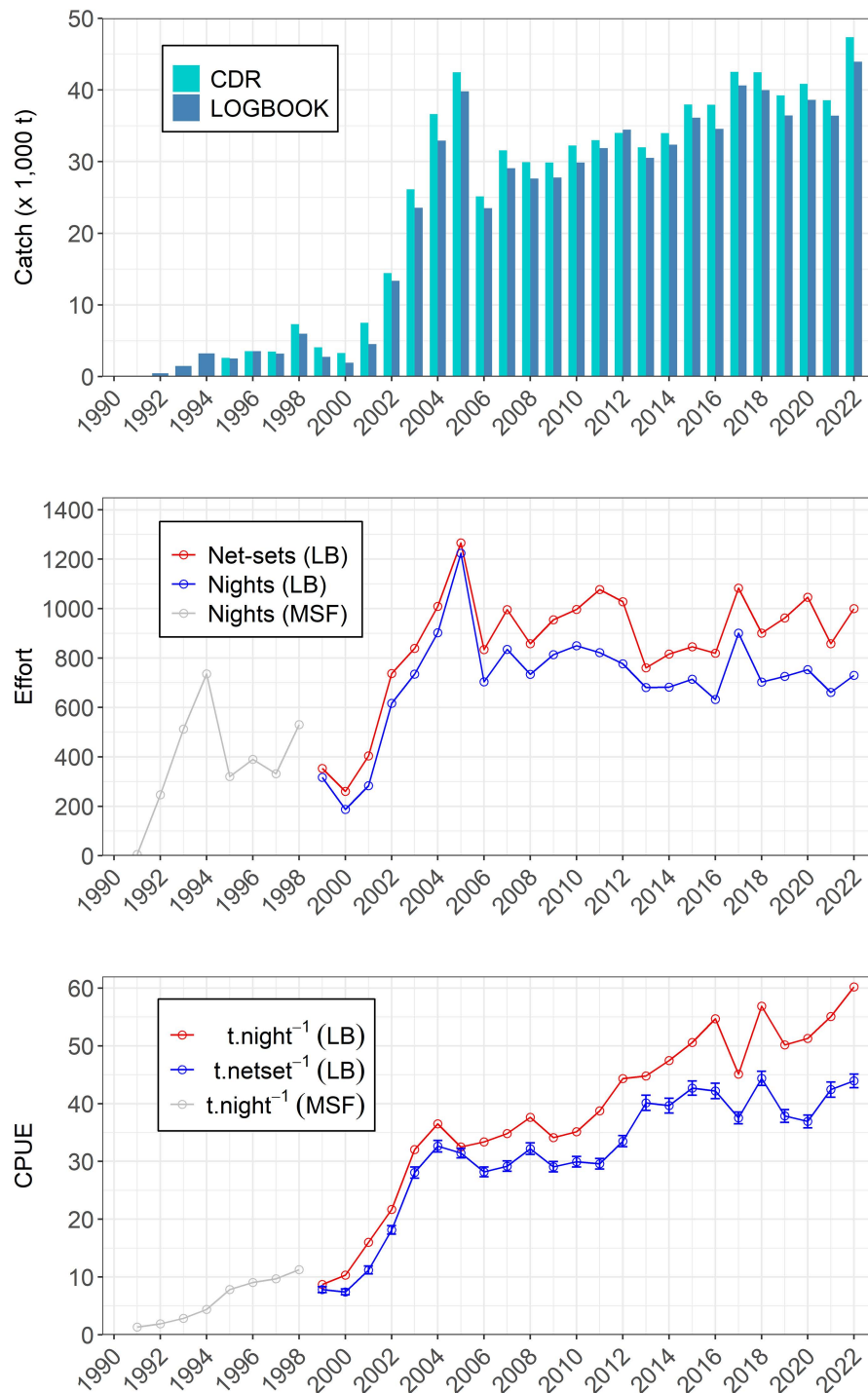
Figure 2-1. Total catches (estimated from logbooks, CDR), fishing effort (nights, net-sets) and mean annual CPUE (t.night^{-1}, t.net-set^{-1}, ± SE). Data prior to 1999 is derived from Marine Scalefish Fishery (MSF) records. Specific SASF logbooks (LB) were introduced in 1999.
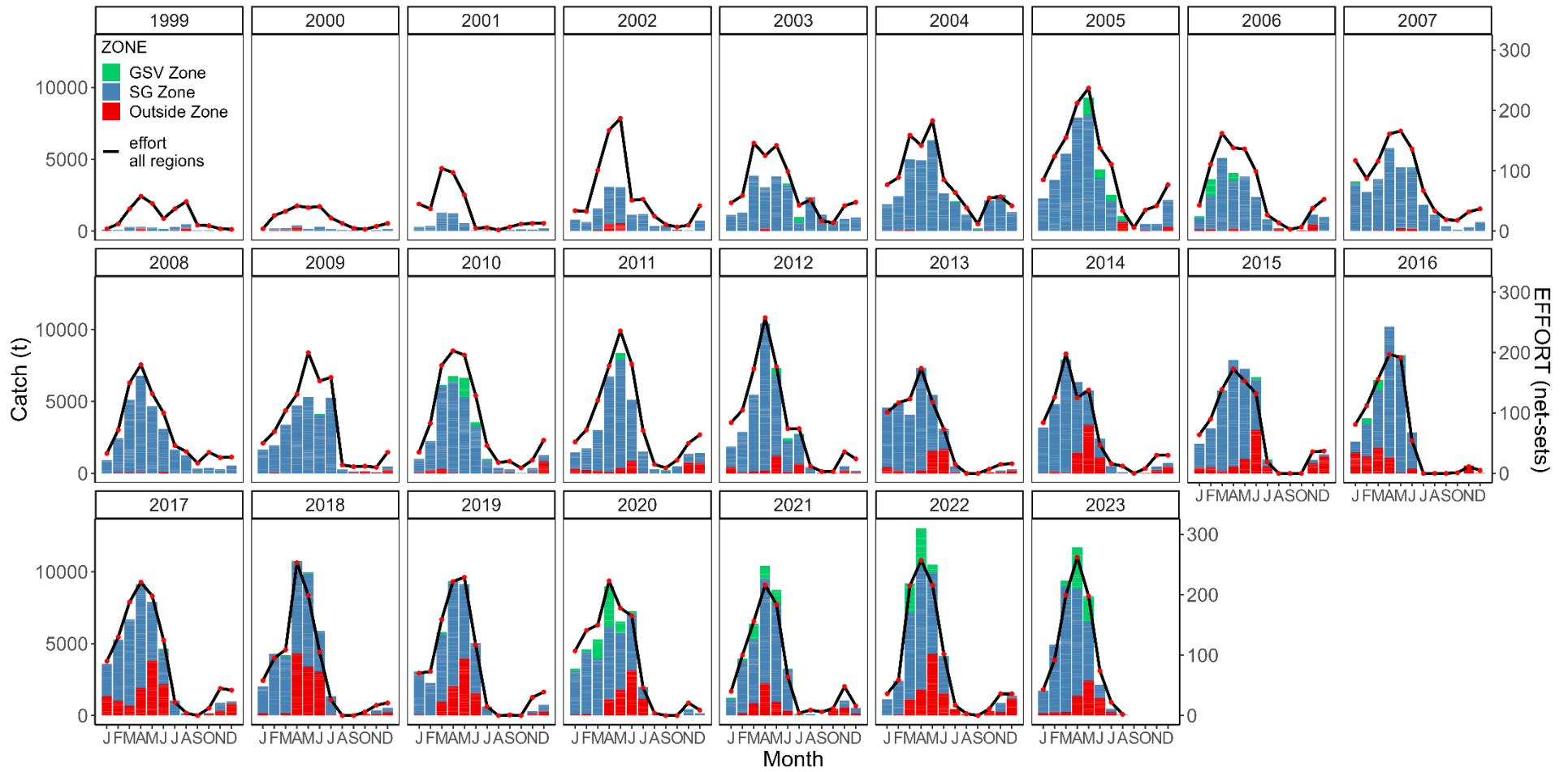
Figure 2-2. Intra-annual patterns in Sardine catch (tonnes, bars) by region and effort (net-sets, red points with black lines, all regions) in SASF between 1999 and 2022. Zones: GSV: Gulf Saint Vincent; SG: Spencer Gulf.
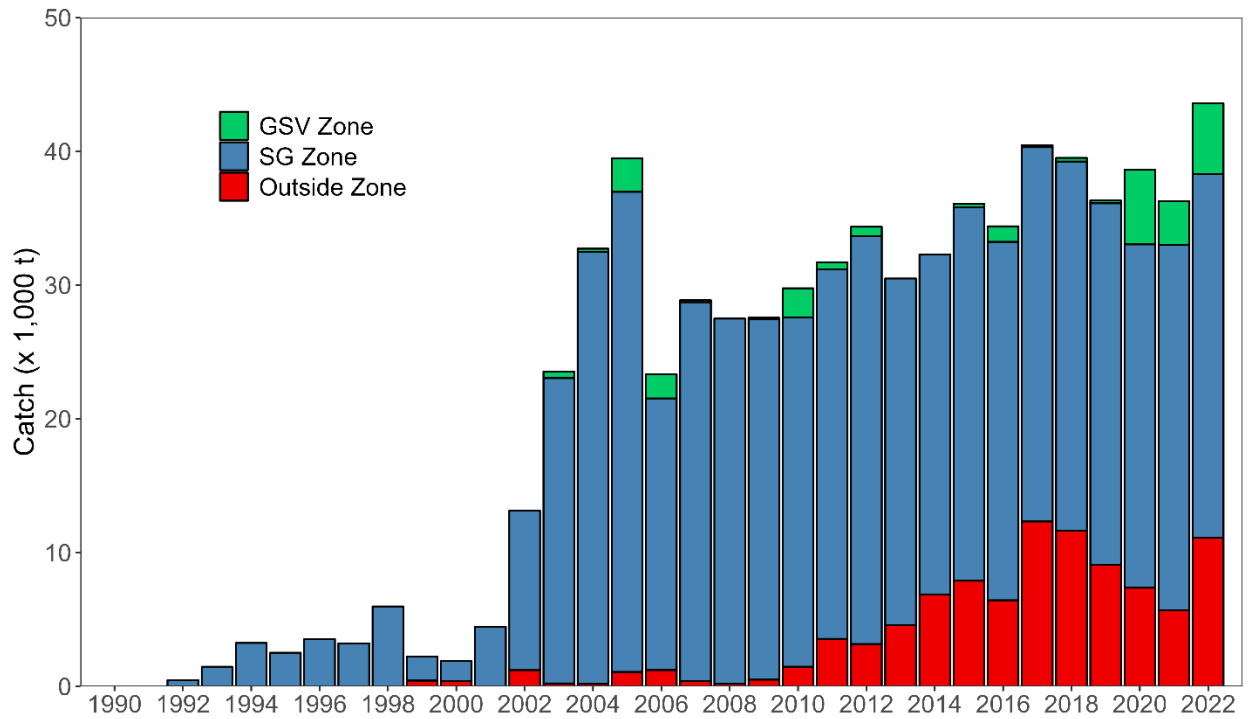
Figure 2-3. Annual Sardine catch (tonnes, logbook data) by zone between 1992 and 2022. Zones: GSV: Gulf Saint Vincent; SG: Spencer Gulf.
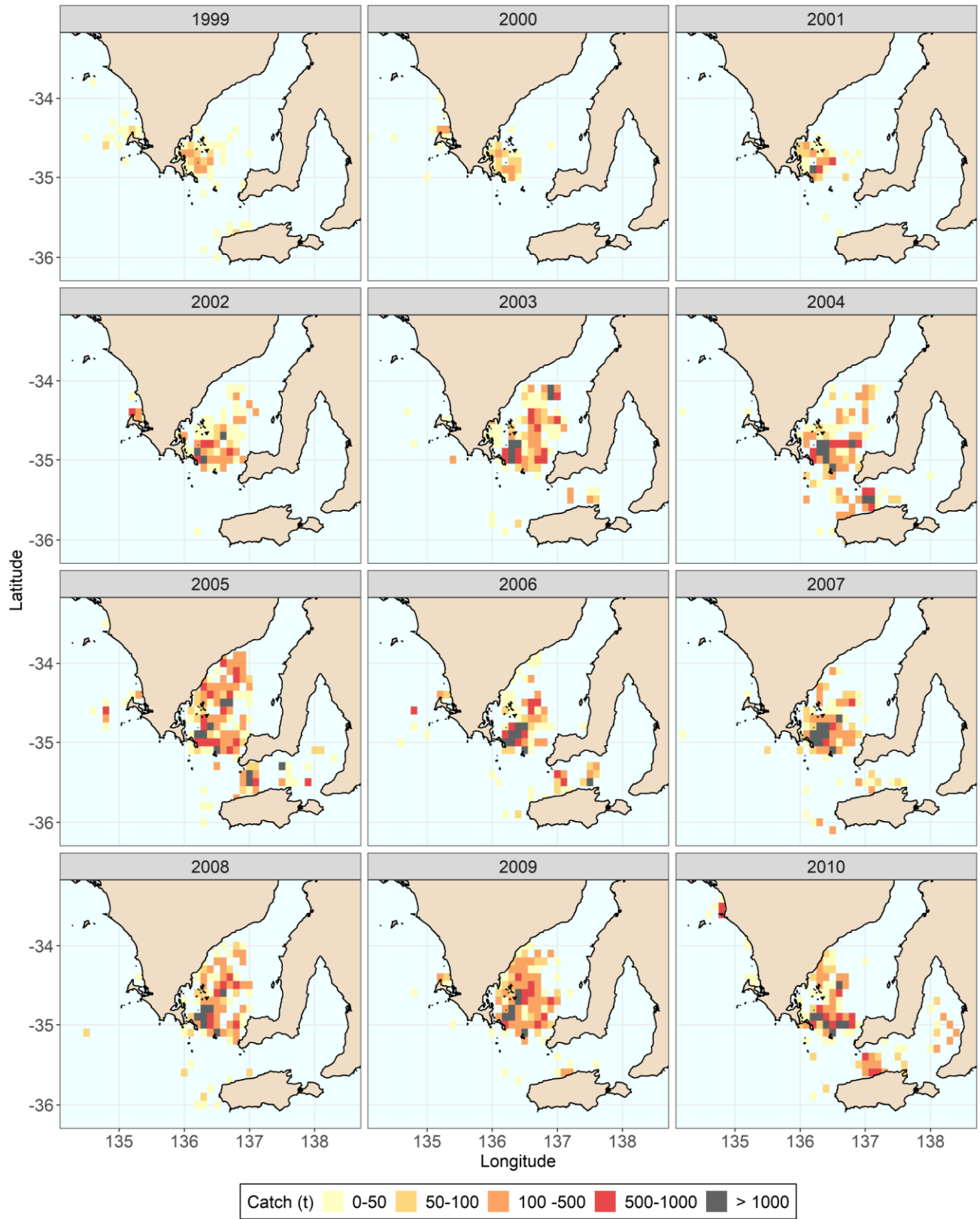
Figure 2-4a. Spatial trends in Sardine catches (tonnes) between 1999 and 2010.
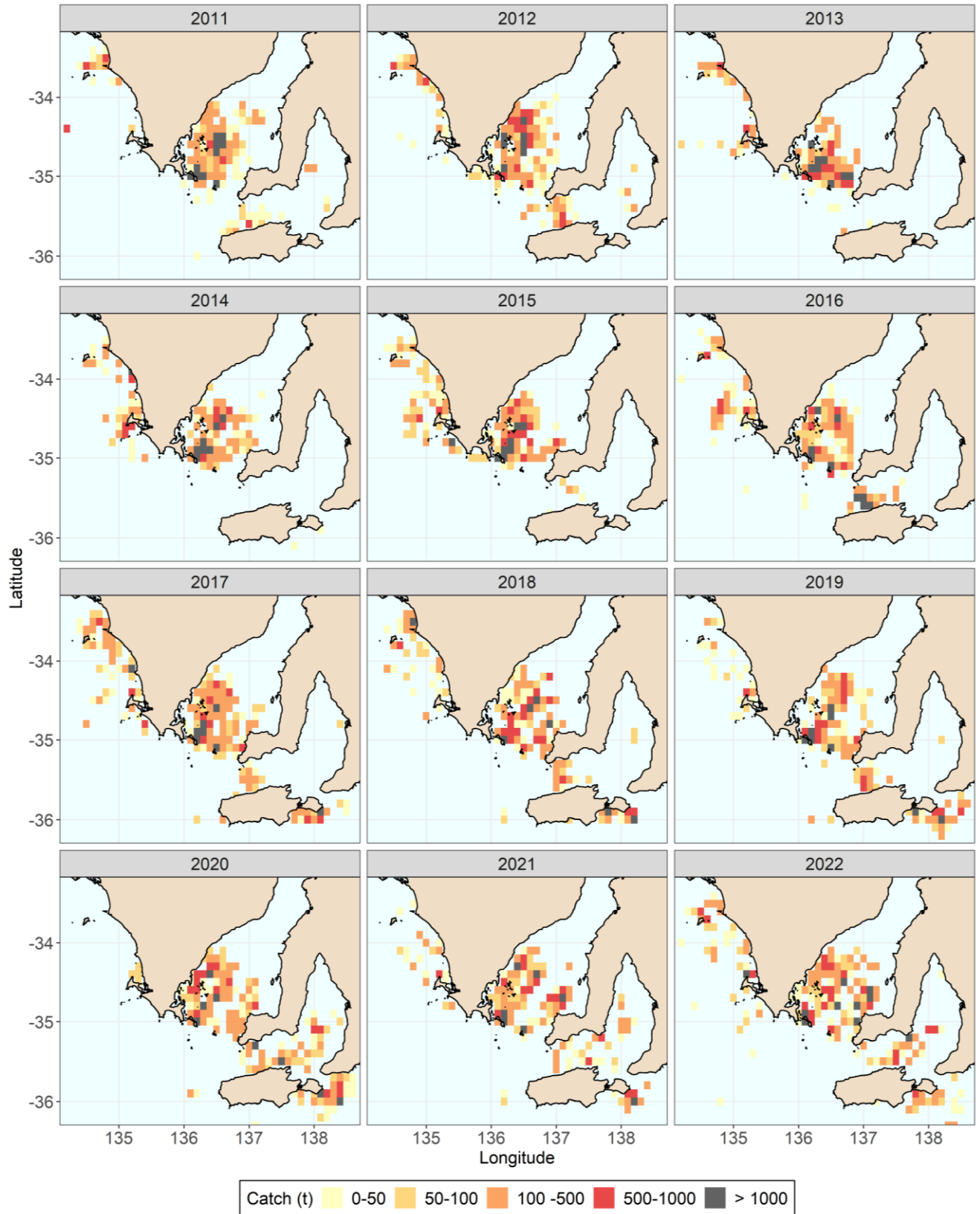
Figure 2-4b. Spatial trends in Sardine catches (tonnes) between 2011 and 2022.

2.3.2 Catch composition

Size frequency

In 1995, the modal size for Sardine caught in the SG Zone was 140 mm FL with fish mostly ranging from 130 to 170 mm FL (Figure 2–5). The modal size in the SG Zone declined to 130 mm FL in 1996 and was 120 mm FL in 1998. Between 1999 and 2002, Sardine from the SG Zone were mostly ≥140 mm FL with modes between 140 and 170 mm FL. In 2003 and 2004, the size structures in catch samples were bimodal, because significant quantities of juveniles (80–120 mm FL) were caught in addition to adults (150–180 mm FL). Prior to 2003, few catch samples from the SG Zone included Sardine ≤100 mm FL. Between 2005 and 2010, size distributions from the SG Zone remained stable with a mode at 140–150 mm FL, and fish ranged from 120 to 190 mm FL. The modal size declined to 130 mm FL in 2011–2013 and increased to 140 mm FL in 2014–2016 and to 150 mm FL in 2017 and 2018. From 2019 to 2021, the modal size declined to 140 mm FL. In 2022, the size structure was bimodal with modes at 130 mm FL and 150 mm FL (Figure 2–5).

Larger size ranges have been caught in the Outside Zone throughout the history of the fishery. In the Outside Zone, Sardine of 150–180 mm FL dominated catches between 1995 and 1998 (Figure 2–6). In 1999, after the second mortality event, the modal length fell to 130 mm FL but increased above 140 mm FL in 2000. In 2004, the modal size was 140 mm FL, and this increased to 170–190 mm FL in 2005–06. Few catch samples were taken in the Outside Zone in 2007–08 and none in 2009. Between 2010 and 2015, the modal size from the Outside Zone remained above 140 mm FL. In 2016 and 2017, sizes were distributed over a wide size range from 90–190 mm FL. The size structure in the Outside Zone was bimodal in 2018 with modes at 140 mm FL and 160 mm FL, and then declined to 130 mm FL in 2019, with few fish above 150 mm FL. In 2020, no samples that corresponded to Sardine catches in the Outside Zone were collected. The size structure was bimodal in 2021 (modes: 140 mm FL and 160 mm FL) and 2022 (modes: 130 mm FL and 160 mm FL).

Catch samples from the GSZ Zone have been available since 2009 with a modal size of 130 mm FL in 2009, 2010 and 2016 (Figure 2–7). No catch samples were available from GSV from 2011 to 2015. In 2018, the size structure was bimodal in the GSV Zone with modes at 120 mm FL and 150 mm FL. The modal size was 140 mm FL in 2019 and increased to 160 mm FL in 2020. The modal size from the GSV Zone was 130 mm FL in 2021 and increased to 140 mm FL in 2022.
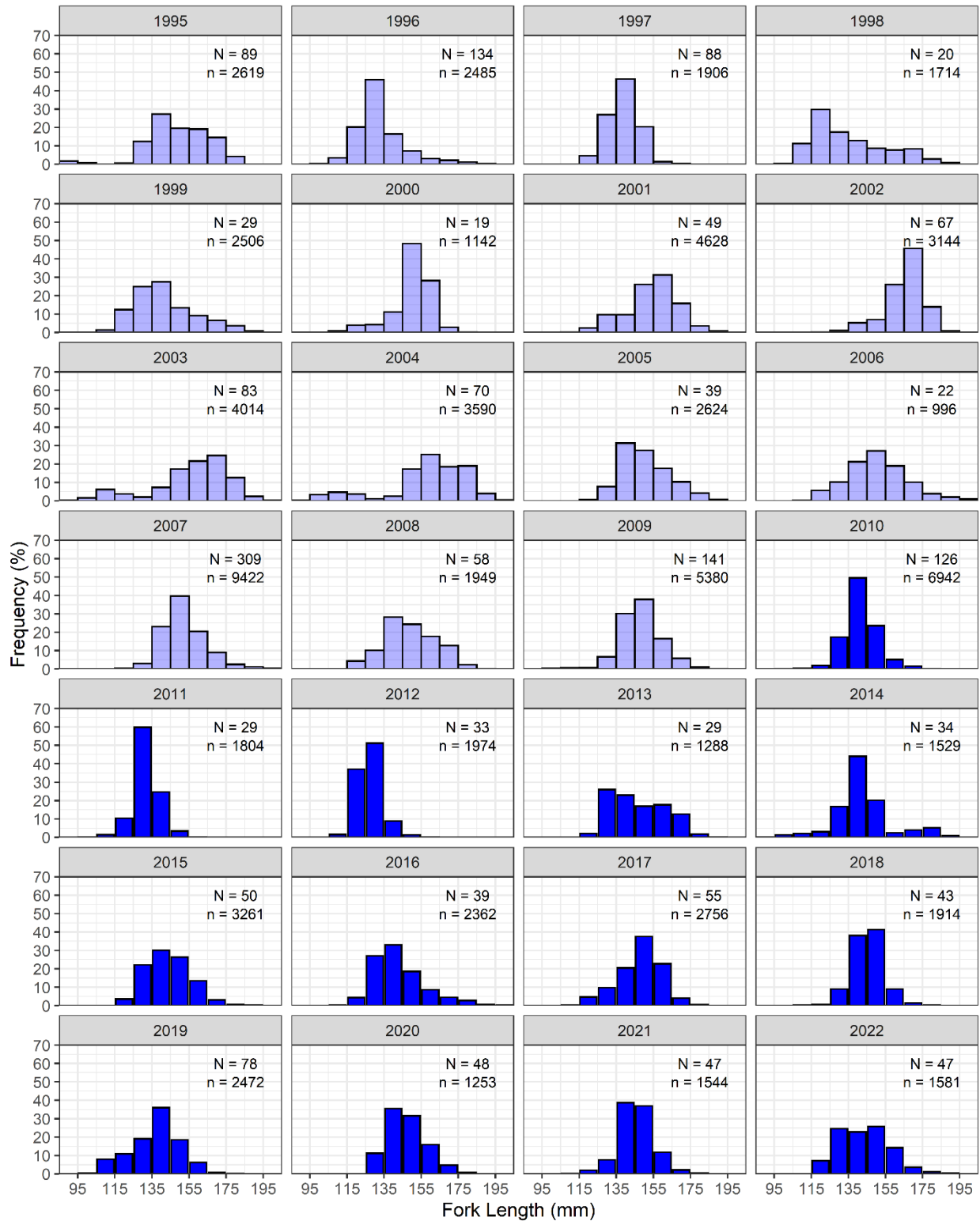
Figure 2-5. Length frequency distributions of Sardine measured (n) from commercial catch samples (N) for the Spencer Gulf Zone between 1995 and 2022. Dark blue: catch weighted distributions; pale blue: not catch weighted.
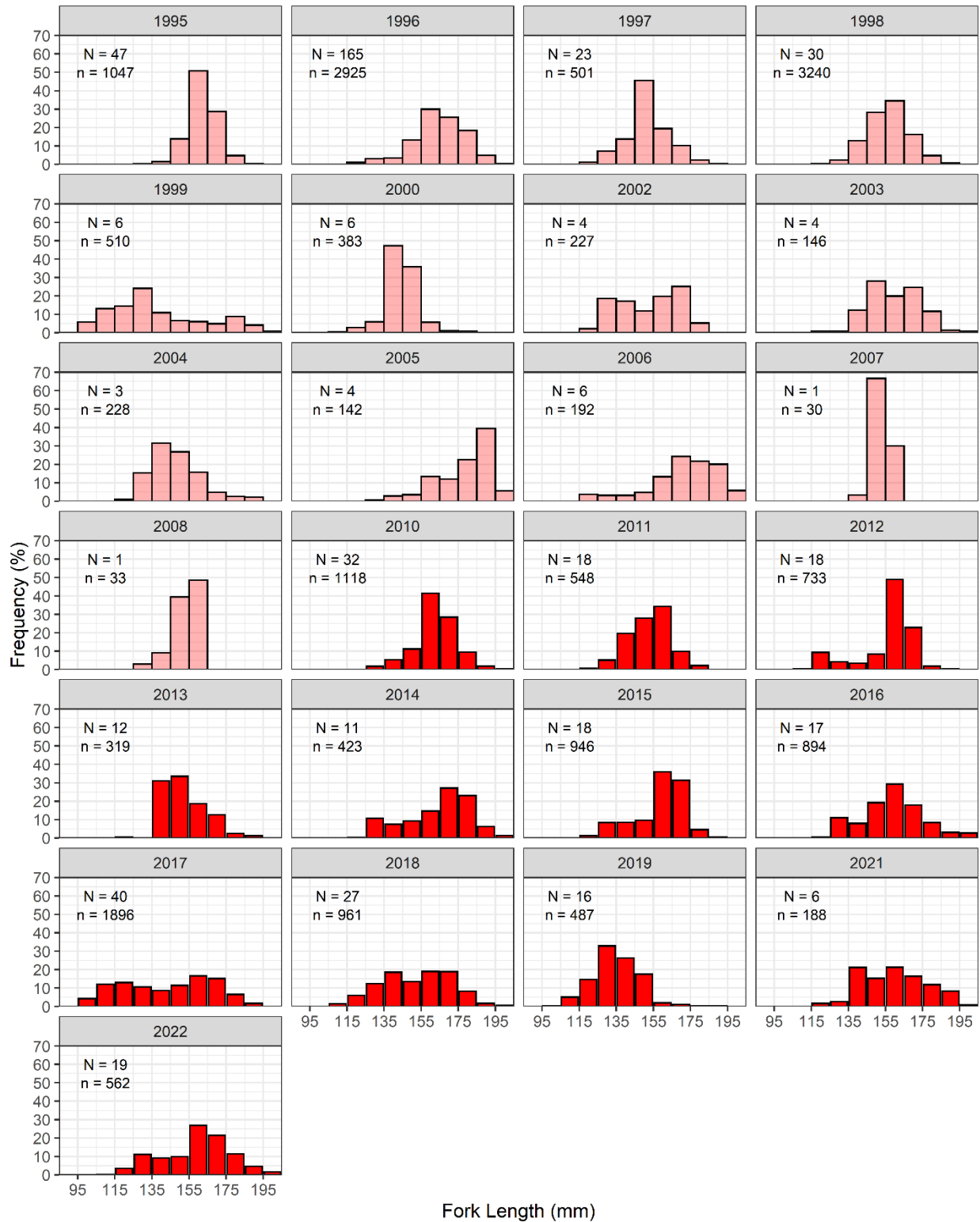
Figure 2-6. Length frequency distributions of Sardine measured (n) from commercial catch samples (N) for the Outside Zone between 1995 and 2022. Bright red: catch weighted distributions; pale red: not catch weighted.
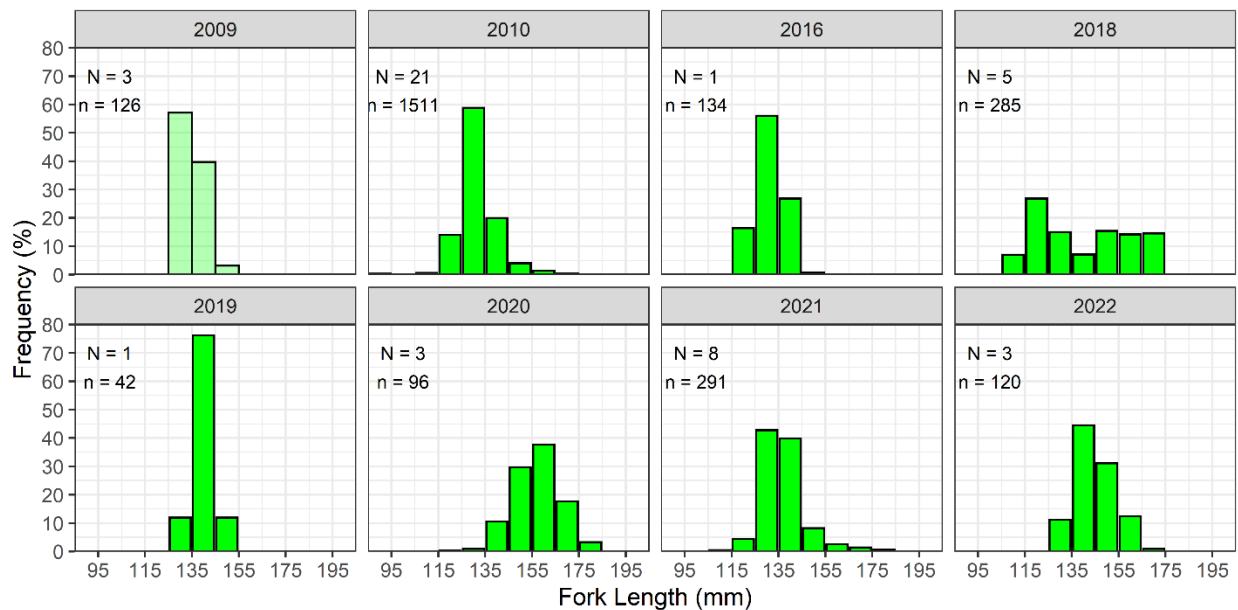
Figure 2-7. Length frequency distributions of Sardine measured (n) from commercial catch samples (N) for the Gulf Saint Vincent (GSV) Zone between 2009 and 2022. Bright green: catch weighted distributions; pale green: not catch weighted.

Mean size

The mean size of Sardine from Spencer Gulf (i.e. SG Zone since 2020) ranged from 133 to 149 mm FL between 1995 and 1999 and increased to 166 mm FL in 2002 (Figure 2–8). Between 2003 and 2009, mean fish size in Spencer Gulf was relatively stable between 149 and 159 mm FL and declined to 128 mm FL in 2012. From 2013 to 2018, the mean size in Spencer Gulf was stable and ranged from 143 to 148 mm FL. The mean size dropped to 138 mm FL in 2019. In 2020 and 2021, the mean size increased to 148 mm FL and 147 mm FL, respectively. In 2022, the mean size of Sardines from Spencer Gulf was 144 mm FL. The drop of the mean size in 2019 to below the reference size of 142 mm FL triggered a reduction in TACC from 30,000 t to 27,000 t for the SG Zone in 2020.

The mean size of Sardine from the Outside Zone was generally higher than Spencer Gulf (Figure 2–8), particularly in 2005 and 2006. Between 2010 and 2016, the mean size remained stable and ranged between 153 and 164 mm FL, but then decreased to 144 mm FL in 2017. In 2018, the mean size from the Outside Zone increased to 153 mm FL, and then fell to 136 mm FL in 2019.

The drop in mean size of Sardine in 2019 from the Outside Zone resulted from substantial catches of small fish (<142 mm FL) taken off the south-eastern coast of Kangaroo Island (SARDI unpublished). In 2020, no samples that corresponded to Sardine catches in the Outside Zone were collected. In 2021 and 2022, the mean size increased to 161 mm FL and 160 mm FL, respectively.

The mean size of Sardine from Gulf Saint Vincent (i.e. GSV Zone since 2020) from 132 to 136 mm FL from 2009 to 2016, then increased to 141 mm FL in 2018 and 2019 and 157 mm FL in 2020. In 2021, the mean size of Sardine from the GSV Zone declined to 138 mm FL, and then increased to 146 mm FL in 2022.
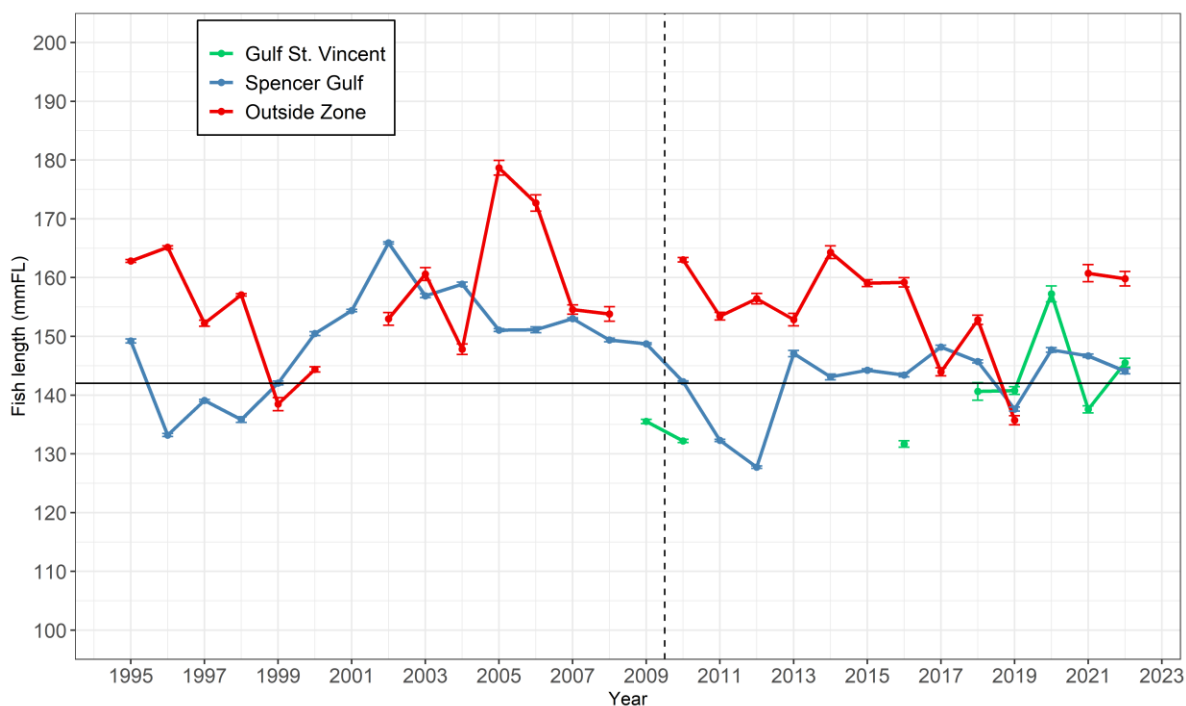
Figure 2-8. Average fork length (mm FL) by year for commercial samples from the three regions of the SASF: Spencer Gulf (SG Zone), Outside Zone, Gulf Saint Vincent (GSV Zone), error bars are standard error. Horizontal line indicates the reference point for maximum catch limit for the Gulf Zone of 142 mm FL (Table 1–2). Vertical dashed line indicated the period from which catch weighting was applied to estimates (2010–2022).

Spatial distribution of size

Between 2010 and 2022, Sardine >155 mm FL from commercial catch samples mainly occurred off the western Eyre Peninsula in the Outside Zone and in the mouth of Spencer Gulf and Investigator Strait (Figure 2–9) in the SG Zone. Sardine ≤ 135 mm FL predominantly occurred in

southwestern Spencer Gulf (Figure 2–9), but also occurred off south-eastern Kangaroo Island and in central GSV (SARDI unpublished; confidential data not shown). Sardine between 135 to 155 mm FL were distributed across the fishing grounds but mainly occurred in the southern Spencer Gulf, Investigator Strait and southern Gulf Saint Vincent (Figure 2–9).
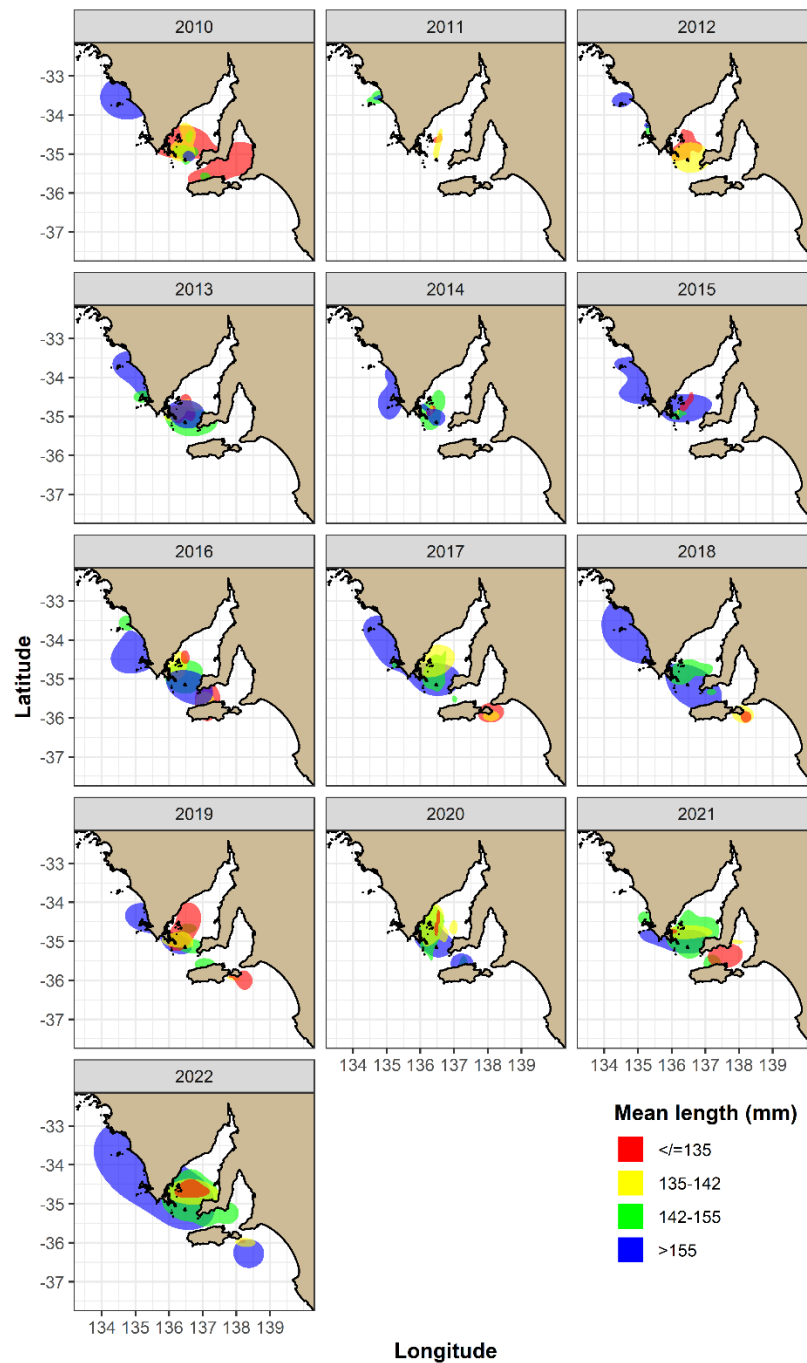
Figure 2-9. Kernal density distributions of the spatial trends in the mean size of Sardine (mm FL) from 2010 to 2022 in commercial catch samples. Data are plotted as kernel density distributions to meet requirements of data confidentiality (≥ 5 licences reporting catch).

Sex ratio

The annual sex ratio (by number) in commercial catches has varied over the history of the fishery. For most years, the sex ratio has been skewed towards females (Figure 2–10; Table A1). The highest proportion of females occurred in both 1995 and 2005 at 63%, while the lowest proportion of females was 47% in both 2000 and 2013 (Figure 2–10; Table A1).
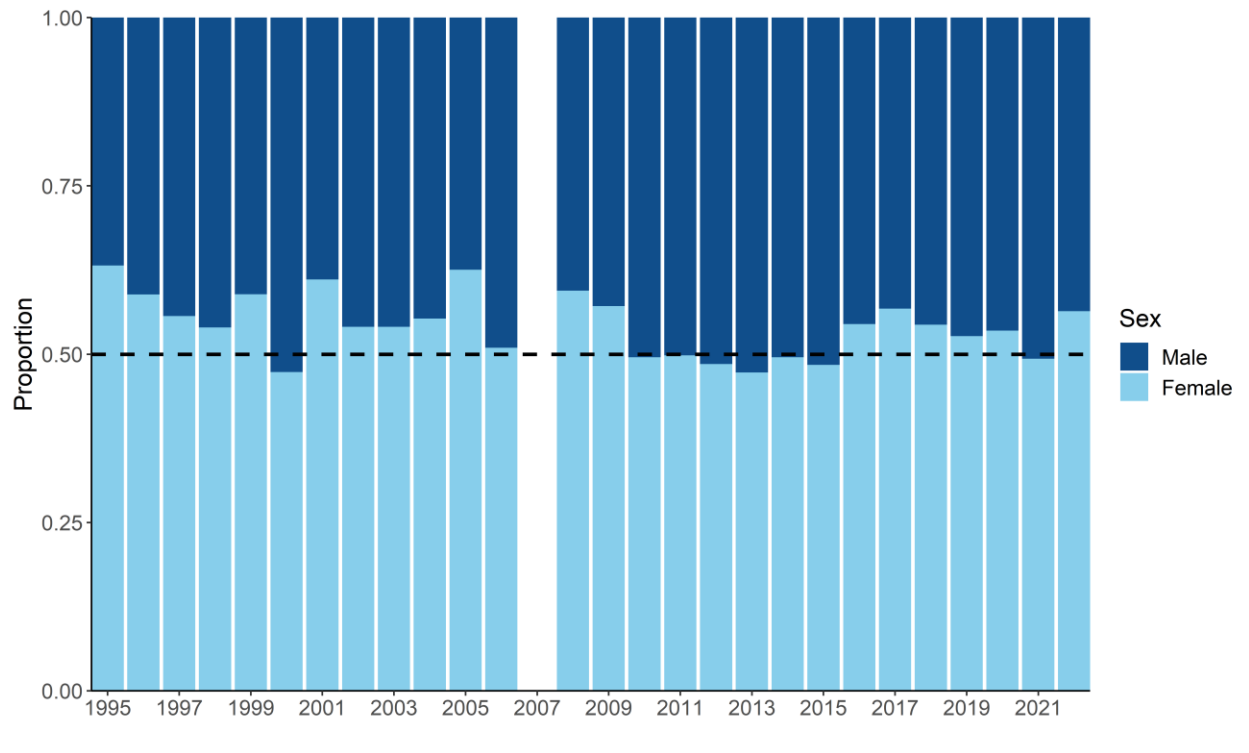
Figure 2-10. Sex ratio of commercial catch samples from all regions between 1995 and 2022. Data are unavailable for 2007 and limited for 2019. Dashed line represents a 1:1 sex ratio. Specific annual values are listed in Table A1.

2.4 Discussion

The SASF has grown rapidly since its inception. The TACC for 2017 to 2021 of 42,750 t was 40 times the TACC in 1992 (1,000 t) and more than ten times the TACC in 2000 (3,500 t). The TACC increased further in 2022 to 45,000 t and to 50,000 t in 2023. This rapid growth has occurred despite the impacts of two mass mortality events, each of which killed more fish than any other single-species mortality event recorded (Jones et al. 1997, Ward et al. 2001b).

Another notable feature of the SASF is the stability in catches over recent years. This stability has been achieved by establishing a precautionary harvest strategy that addresses the imprecision in estimates of spawning biomass obtained using the DEPM. Under the current harvest strategy for the SASF, the maximum TACC of 55,000 t can only be set when DEPM surveys and integrated stock assessments are done annually, and the spawning biomass is greater than the target reference point of 200,000 t. The fishery is currently positioned at Tier 2 with a maximum TACC of 50,000 t. At Tier 2, DEPM surveys are done annually with integrated stock assessments done every second year. At all Tiers, an ecosystem assessment is required every four years, and under the current harvest strategy, is set to occur in 2025 (PIRSA 2023).

Fishing effort of the SASF is concentrated in a relatively small proportion of the total area where the managed population is distributed. Since 2010, a range of management arrangements have been implemented to limit the catch from the SG and GSV Zones (particularly Spencer Gulf), reduce the capture of small fish from those Zones, and increase the catch from the Outside Zone. This approach established explicit rules to limit the total catch that can be taken from the Gulfs Zone (SG + GSV) based on the mean size of fish taken from that Zone in the previous year. In 2020, a third zone was implemented that separated the Gulfs Zones into the SG Zone and the GSV Zone (PIRSA 2020). These management approaches have been successful in increasing the mean size of fish taken from the Gulf Zones and shifting effort and catch across the region. The spatial management arrangements of three zones (trialled since 2020) have been permanently applied in the current Management Plan (PIRSA 2023). The percentages of the catch taken in the Outside Zone and the GSV Zone have increased substantially since 2010. The maximum catch recorded in logbooks from the Outside Zone was 12,479 t in 2017, which represented 31% of the total catch that year. Prior to 2020, relatively little catch was taken from the GSV Zone. In 2022, 12% of the total catch was taken from the Outside Zone, 7% from the GSV Zone and 62% from the SG Zone.

Changes in management arrangements and fishing patterns over the history of the SASF have influenced the size composition of fish taken in catches. Size-based decision rules implemented in 2010 have resulted in fishers selectively targeting larger fish in the Gulf Zones, i.e. > 142 mm FL. However, in 2019, the mean size of fish taken from the combined Gulfs Zone (SG + GSV) dropped to below the reference size of 142 mm FL and caused a reduction in TACC in 2020 from 30,000 t to 27,000 t for the SG Zone. Catches in 2022 from the both the Outside and GSV Zones have contained larger fish than catches from the SG Zone, although small fish do occur in areas of both Zones, e.g. northerly fishing grounds in GSV and off southeast Kangaroo Island (SARDI unpublished). A spatial pattern of the size-based distribution of Sardine off South Australia, based on size composition data from commercial catches, is beginning to emerge. Further understanding of the size-based distribution of Sardine in South Australian waters would be useful, given that size selectivity in the SASF has likely changed over time.

The increase in CPUE over the history of the SASF reflects increased catch capacity of the fleet. The reduction in CPUE in 2017 was interpreted by fishers to reflect a change in schooling behaviour of Sardine during that year. CPUE also declined in 2019 and 2020. The results of the DEPM survey for 2017, 2019 and 2020 did not suggest that the population had declined in those years. A divergence of $CPUE_{night}$ (small increase) and $CPUE_{net-set}$ (small decrease) since 2020 may warrant further investigation in light of the changing spatial nature of the fishery, in particular the increased use of the GSV Zone. These results reaffirm the unsuitability of CPUE for monitoring the abundance of pelagic fishes taken in a purse-seine fishery. CPUE is not used as an index of abundance in the population modelling undertaken in Chapter 5.

3. AGE COMPOSITION AND REPRODUCTIVE BIOLOGY

3.1 Introduction

Age determination studies of Sardine have involved counting growth increments in scales (Blackburn 1950) and sagittal otoliths (ear bones) (Butler et al. 1996, Fletcher and Blight 1996), and modelling the formation of marginal increments in otoliths (Kerstan 2000). Daily deposition of growth increments in the otoliths of larvae and juveniles has been validated in laboratory trials (Hayashi et al. 1989). Age validation studies involving the capture and maintenance of Sardine and other clupeoids have been problematic owing to logistical difficulties (Fletcher 1995) and sensitivity to handling (Rogers et al. 2003). Other methodological approaches have been used to show that translucent zones form annually in the sagittal otolith of 1+ year old Sardine off South Africa (Waldron 1998), ≤2+ year olds off North America (Barnes et al. 1994) and ≥4+ year olds off Western Australia (Fletcher and Blight 1996). Despite this theoretical basis for using increment-based age-determination methods, the application of these standard approaches has been problematic in Western Australia, South Australia and California due to difficulties associated with interpreting and counting opaque and translucent zones (Butler et al. 1996, Fletcher and Blight 1996, Rogers and Ward 2007).

Studies of growth dynamics of Sardine in the Benguela and California Current systems suggest that growth rates of larvae (up to 0.85 mm.day^{-1}) and juveniles (0.48–0.63 mm.day^{-1}) are high (Butler et al. 1996, Quinonez-Velazquez et al. 2000). In South Africa, Sardine were found to reach larger asymptotic sizes (L_∞ = 221 mm) and have lower growth constants (k = 1.09 year^{-1}) than those off southern California (L_∞ = 205 mm, k = 1.19 year^{-1}) (Thomas 1984, Butler et al. 1996). Parameter estimates for Sardine in Western Australia (Fletcher and Blight 1996) suggest that growth in this area is slower and that fish reach smaller asymptotic sizes than those in the more productive eastern boundary current systems.

A detailed study by Rogers and Ward (2007) showed that the growth rates of Sardine are higher in South Australian waters than off other parts of the Australian coastline, but lower than those in more productive boundary current ecosystems (Ward et al. 2006). A notable finding of the study was that fish in commercial catches were younger (and smaller) than those obtained in fishery-independent samples. This finding has implications for the use of age structured models (based on fishery samples) for stock assessment of the SASF (see Chapter 5).

This chapter describes the methods used to determine age compositions from the commercial catch of Sardine in South Australian waters. Catch-at-age information presented in this chapter is a key input to the population model presented in Chapter 5.

3.2 Methods

3.2.1   Age-determination

Otolith preparation and interpretation

Sagittal otoliths were collected from sub-samples (n = 10–20) of the commercial catch samples and fishery-independent samples (Chapter 2). Otoliths were cleaned of excess tissue, rinsed in distilled water and dried in IWAKI™ plastic microplates. Translucent zone counts were made for one whole otolith from each fish under reflected light, immersed in water against a flat black background (Butler et al. 1996).

Readability index

Sardine otoliths were classified as 1 = excellent, 2 = good, 3 = average, 4 = poor and 5 = unreadable based on standard criteria relating to their interpretability (see Rogers and Ward 2007).

Decimal age estimates from annuli counts

To estimate decimal age for adults with a translucent zone count of one or more, an arbitrary birth-date of March 1 was assigned, which represents the time of peak spawning. The midpoint of translucent zone formation was assumed to be mid-winter (Rogers and Ward 2007). Decimal age *A* was calculated as:

$$A = \begin{cases} (\alpha - \beta_p)/365 + TZC + 0.334 & \alpha \le \beta_s \\ (\alpha - \beta_s)/365 + TZC + 0.334 & \alpha > \beta_s, \end{cases}$$

where α is the date of capture, β_s is the assumed translucent zone formation date from the same year as α, β_p is the assumed translucent zone formation date from the previous year, TZC is the translucent zone count and 0.334 (4 decimal months) adjusts for the difference between the assigned birth-date and the approximate timing of the first translucent zone.

Age estimations from otolith weight

The relationship between age and otolith weight was determined using a linear model fitted to decimal age and otolith weight data from those otoliths with readability index scores of 1 and 2. Aged otoliths from commercial catch samples between 1995 and 2022 and fishery-independent samples between 1998 and 2018 were pooled for the analysis. The resulting model was used to derive an age estimate for all otoliths based on otolith weight. Due to the change in the spatial patterns of fishing over time it is not possible to separate annual effects from regional effects on the relationship (i.e. region and season were confounded), so data from all regions were used in the analysis. Otoliths collected in 2017 and 2018 were unusually opaque and were unable to be visually assigned an age. Therefore, ages were assigned to these otoliths using the linear relationship for age–otolith weight.

3.2.2 Size-at-maturity

Ovaries were staged macroscopically where stage 1 = immature, stage 2 = maturing, stage 3 = mature, stage 4 = hydrated (spawning) and stage 5 = spent (recently spawned). Testes were staged where stage 1 = immature, stage 2 = mature and stage 3 = mature (running ripe). Only fish sampled during the spawning season (1 December to 31 March) were included as outside of this period as stages 2 and 5 are difficult to macroscopically differentiate.

The length at which 50% of the population was mature (L_{50}) was estimated using a binomial generalised linear model (GLM) with a logit link function. The model was fitted separately to males and females using binary maturity assignments where immature = 0 (stage 1) and 1 = mature (stages ≥ 2). The proportion of the mature population at length L calculated as:

$$P(L) = P_{max}\left(1 + e^{-\ln(19)\left(\frac{L - L_{50}}{L_{95} - L_{50}}\right)}\right)^{-1}$$

where *P(L)* is the proportion of the population mature at fork length L and P_{max} is the maximum proportion of mature individuals. Size-at-maturity models were fit to each sampling year to determine if L_{50} has changed over the history of the fishery. Some years were omitted as insufficient data were collected within the spawning season to accurately fit the model.

A size-at-maturity ogive was produced using the data pooled across all years and fishery dependent and independent sampling. These data were also restricted to within the spawning season and the two Gulf Zones (SG and GSV).

To examine any changes in *L₅₀* during the spawning season, size-at-maturity ogives were produced per month using the data pooled across all years and fishery dependent and independent sampling and restricted to within the spawning season and the two Gulf Zones (SG and GSV). To further interrogate any change in *L₅₀* over the history of the fishery, data were then restricted by month (December–April) in each year and size-at-maturity models were fitted to each sampling year. Some years were omitted as insufficient data were collected within the spawning season to accurately fit the model.

3.2.3 Growth

Length-at-age was estimated using the standard von Bertalanffy growth function (VBGF) fitted to individuals that were aged with a readability index score of 1 or 2. Discrete ages were converted to decimal ages using the methods outlined previously. Preliminary analyses indicated that growth was not sex dependent and therefore the sexes were pooled. This allowed the inclusion of juvenile fish that were aged using daily ring counts and had been too young to accurately determine sex (Rogers and Ward 2007). The VBGF was represented by the equation:

$$L_t = L_\infty - (L_\infty - L_0)e^{-kt}$$

Where L_t was the length at time *t*, L_∞ was the asymptotic length, *k* was the growth completion parameter (yr^{-1}) and L_0 was the length-at-age-zero. Length-at-age 95% confidence intervals were computed using 1000 bootstrap iterations.

3.2.4 Gonadosomatic index (GSI)

Mean monthly gonadosomatic indices (GSI) were calculated from both fishery independent and commercial samples using the equation:

$$GSI = \left[\frac{Gwt}{Fwt_{gonadfree}} \right].100$$

where *Gwt* is gonad weight and *Fwt* is gonad-free fish weight for fish with gonads of macroscopic stages ≥ 2. The mean estimate of GSI of all fish above size-at-maturity was used for both males and females to determine spawning season. It is important to note that it is sometimes difficult to macroscopically distinguish between Stage 2 and Stage 5 gonads in frozen samples.

3.3 Results

3.3.1 Age-determination

Between 1995 and 2022, a total of 22,546 otoliths from commercial and fishery-independent samples were read (Figure 3–1, Table A2). Less than 0.1% were assigned a readability index score of 1, while 5.5%, 49.0% and 28.8% were assigned scores of 2, 3 and 4, respectively. A readability index score of 5 was assigned to 16.5% of the otoliths (Figure 3–1, Table A2).
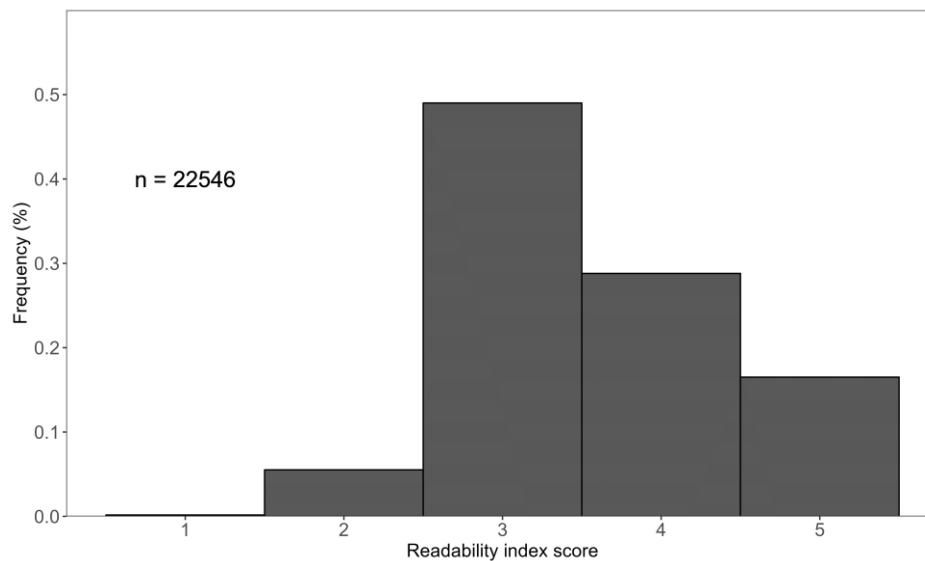
Figure 3-1. Readability index scores assigned to otoliths from all samples between 1995 and 2022.

Otolith weight relationship

The modelled relationship between decimal age (years) and otolith weight (mg) provided a reasonable fit to the data (r^2 = 0.827; Figure 3–2). However, while the 95% confidence intervals for the linear regression fit were narrow, the variation around the linear relationship was large. Therefore, while age can be inferred from otolith weight, the lack of precision resulting from this method means that these age estimates must be used with caution.
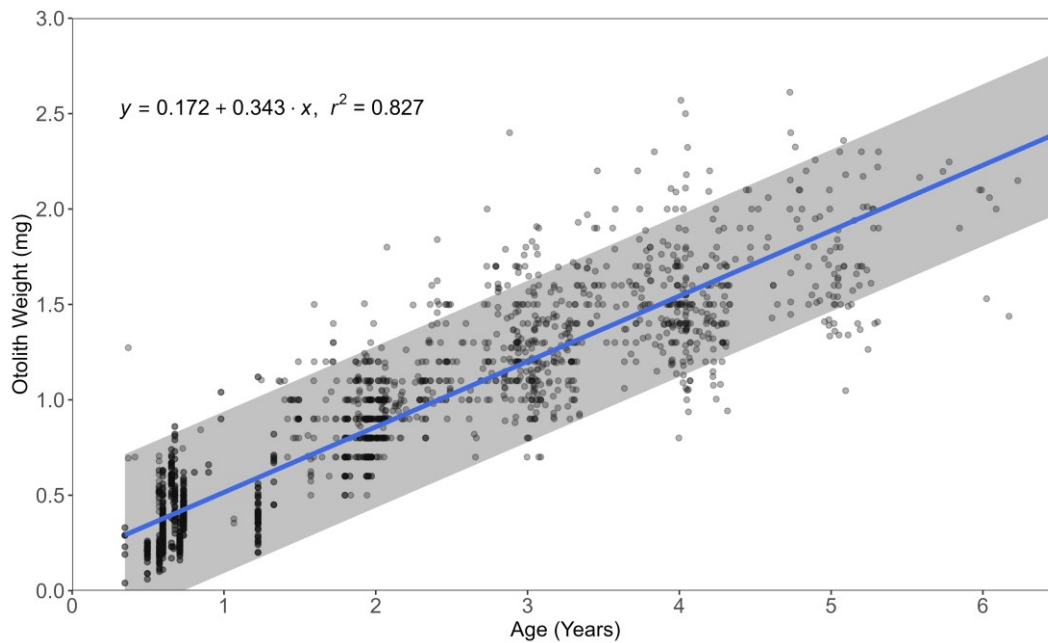
Figure 3-2. Regression of decimal age and otolith weight for Sardine otoliths with readability index scores of 1 and 2 from commercial and fishery-independent samples collected between 1995 and 2022. The light grey area represents 95% confidence intervals.

3.3.2 Age composition

Age composition data from commercial catches were available from 1995 to 2022, except for 2007 when no otoliths were collected. Ages ranged from 0+ to 8+ years. In 1995, fish aged 2+, 3+, and 4+ years dominated catches from the SG Zone, but from 1996 to 1998, catches were mostly dominated by age 1+ and 2+ fish, with a noticeable reduction in older fish in 1997 (Figure 3–3). These trends reflect the 1995 mass mortality event which mainly affected adult fish. In 1999, 2+ year olds (fish that were juveniles in 1998 and largely unaffected by the 1998 mass mortality event) dominated the catch. Fish that were spawned during 1997 and 1998 continued to dominate catches from the SG Zone as 2+ and 3+ year olds in 2000. From 2001 to 2022, 3+ year olds dominated the catch from the SG Zone in all years, except 2006, 2011 and 2019, when 2+ year olds were most abundant (Figure 3–3).

Catches from the Outside Zone have generally been comprised of older fish than those from the two Gulf Zones (Figure 3–4). In most years, fish aged 3+, 4+ and 5+ years dominated catches from the Outside Zone. However, fish aged 2+ years dominated catches in 1999, immediately after the 1998 mortality event, as well as in 2000. In 2019, 2+ year old fish were again the dominant year class with fewer older year classes present. Since 2021, the age composition was once again comprised of 3+ and 4+ year olds, although the sample size was limited.
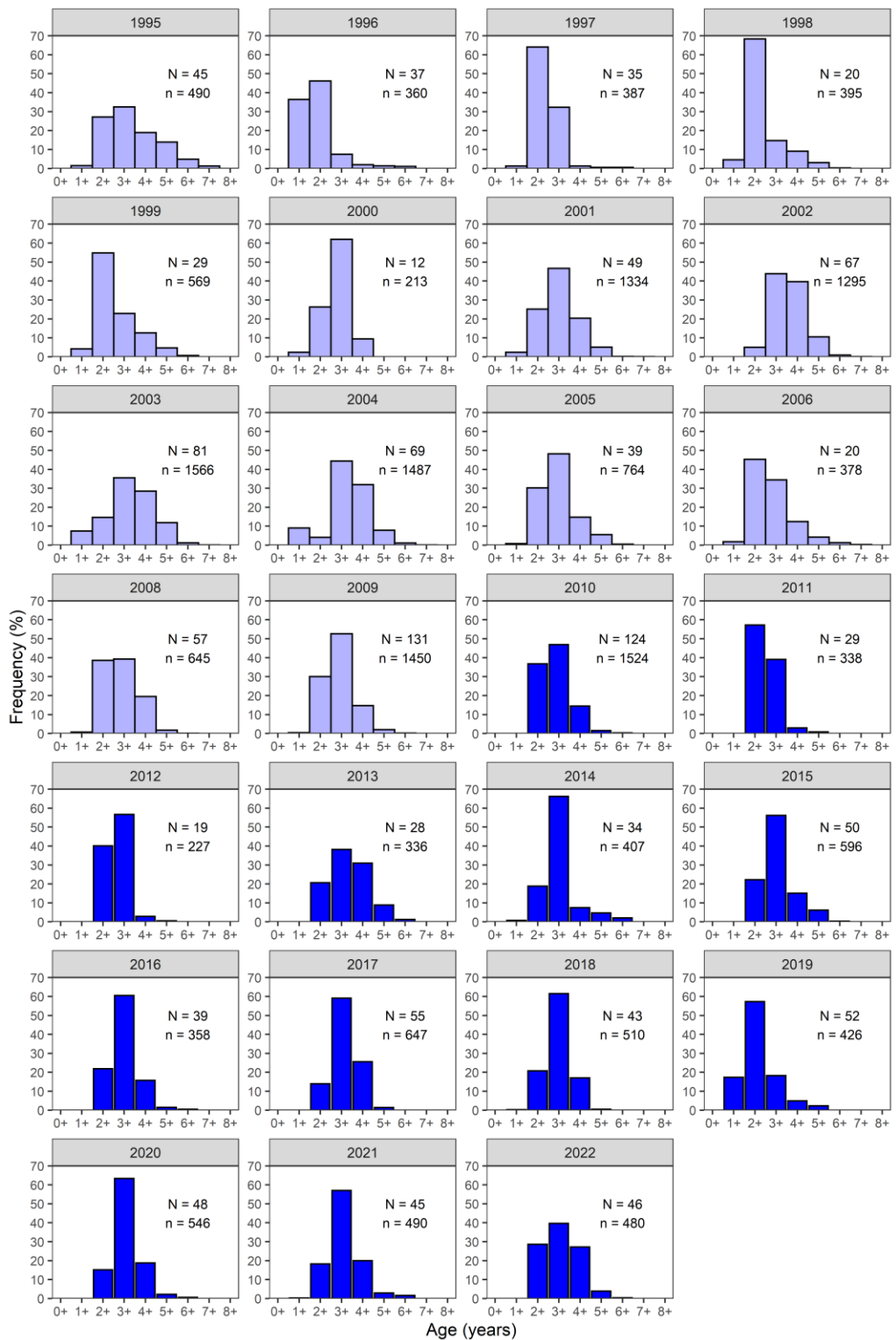
Figure 3-3. Age distributions for commercial catch samples of Sardine from the Spencer Gulf Zone between 1995 and 2022. Ages are derived from an otolith-weight-age relationship calculated for all years from otoliths with readability index scores of 1 and 2 and applied to all weighed otoliths for each year. Data were not available for 2007. Dark blue: catch weighted distributions; pale blue: not catch weighted. N: number of samples; n: number of fish.
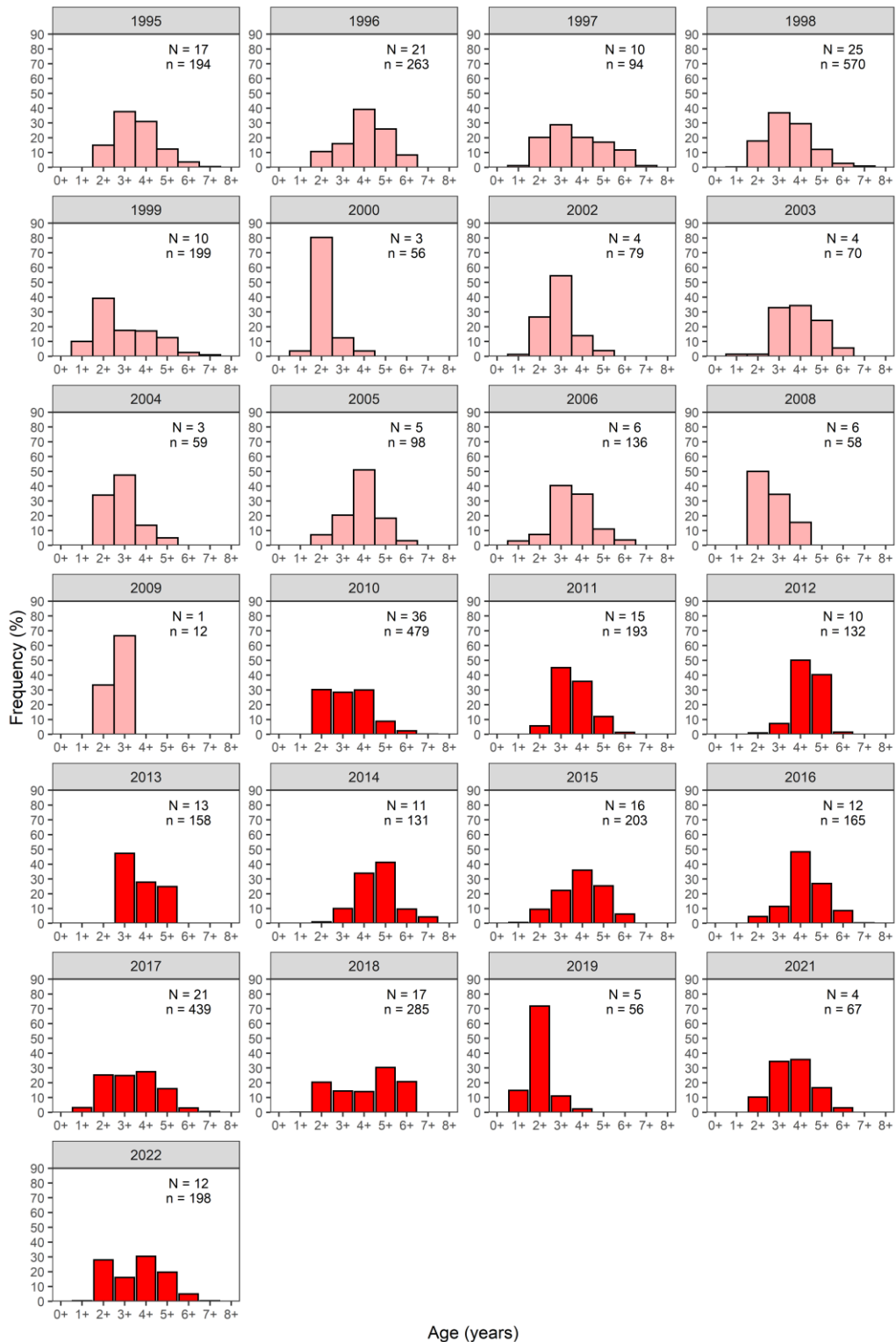
Figure 3-4. Age distributions for commercial catch samples of Sardine from the Outside Zone between 1995 and 2022. Ages are derived from an otolith-weight-age relationship calculated for all years from otoliths with readability index scores of 1 and 2 and applied to all weighed otoliths for each year. Data were not available for 2007. Bright red: catch weighted distributions; pale red: not catch weighted. N: number of samples; n: number of fish.

Between 2009 and 2010, catches from the GSV Zone were dominated by fish aged 2+ years; in 2016, fish aged 3+ years were more abundant than 2+ year olds (Figure 3–5). In 2018, the age of Sardine from the GSV Zone was bimodal with modes at 2+ and 4+ years. The age mode declined to 2+ years in 2019 and rose to 4+ years in 2020. The modal age of Sardine from the GSV Zone was 2+ year olds in 2021 and 3+ year olds in 2022. The number of samples available from Gulf Saint Vincent were small in all years.
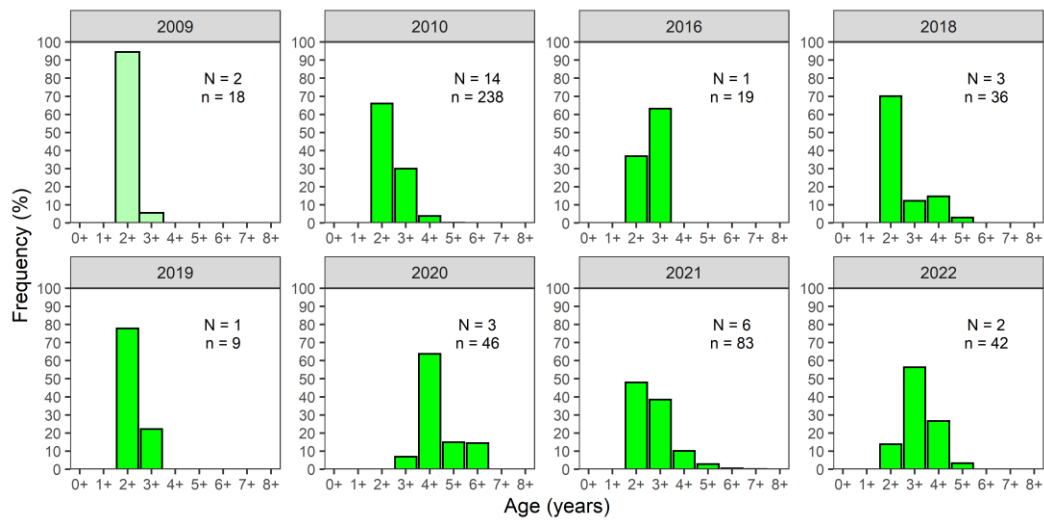
Figure 3-5. Age distributions for commercial catch samples of Sardine from Gulf Saint Vincent between 2009 and 2022. Ages are derived from an otolith-weight-age relationship calculated for all years from otoliths with readability index scores of 1 and 2 and applied to all weighed otoliths for each year. Bright green: catch weighted distributions; pale green: not catch weighted. N: number of samples; n: number of fish.

3.3.3 Growth

Fixing t_0 is a common approach for species whose life history includes a larval phase. The best fitting VBGF curve provided parameter estimates of: L_∞ = 177.7 mm FL, k = 0.71 year^{-1}, L_0 = 3.49 mm FL (Figure 3–6).
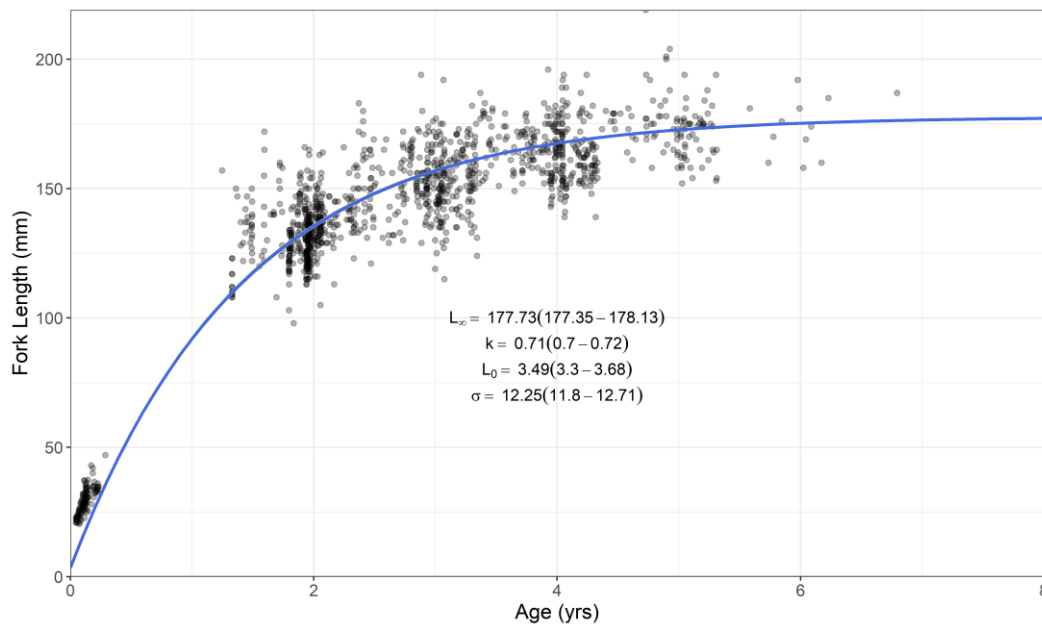
Figure 3-6. von Bertalanffy growth model fitted to length-at-age data (grey points) of individuals with otoliths that had readability index scores of 1 or 2 collected between 1995 and 2022.

3.3.4 Size-at-maturity

Size-at-maturity (L_{50}) estimated for Sardine from the commercial catch samples from the Gulf Zones (SG +GSV) between 1995 and 2016 has varied slightly among years (Figure 3–7). A declining trend in L_{50} appears to be occurring over the time series for both females and males (Figure 3–7). L_{50} could not be estimated in 1998, 2007, 2012, 2013 and 2014 due to a lack of commercial samples collected during the spawning season. Samples from 2019 were too deteriorated to stage after a freezer break down. The interpretation of gonads for samples collected during 2020 appeared to be inconsistent with previous years and those data were unable to be used to determine L_{50} in that year. All females below 118 mm FL and males below 116 mm FL had immature gonads. The estimate of L_{50} using data from all years combined was 141.8 mm FL for females and 137.7 mm FL for males (Figure 3–8).
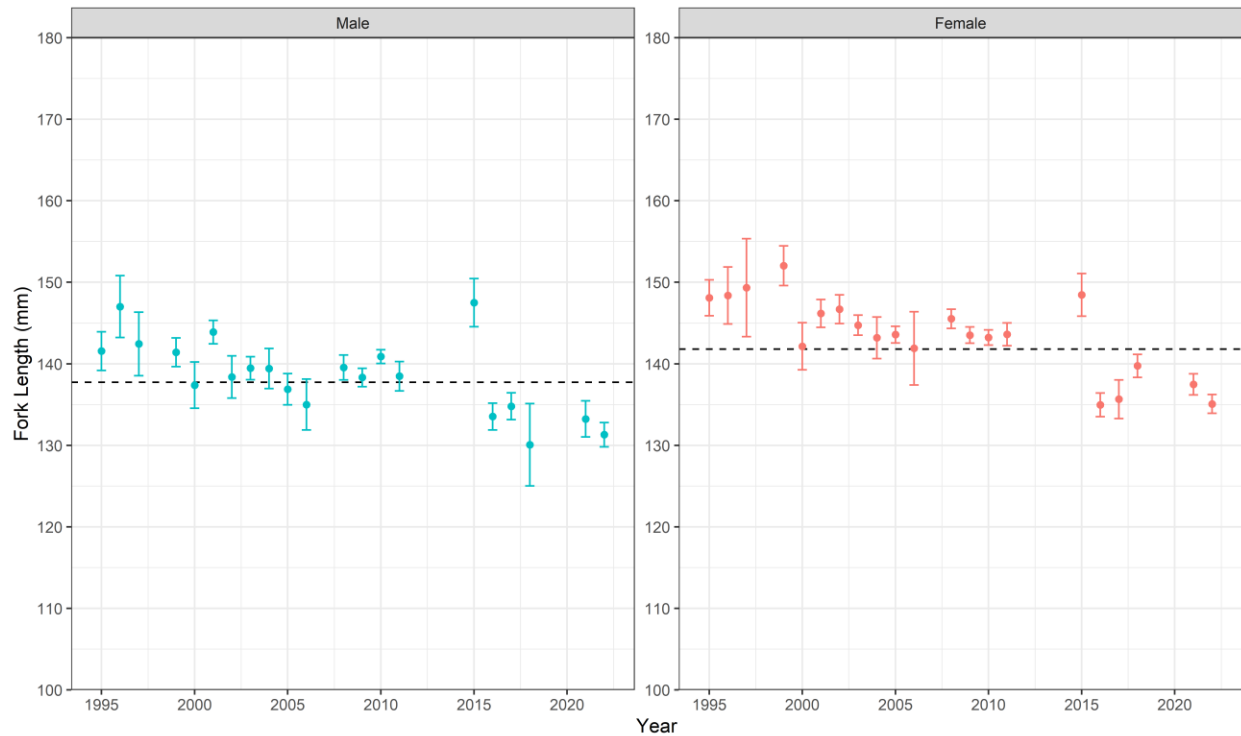
Figure 3-7. Size-at-maturity (*L₅₀*) for male and female Sardine collected in the two Gulf Zones (SG and GSV) by year, between 1995 and 2022. Some years were omitted due to low sample size and/or deteriorated samples. Error bars are 95% confidence intervals. Dashed lines represent the mean *L₅₀* across all years calculated in Figure 3–8.
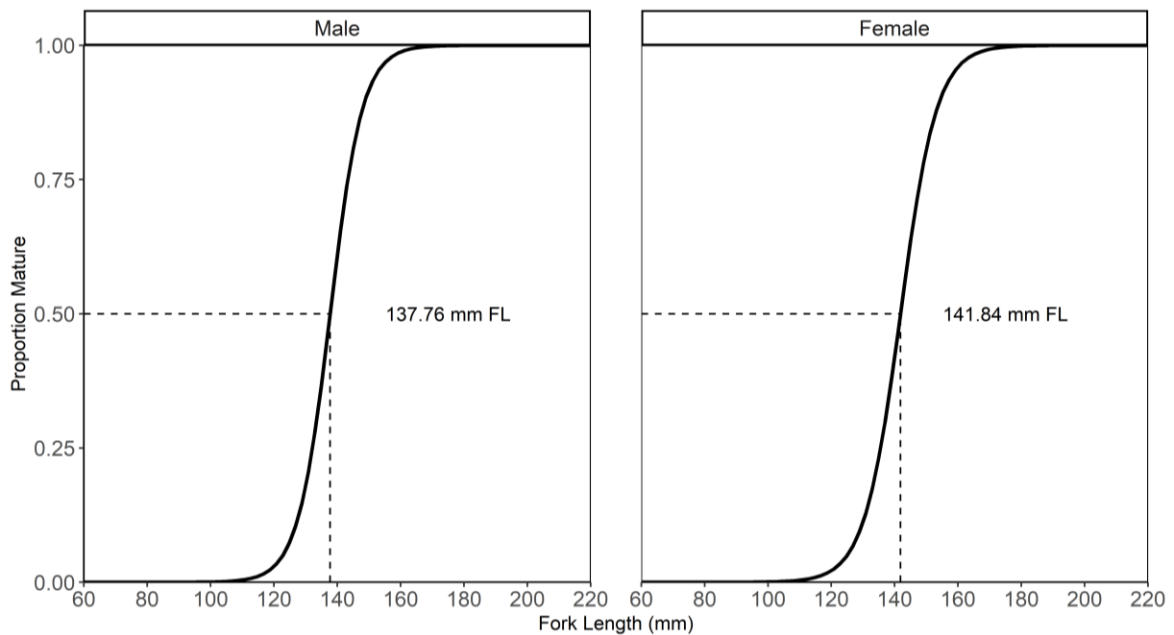
Figure 3-8. Size-at-maturity (*L₅₀*) for male and female Sardine collected from the two Gulf Zones (SG and GSV) for all years combined.

Estimates of L_{50}, using data from all years combined and partitioned by month, decreased for both males and females over the spawning season, reducing from 141 mm FL (December) to 134 mm FL (March) in males and from 150 mm FL (December) to 138 mm FL (March) in females (Figure 3–9). The estimate of L_{50} increased in April for both males (136 mm FL) and females (139 mm FL). This may be due to the recruitment of small juveniles into the mature population early in the season (decreased L_{50}), and the cessation of juvenile recruitment later in the season combined with the continuing growth of mature fish in the population (increasing L_{50}). These results complicate interpretation of annual trends in L_{50}, as catch samples were not uniformly collected over the spawning season through time. For example, catch samples have not been collected in December since 2006 and samples have been generally limited for January (Figure 3–10). However, inter-annual comparisons of L_{50} by month continued to show a declining trend through time for both males and females where adequate samples were available, e.g. January to April (Figure 3–10).
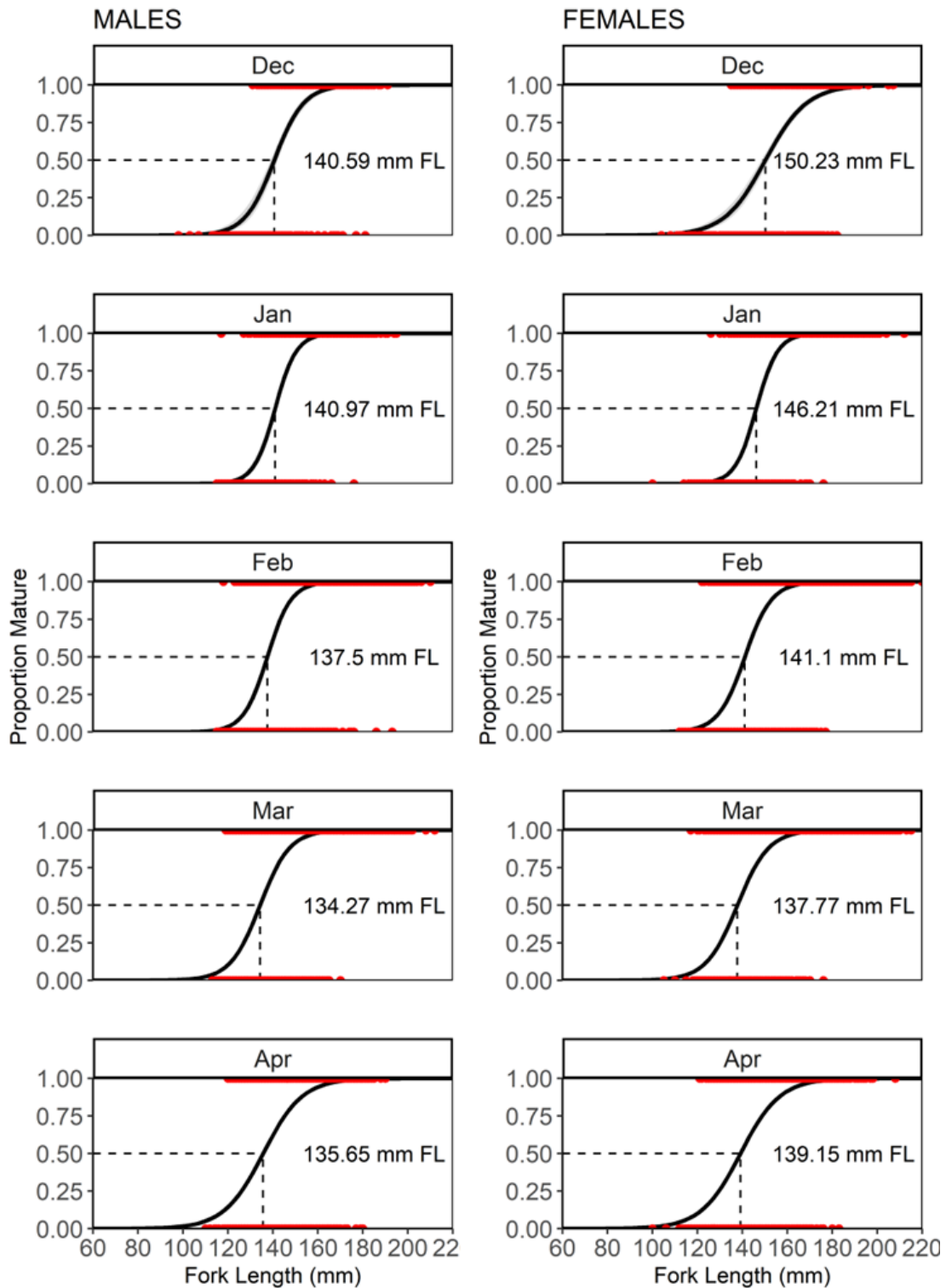
Figure 3-9. Size-at-maturity (L_{50}) for male and female Sardine collected from the two Gulf Zones (SG and GSV) per month over the spawning season (December to March and April) for all years combined. Red: length ranges for mature (top) and immature (bottom) fish included for each month.
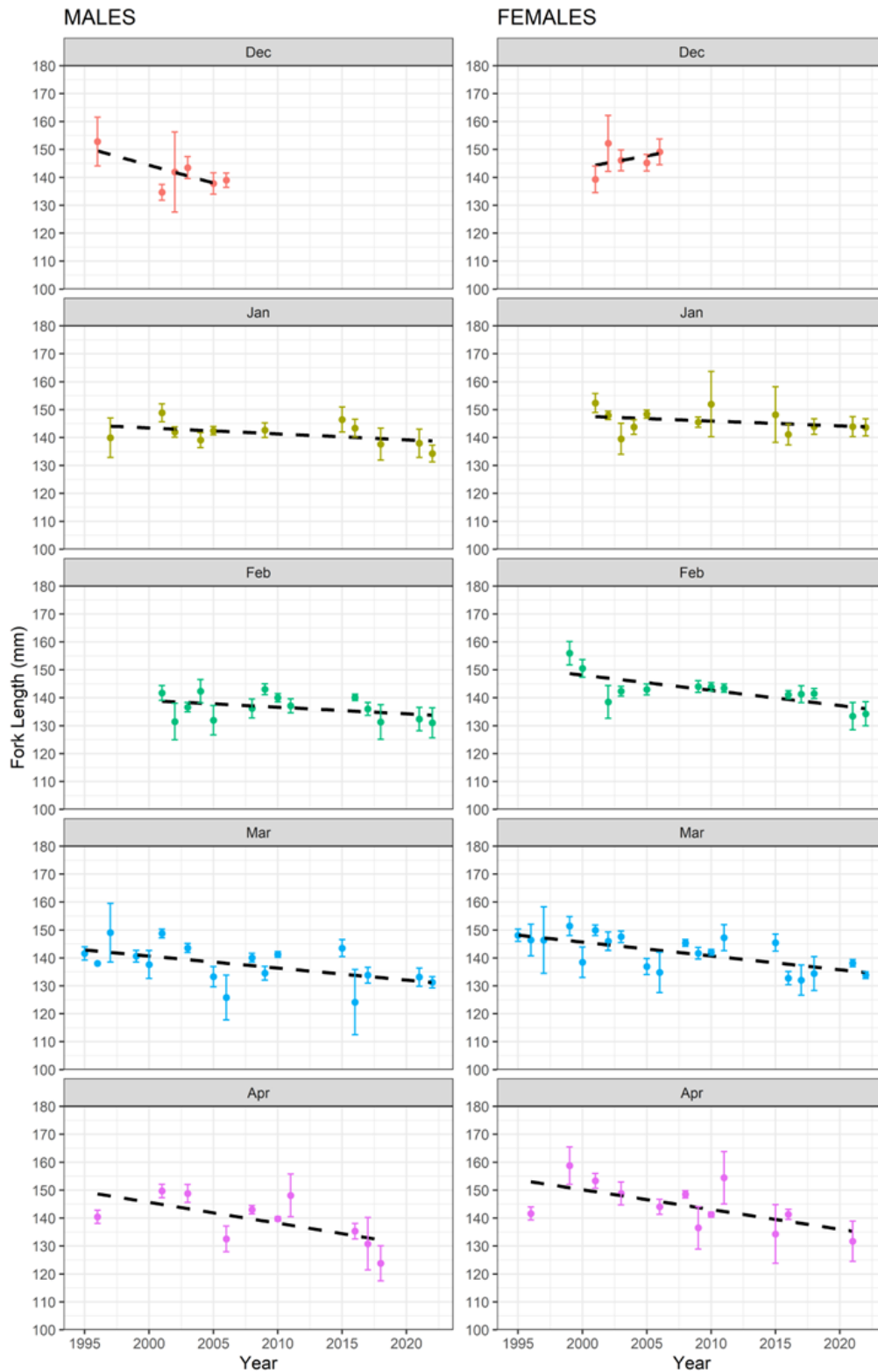
Figure 3-10. Size-at-maturity (L_{50}) for male and female Sardine collected in the two Gulf Zones (SG and GSV) per month by year, between 1995 and 2022. Some years were omitted due to low sample size and/or deteriorated samples. Error bars are 95% confidence intervals. Dashed lines represent the linear trend through time.

3.3.5　Gonadosomatic index (GSI)

There was a large amount of seasonal variability in GSI (Figure 3–9). However, sample size was variable, with sufficient samples obtained only from the two Gulf Zones in most years. GSI peaked between November and April (Figure 3–9). Higher mean GSI values were observed for males than females, which may be caused by male gonads not decreasing in size as much as females after each spawning event. Higher mean GSI values were also observed from larger fish.
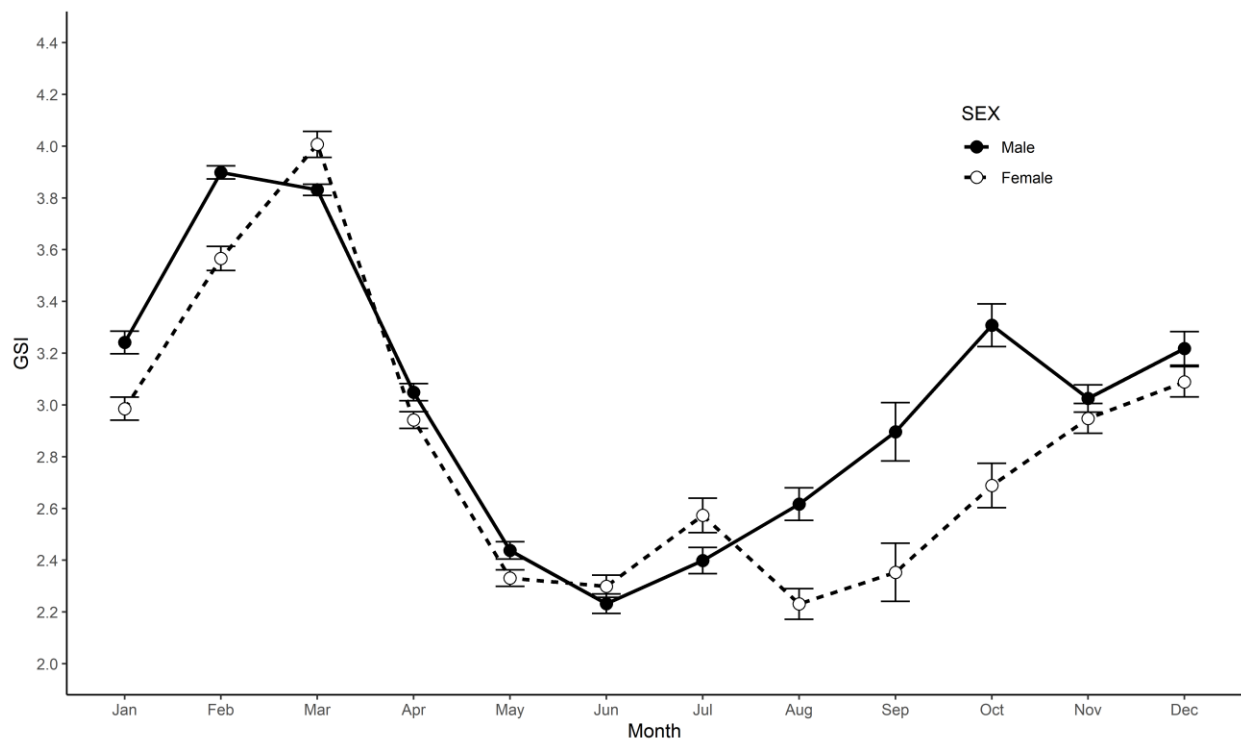
Figure 3-11. Mean monthly gonadosomatic index of male and female Sardine from commercial samples from the two Gulf Zones (SG and GSV) from 1995 to 2022, combined. Error bars are standard error. Fish below the size-at-maturity have been excluded.

3.4 Discussion

The relatively high level of uncertainty associated with estimating the age of Sardine from annual growth increments in otoliths has been noted elsewhere (Fletcher 1994, Rogers and Ward 2007). This issue can be partly overcome by using an age-otolith weight relationship developed from otoliths with high readabilities to estimate the age of Sardine with otoliths that are more difficult to read. This approach requires a relatively large number of otoliths to be read each year to provide adequate numbers of otoliths with high readability. This approach should be applied with caution as the relationship between otolith weight and fish age is relatively imprecise. The use of alternative approaches to assigning ages warrants consideration.

The growth rates of individual Sardine vary with age (Rogers and Ward 2007), with moderate to high growth rates occurring prior to sexual maturity, with slower growth rates as adults. Several studies have found that fish lengths have limited modal progression through samples, whereas cohorts could be tracked using otolith weight (Fletcher 1994, Rogers et al. 2004). This variability in growth rates limits the use of age-length keys for estimating the age of Sardine.

As discussed in the previous chapter (with respect to fish size), changes in management arrangements and fishing practices over the history of the fishery have driven changes in the sampled age composition of catches. As a result, age composition data from commercial catches are unlikely to be representative of the total population, and size/age selectivity have likely changed over time. The effects of these limitations of the age structure data need to be considered when interpreting the outputs of the population model (Chapter 5).

Despite these sampling limitations, a consistent pattern of the spatial distribution by size and age is emerging for the southern stock of Sardine. Sardine taken from the Gulf Zones are usually younger and smaller than those taken from the Outside Zone (Figure 2–9). However, smaller and younger fish have been regularly caught off the southeast coast of Kangaroo Island in the Outside Zone since 2017 (SARDI unpublished data). Sardine taken from the most northerly fishing grounds in the SG and GSZ Zones are also smaller and younger than those taken further south (Figure 2–9). These findings are consistent with observations for many species of small and medium-sized pelagic fishes (e.g. Australian anchovy, Jack Mackerel), where larger, older fish tend to be found in deeper waters and further offshore than smaller, younger fish (Dimmlich and Ward 2006, Sexton et al. 2017).

A coherent picture is also emerging in the temporal patterns in the size and age of Sardine taken from the Gulf Zones. In 1995, before the two mass mortality events, Sardine taken from Spencer

Gulf had a modal age of 3+ years. From 1996 to 1999, the modal age was reduced to 2+ years but re-stabilised at 3+ years from 2000 to 2005. However, the modal age of Sardine taken from Spencer Gulf fell to 2+ years in 2006, after 38,734 t were taken from the Gulfs Zone (SG +GSV) in 2005. The modal age increased to 3+ years in 2008, before falling to 2+ years in 2011. The modal age returned to 3+ years from 2012 onwards, when rules capping the catch from the Gulfs Zone (SG + GSV) were introduced. As mentioned in the previous chapter, the mean size of fish taken from the Gulfs Zone (SG +GSV) in 2019 dropped below the reference size of 142 mm FL and caused a reduction in TACC in 2020 from 30,000 t to 27,000 t for the SG Zone. The larger (older) size (age) structures of fish taken from the Gulf Zones since 2013 (except 2019) demonstrates the success of the size-based decision rules in reducing the capture of smaller-sized Sardine and preventing growth overfishing in the SASF.

The declining trend in L_{50} over the time series does not appear to be caused by a change in the size or age structure of the Sardine in the Gulf Zones, since there is no evidence that a similar change to the size or age structure has occurred. Uneven catch sampling across the spawning season may influence the decline but is unlikely to be the main driver, given the trend was still apparent when L_{50} was plotted by month across the time series. It is unclear if the change in L_{50} over time is a result of a genetic change to the population due to fishing (e.g. selectively targeting fish above the size at maturity; Rijnsdorp 1993, Grift 2003), a physiological response in the population to a change in environmental conditions (e.g. size at maturity declines with increasing water temperatures; Jonsson et al. 2013, Yoneda et al. 2015), or a combination of the two (Rijnsdorp 1993, Véron et al. 2020). Both scenarios warrant further investigation and consideration.

4.   SPAWNING BIOMASS OF SARDINE OFF SOUTH AUSTRALIA BETWEEN 1995 AND 2023

4.1 Introduction

This chapter present the time series of spawning biomass for Sardine off South Australia for the period from 1995 to 2023. Data from the spawning biomass survey in 2023 (Grammer and Ivey 2023) have been incorporated into the analyses. The estimates of spawning biomass are a key input into the population model in Chapter 5.

The Daily Egg Production Method (DEPM) was developed for stock assessment of the Northern Anchovy, *Engraulis mordax* (Parker 1980, Lasker 1985), and has been applied to more than 20 species of small to medium-sized pelagic fishes (e.g. Stratoudakis et al. 2006, Dimmlich et al. 2009, Neira et al. 2009, Grammer et al. 2022). The method is widely used in coastal fisheries because it is often the most practical option available for assessment of pelagic species (Ward et al. 1998). The DEPM has been used to estimate the spawning biomass of Sardine off South Australia since 1995 (Ward et al. 2021, Grammer and Ivey 2023).

The DEPM relies on the premise that spawning biomass can be calculated by dividing the mean number of pelagic eggs produced per day throughout the spawning area (i.e. total daily egg production) by the mean number of eggs produced per unit mass of adult fish (i.e. mean daily fecundity, Parker 1980, Lasker 1985). Total daily egg production is the product of mean daily egg production (P_0) and total spawning area (A). Mean daily fecundity is the product of mean sex ratio (by weight, R), mean spawning fraction (proportion of mature females spawning each day/night, S) and mean relative fecundity (number of eggs produced per gram of total female weight; F'). Spawning biomass (SB) is calculated according to the equation:

$$SB = P_0 * A/(R * S * F')$$ Equation 1

The DEPM, as applied to Sardine off South Australia, underwent a comprehensive review in 2020 (Ward et al. 2021). This review reanalysed data collected between 1995 and 2019 for South Australian Sardine and identified several ways to increase the precision of estimates of spawning biomass: 1) increase the precision of totally daily egg production (P_0*A) by using the estimate of P_0 obtained from all historical data rather than annual estimates of P_0; 2) continue to use the log-linear model to estimate P_0 for the Southern stock of Sardine; 3) increase the precision of mean daily fecundity ($R * S * F'$) by using the estimates of sex ratio (R), spawning fraction (S) and

relative fecundity (*F'*) obtained from all historical data rather than annual estimates; and 4) combine batch fecundity (*F*) and female weight (*W*) into a single parameter: relative fecundity (*F' = F̂/W*). The revised methods for the DEPM have been applied to estimates of spawning biomass for Sardine in South Australia since 2020 (Ward et al. 2021, Grammer et al. 2021, Grammer and Ivey 2023).

4.2 Methods

4.2.1 Total daily egg production

Ichthyoplankton surveys

Ichthyoplankton surveys have been conducted during the spawning season (January–April) of Sardine off South Australia since 1995. The surveys take about 28 days and have been done from the *RV Ngerin*. Surveys were undertaken every year between 1995 and 2023, except for 2008, 2010, 2012, 2015 and 2021. The orientation of transects and the number of sites sampled have varied among surveys (Figure 4–1). Changes in the area surveyed reflect the changes in the objectives of the sampling program over time. During 1995-97, the primary goal was to identify the main spawning grounds and develop an appropriate survey design. The sampling design and area sampled continued to be refined between 1998 and 2004, primarily to ensure that the spawning area was being covered (Figures 4–1). During 1995 and 1996, when the primary goal was to identify areas where Sardine spawned, transects were orientated from north to south and relatively few sites were sampled. After 1997, transects were orientated from north-east to south-west to improve sampling efficiency. From 1998 onwards, there has been a general increase in the number of sites sampled during each survey. From 2006 onwards, the number of sites sampled in Spencer Gulf has been doubled.

An adaptive approach to egg sampling has been applied since 2014 to ensure that each survey covered as much of the spawning area as possible (see Ward et al. 2017). Under this adaptive sampling protocol, additional samples have been taken at sites located outside the area covered by the historical pre-determined sampling sites (Figure 4–1). Decisions about whether to take additional samples were based on the presence/absence of eggs in samples taken using the Continuous Underway Fish Egg Sampler (CUFES) at sites located on the seaward end of transects. Sampling at additional sites continued until Sardine eggs were not present in the CUFES samples.
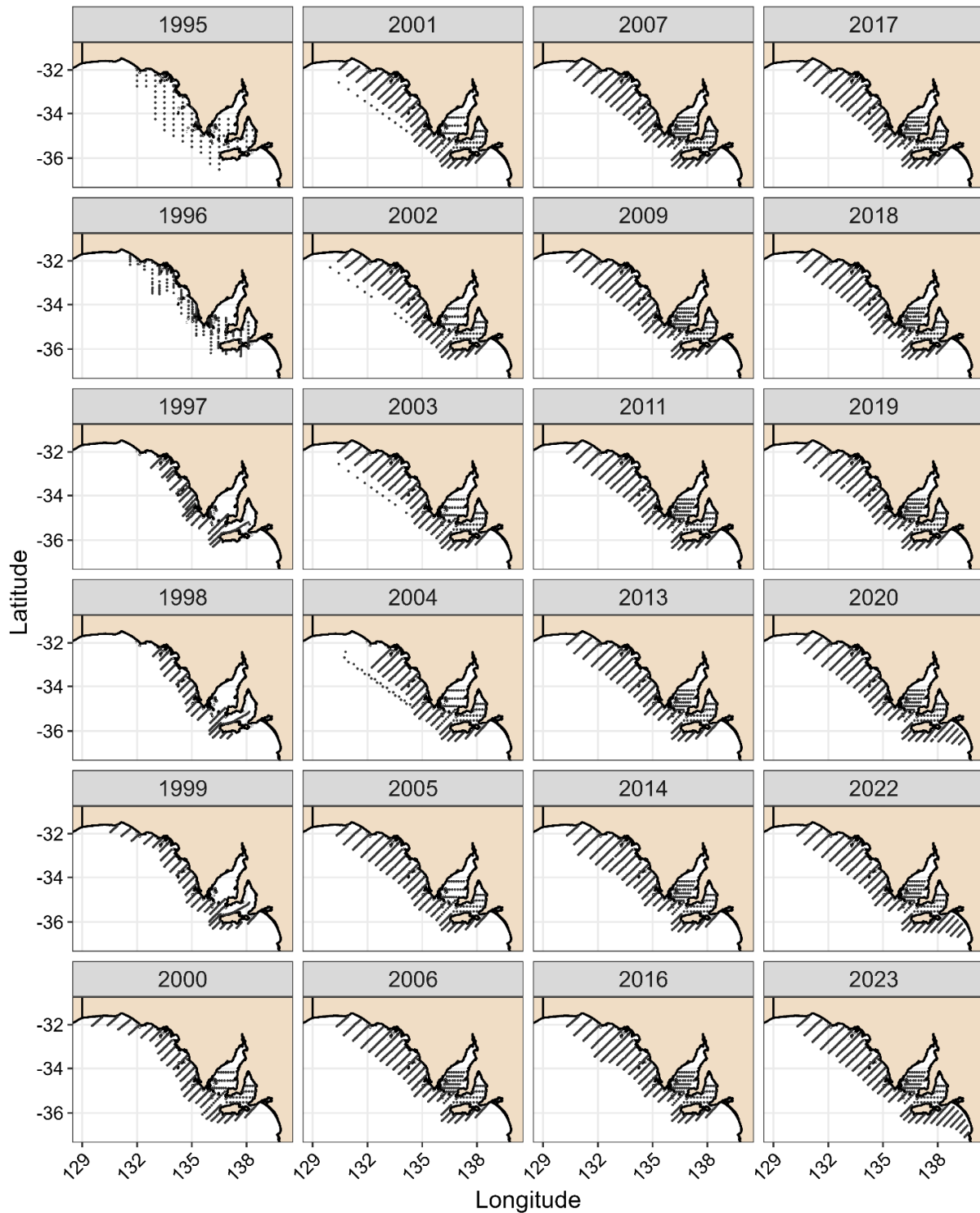
Figure 4-1. Location of sites sampled during ichthyoplankton surveys conducted off South Australia between 1995 and 2023.
Plankton sampling

Since 2020, an additional 62 sites have been added to the south-eastern end of the survey to the east of Kangaroo Island (6 transects) and along the outer end of transects in the GAB. The south-eastern sites were added in response to the expansion of the fishery into this region and recent observations that Sardine eggs had become more common in the area (Ward et al. 2020a; Figure 4-1).

Samples were collected at each site in each year shown in Figure 4-1 using paired Californian Vertical Egg Tow (CalVET) plankton nets. The CalVET nets have an internal diameter of 0.3 m, 330 µm mesh and plastic cod-ends. During each tow, the nets were deployed to within 10 m of the seabed at depths <80 m or to a depth of 70 m at depths >80 m. Nets were retrieved vertically at a speed of ~1 m.s^{-1}. A *Sea-Bird* Conductivity-Temperature-Depth (CTD) profiler attached to the CalVET nets was used to measure oceanographic parameters (e.g. temperature, salinity, fluorescence) at each site. General Oceanics™ flowmeters were used to estimate the distance travelled by each net. Samples from the two cod-ends were combined and stored in 5% buffered formaldehyde and seawater solution.

Egg identification and staging

Sardine eggs were identified using published descriptions (Neira et al. 1998, White and Fletcher, 1998). Eggs were staged based on the descriptions by White and Fletcher (1998). Total counts of eggs of each developmental stage in each sample were recorded. Eggs in the first and last stages were excluded from the statistical analyses because they can be under- and over-represented in plankton samples, respectively (Ward et al. 2018).

Egg ageing, treatment of zero count egg samples and egg density

The development rate of Sardine eggs is dependent on ambient water temperature (Picquelle and Stauffer 1985, Pauly and Pullin 1988). Based on the temperature data from the CTD, egg samples were allocated to one of three temperature bins that covered the range of temperatures encountered during surveys (14–18°C, 18–22°C, and 22–26°C). The temperature bins were comparable to those used by Le Clus and Malan (1995) to describe the developmental rates of Sardine eggs. These published development rates were used to assign a mean age to each egg in each sample (see Ward et al. 2018).

After each egg was assigned an age, the eggs in each sample were grouped into daily cohorts. This was done because a sample usually included eggs spawned on more than one night. The total number of eggs in each daily cohort was calculated by summing the number of eggs of each

stage assigned to a spawning day (i.e. day 0, day 1, day 2). The age of a daily cohort was calculated from the average age of each stage within the daily cohort, weighted by the number of eggs in each stage.

Samples with eggs could contain several possible combinations of daily cohorts depending on water temperature, spawning time (peak around 2:00 am) and sampling time. Zero counts were allocated for daily cohorts where the cohort was expected to be present but was not found within the sample (Ward et al. 2018). Samples with no eggs were excluded from the analyses and not considered part of the spawning area.

The number of eggs of each stage under one square metre of water (P_t) was estimated at each site according to Equation 2 (Table 4-1).

Table 4-1. Equations used when applying the DEPM to estimate the spawning biomass of Sardine.

Calculation	Equation	Eq. no.	Parameters	Reference
Egg Density (sample)	$P_s = \dfrac{C\,D}{V}$	2	P_s: density of eggs in a sample C: number of eggs of each age in each sample V: volume of water filtered (m^3) D: depth (m) of net cast	Smith and Richardson (1977)
Negatively biased estimate (P_b)	$\ln P_b = \ln(P_{i,t} + 1) - Zt$	3	P_b: negatively biased P_0 $P_{i,t}$: density of eggs of age t at site i z: instantaneous rate of daily egg mortality	Picquelle and Stauffer (1985)
Bias corrected (P_0)	$P_0 = e^{\left(\ln P_b + \sigma^2/2\right)} - 1$	4	P_b: negatively biased estimate of daily egg production σ^2: variance of P_b estimate	Wood (2006), Ward et al. (2011, 2018)
Generalised Linear Model (GLM) with negative binomial error structure	$E[P_0] = g^{-1}(-zt + \varepsilon)$	5	$E[P_0]$: expected value of P_0 g^{-1}: inverse-link function zt: the instantaneous rate of daily egg mortality at age t ε: error term	Wood (2006), Ward et al. (2011, 2018)
Female Weight	$W = \left[\dfrac{\overline{W_i\,n_i}}{N}\right]$	6	$\overline{W}_i$: mean female weight of each sample i; n: number of fish in each sample N: total number of fish collected in all samples	Lasker (1985)
Sex Ratio: sample	$\overline{R}_i = \dfrac{F_i}{F_i + M_i}$	7	F_i: total weight of mature females in each sample i M_i: total weight of mature males in each sample i	Lasker (1985)
Sex Ratio: population	$R = \left[\dfrac{\overline{R_i\,n_i}}{N}\right]$	8	$\overline{R}_i$: mean sex ratio of each sample i n: number of fish in each sample i N: total number of fish collected in all samples	Lasker (1985)
Spawning Fraction: sample	$\overline{S}_i = \dfrac{d0 + d1 + d2}{3\,n_i}$	9	$d0$, $d1$ and $d2$: the number of mature females with POFs aged day 0, 1 or 2 in each sample n_i: is the total number of females within a sample.	Lasker (1985)
Spawning Fraction: population	$S = \left[\overline{S}_i * \dfrac{n_i}{N}\right]$	10	$\overline{S}_i$: mean spawning fraction of each sample i n: number of fish in each sample i N: total number of fish collected in all samples	Lasker (1985)

Spawning area

The spawning area (*A*) was estimated for each survey (Lasker 1985, Somarakis et al. 2004) using the Voronoi natural neighbour method (Watson 1981). The survey area was divided into a series of contiguous polygons approximately centred on each site using the 'deldir' package in the statistical program R (R Core Team 2023, Turner 2023). The area represented by each site (km^2) was calculated. *A* was defined as the total area of the polygons where live Sardine eggs were present in the plankton sample (see Fletcher et al. 1996).

Mean Daily Egg Production (P_0)

The underlying model used to calculate mean daily egg production (P_0) was the exponential egg mortality mode with a bias correction factor (the 'log-linear model'). A linear version of the exponential egg mortality model was fitted to estimates of egg age and density for each daily cohort at each site (Picquelle and Stauffer 1985; Equation 3, Table 4-1).

Estimates of P_b from the log-linear version of the exponential mortality model have a negative bias, therefore a bias correction factor was applied (Equation 4, Table 4-1). This equation is hereafter referred to as the 'log-linear model'.

A general linear model (GLM) with a negative binomial error structure (NB1), was also used to estimate P_0 (Equation 5, Table 4-1). The negative binomial error structure used is considered suitable for over-dispersed data, such as egg density by age (e.g. Ward et al. 2011, 2018, 2021). For NB1, variance increased linearly with the mean ($\sigma = \mu*(1+ \mu +\varphi)$), where μ is the model estimate, σ is the model variance and φ is the over-dispersion parameter. The GLM used a log-link function (Wood 2006) and was fit using the glmmTMB R package (Brooks et al. 2017).

Estimates of P_0 and *z* obtained by fitting the two models to egg data collected each year and to data obtained in all years from 1998 to 2023 (combined) are presented in Appendix A (Table A3).

4.2.2 Mean daily fecundity

Adult parameters

Adult parameters used to calculate spawning biomass are derived from all adult samples of Sardine collected for DEPM surveys off South Australia between 1995 and 2018 (see Ward et al. 2021).

Adult sampling

Mid-water trawling and sampling from commercial catches undertaken during 1995–1997 did not provide samples suitable for estimating adult reproductive parameters of Sardine off South Australia. The lack of reliable estimates of these adult parameters reduced the reliability of estimates of spawning biomass obtained during this period (e.g. Ward et al. 2001a).

From 1998 to 2018, samples of mature Sardine were collected from sites located in the eastern Great Australian Bight, southern Spencer Gulf and Investigator Strait using a gill-net (Figure 4–2). In the late afternoon, a dual frequency echo sounder (60 and 180 KHz) was used to search areas where schools of adult Sardine were known to aggregate. A gillnet comprised of three panels, each with a different multi-filament nylon mesh size (see Ward and McLeay 1998) was deployed from the port side of the *RV Ngerin* at protected locations where schools were encountered. Surface and sub-surface lights (150 W) were illuminated near the net after it was set. Net soak times varied from 15 minutes to 3 hours depending on the number of fish caught.

After the net was retrieved, fish were removed and dissected immediately. All Sardine collected were counted and sexed. Mature males and immature fish were frozen. Mature females were fixed in 10% buffered formaldehyde seawater solution.
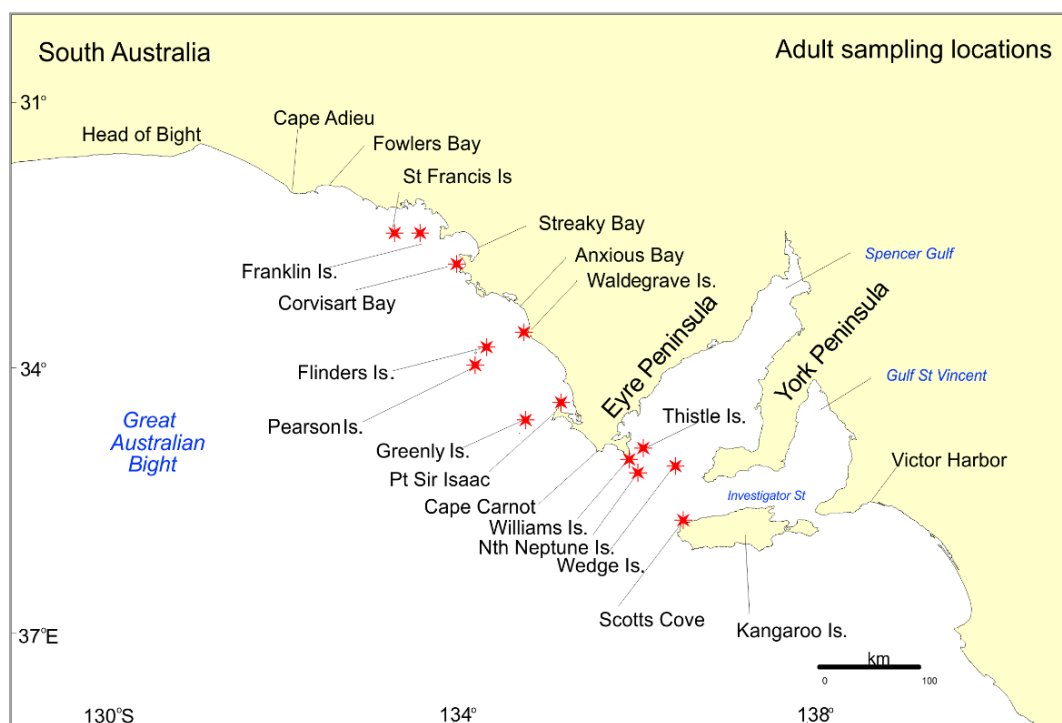
Figure 4-2. Location of sampling sites for adult Sardine off South Australia.

Female weight (W) and Male weight

Mature females from each sample were removed from the formalin solution and weighed (± 0.01 g). Fixation in formalin has a negligible effect on fish weight (Lasker 1985). The mean weight of mature females in the population was calculated from the average of sample means weighted by proportional sample size (Equation 6, Table 4-1). Mature males in each sample were thawed and weighed (± 0.01 g).

Sex ratio (R)

The mean sex ratio of mature individuals in the population was calculated from the average of sample means weighted by sample size (Equations 7 and 8, Table 4-1).

Spawning fraction (S)

Ovaries of mature females were sectioned and stained with haematoxylin and eosin. Several sections from each ovary were examined to determine the presence/absence of post-ovulatory follicles (POFs). POFs were aged according to the criteria developed by Hunter and Goldberg (1980) and Hunter and Macewicz (1985). The spawning fraction of each sample was estimated as the mean proportion of females with hydrated oocytes plus day-0 POFs ($d0$) (assumed to be spawning or have spawned on the night of capture), day-1 POFs ($d1$) (assumed to have spawned the previous night) and day-2 POFs ($d2$) (assumed to have spawned two nights prior). The mean spawning fraction of the population was then calculated from the average of sample means weighted by proportional sample size (Equations 9 and 10, Table 4-1).

Batch fecundity

Batch fecundity (F) was estimated from ovaries containing hydrated oocytes using the methods of Hunter and Macewicz (1985). Both ovaries were weighed and the number of hydrated oocytes in three weighed ovarian sub-sections counted. The total batch fecundity for each female was calculated by multiplying the mean number of oocytes per gram of ovary segment by the total weight of the ovaries. Methods to estimate the batch fecundity for mature females without hydrated ovaries ($\hat{F}$) followed those of Ward et al. (2021).

Relative Fecundity (F') was calculated by dividing batch fecundity ($\hat{F}$) determined from all years data (1998-2018) by total female weight (W).

4.2.3 Spawning biomass

Spawning biomass was calculated using the all-years estimate of P_0 (1998 to 2023) obtained from the log-linear model, spawning area (A) in each year and estimates of S, R and F' obtained from adult samples collected between 1998 and 2018.

The reliability of model fits, 95% confidence intervals (CIs) and coefficients of variation (CVs) for P_0 were estimated using bootstrap resampling methods with 10,000 iterations. Coefficients of variation and CIs for R, S, F, W and F', were calculated from the all-years adult data. *A* ratio estimator was used calculate the variance for S, R, and F' (Rice 1995). The variance for the spawning biomass estimates were calculated by summing the squared CVs for each parameter and multiplying by the square of the estimate of spawning biomass (Parker 1985). Uncertainty estimates presented for all parameters are 95% CIs. Data analyses were done in the R programming environment (R Core Team 2023).

4.3 Results

4.3.1 Total daily egg production

Total area sampled

The total area sampled during the ichthyoplankton surveys varied from 48,379 km^2 in 1998 to 136,471 km^2 in 2023 (Figure 4–3). Differences in the area surveyed between 1995 and 2004 reflect changes in the objectives of the sampling program over this period (i.e. identify main spawning grounds and develop/refine appropriate survey design). The total survey area was stable at about 119,000 km^2 between 2006 and 2013. Total survey area increased in 2014 to 125,249 km^2, after the adaptive sampling protocol was implemented in response to the incomplete coverage of the spawning area in 2013 (Figure 4–4). Since 2020, the survey has expanded to 136,471 km^2 in 2023 (Grammer and Ivey 2023) to include shelf waters between Kangaroo Island and Kingston, South Australia in response to an expansion of the fishery into this area (Figure 4–1, 4–4). Adaptive sampling remains a key element of the current survey design and is also a reason the total survey area varies slightly from year to year.
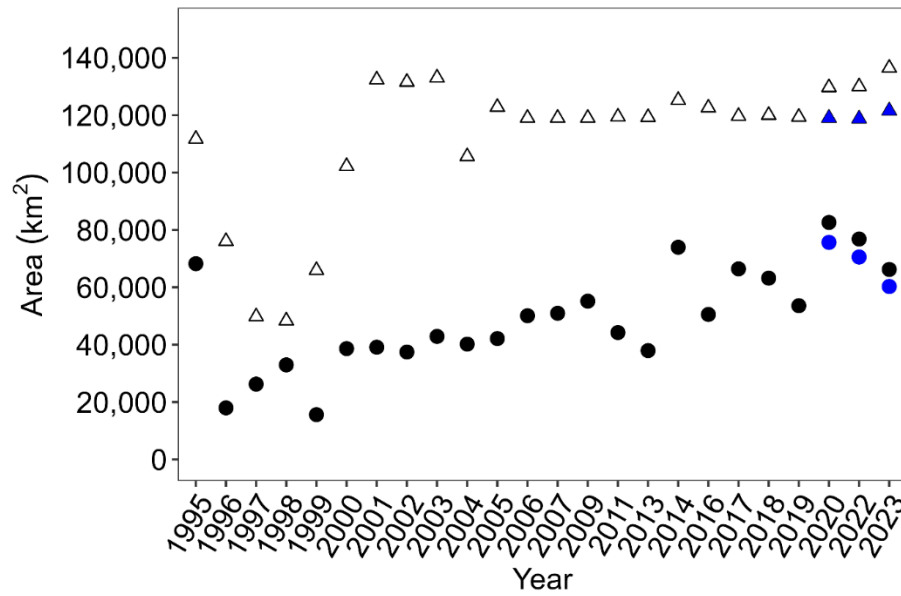
Figure 4-3. Total area sampled (km^2) (triangles) and corresponding spawning area (A, km^2) (circles) for DEPM surveys between 1995 and 2023. For comparison: blue points for A in 2020, 2022 and 2023 exclude additional sites added since 2020.

Spawning area (A)

Estimates of spawning area varied among years and reflected both the size of the survey area and the spawning biomass. The spawning area declined substantially following the two mass mortality events, from 68,260 km^2 in 1995 to 17,990 km^2 in 1996 and from 32,980 km^2 in 1998 to 15,637 km^2 in 1999 (Figure 4-3). Between 2000 and 2005, the spawning area remained between 37,000 and 42,200 km^2, before increasing to >50,000 km^2 from 2006 to 2009. In 2011 and 2013, the spawning area was below 45,000 km^2, but the 2013 survey did not cover the entire spawning area as the stock had moved offshore. Spawning area increased to 73,900 km^2 in 2014 and remained above 50,000 km^2 from 2015 to 2019 (Figure 4–3). Spawning area peaked at 82,600 km^2 in 2020. The spawning area in 2023 was 66,248 km^2, which was lower than the spawning areas in 2020 and in 2022 (76,842 km^2; Grammer and Ivey 2023). Excluding the additional sites added since 2020 results in a spawning area of 60,300 km^2 for 2023, which is the sixth highest on record for South Australian Sardine (Figure 4–3).
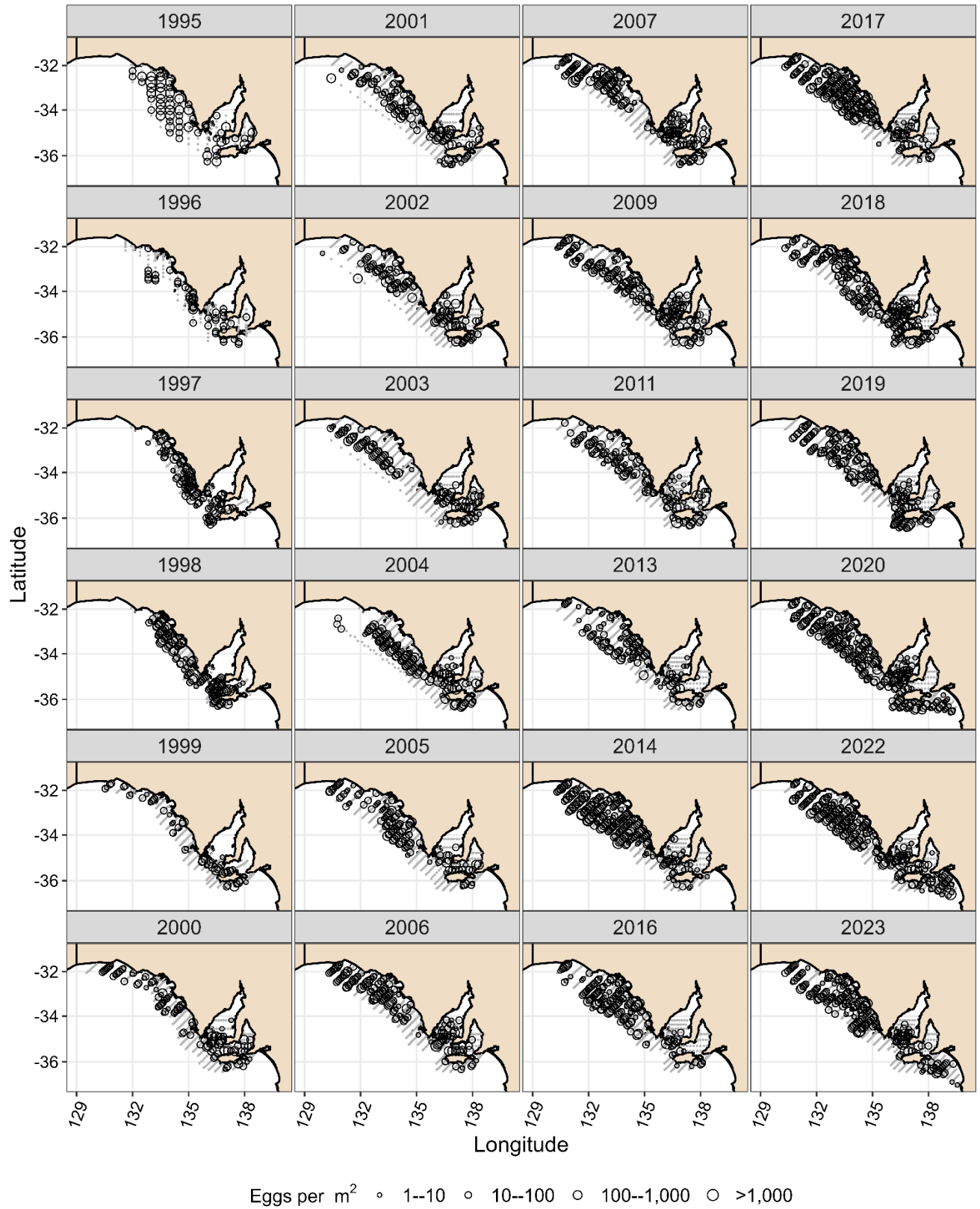
Figure 4-4. Distribution and abundance of Sardine eggs collected during surveys between 1995 and 2023.

Egg distribution and abundance

The distribution and abundance of Sardine eggs has varied considerably among years. Areas where large numbers of eggs are sometimes found include shelf waters of the eastern Great Australian Bight, between Coffin Bay and the Head of Bight, southern Spencer Gulf, and the western end of Investigator Strait (Figure 4–4). Large numbers of eggs regularly occur to the south and east of Kangaroo Island. Mass mortality events in 1995 and 1998 reduced both the total abundance of eggs and their spatial distribution off South Australia (see Ward et al. 2001a). The presence of eggs into offshore waters in 2013 was a major change from the historical patterns.

Mean daily egg production (P_0)

The estimate of P_0 obtained by fitting the log-linear model to all data from 1998 to 2023 was 84.1 (95% CI: 75.9–93.0) eggs.day^{-1}.m^{-2} (Grammer and Ivey 2023). The estimate of P_0 obtained by fitting GLM NB1 to all data from 1998 to 2020 was 99.3 (95% CI: 84.9–116.9) eggs.day^{-1}.m^{-2} (Grammer and Ivey 2023). Estimates of P_0 for individual years (log-linear model) ranged from 39.0 in 2013 to 145.3 in 2004 (Table A3).

4.3.2 Adult parameters

Mean female weight

The mean weight of mature females (W, 95% CI) estimated from 16,995 fish (255 samples) collected between 1998 and 2018 was 58.4 g (23.1–93.7) (Ward et al. 2021). Estimates of W for individual years ranged between 46.5 g in 1998 and 78.7 g in 2004 (Table A3).

Sex ratio

The mean sex ratio by weight (R, 95% CI) calculated from all fish collected between 1998 and 2018 was 0.55 (0.52–0.58) (Ward et al. 2021). Estimates of R for individual years ranged from 0.36 in 2009 to 0.70 in 2018 (Table A3).

Batch fecundity

Between 1998 and 2018, 1,099 females with hydrated oocytes were collected (Ward et al. 2021). The fecundity-weight relationship estimated from these samples was: Batch Fecundity = 335 × Gonad Free Female Weight – 797 (R^2 = 0.53) (Ward et al. 2021). Mean gonad free female weight

between 1998 and 2018 was 55.5 g and ranged between 43.2 and 75.0 g (Table A3). Overall mean batch fecundity ($\hat{F}$, 95% CI) was 17,835 (3,790–31,880) oocytes (Table A3).

The overall estimate of F' was 305.4 (95% CI: 304.2–306.6) eggs.g^{-1} (Ward et al. 2021). Estimates of F' for individual years ranged from 295.9 eggs.g^{-1} in 2000 to 312.9 eggs.g^{-1} in 2011 (Table A3).

Spawning fraction

The spawning fraction (S, 95% CI) calculated from all data collected between 1998 and 2018 was 0.108 (0.100–0.119) (Ward et al 2021). A total of 16,334 ovaries were examined; 2,578 had day-0 POFs or hydrated oocytes, 1,540 had day-1 POFs and 1,046 day-2 POFs (Ward et al. 2021). Estimates of S for individual years ranged from 0.041 in 2014 to 0.179 in 2001 (Table A3).

4.3.3 Spawning biomass

Estimates of spawning biomass obtained through the application of the DEPM over time were improved by the re-analysis of historical data (Ward et al. 2021). In particular, the estimates of adult parameters obtained from data collected from 1998 to 2018 helped to resolve uncertainties in estimates of mean daily fecundity for 1995 to 1997 that were driven by the limited number of adult samples collected during this initial period. Similarly, the preliminary estimates of P_0 obtained from the limited plankton sampling undertaken in the early years of this time series were likely improved by applying refined analytical methods.

The overall estimate of P_0 (84.0 eggs.day^{-1}.m^{-2}; log-linear model) was updated for 2023 using egg data collected during the 2023 DEPM survey. The annual estimates of spawning biomass were also updated using this new value of P_0 (Figure 4–5). In 1995, prior to the two mass mortality events, spawning biomass was approximately 320,000 t. Spawning biomass fell to 84,000 t in 1996 and 73,000 t in 1999 following the events, but recovered rapidly to 180,000 t in 2000 and then 260,000 t in 2009 (Figure 4–5). The relatively low estimate of spawning biomass in 2013 largely reflects the incomplete coverage of the spawning area in that year. Since the adaptive approach to sampling was adopted in 2014, estimates of spawning biomass have been above 230,000 t. Spawning biomass peaked in 2020 at approximately 380,000 t and estimates have been greater than 300,000 t since then. The estimate of spawning biomass for 2022 was 355,075 t (299,956–410,193 t) (Grammer and Ivey 2022). In 2023, spawning biomass was estimated to be 307,881 t (260,468–412,113 t), which is comparable to estimates since 2014 (Figure 4–5; Grammer and Ivey 2023). The estimate for 2023 calculated using the value of A without the stations added since 2020 was 280,239 t (Grammer and Ivey 2023).
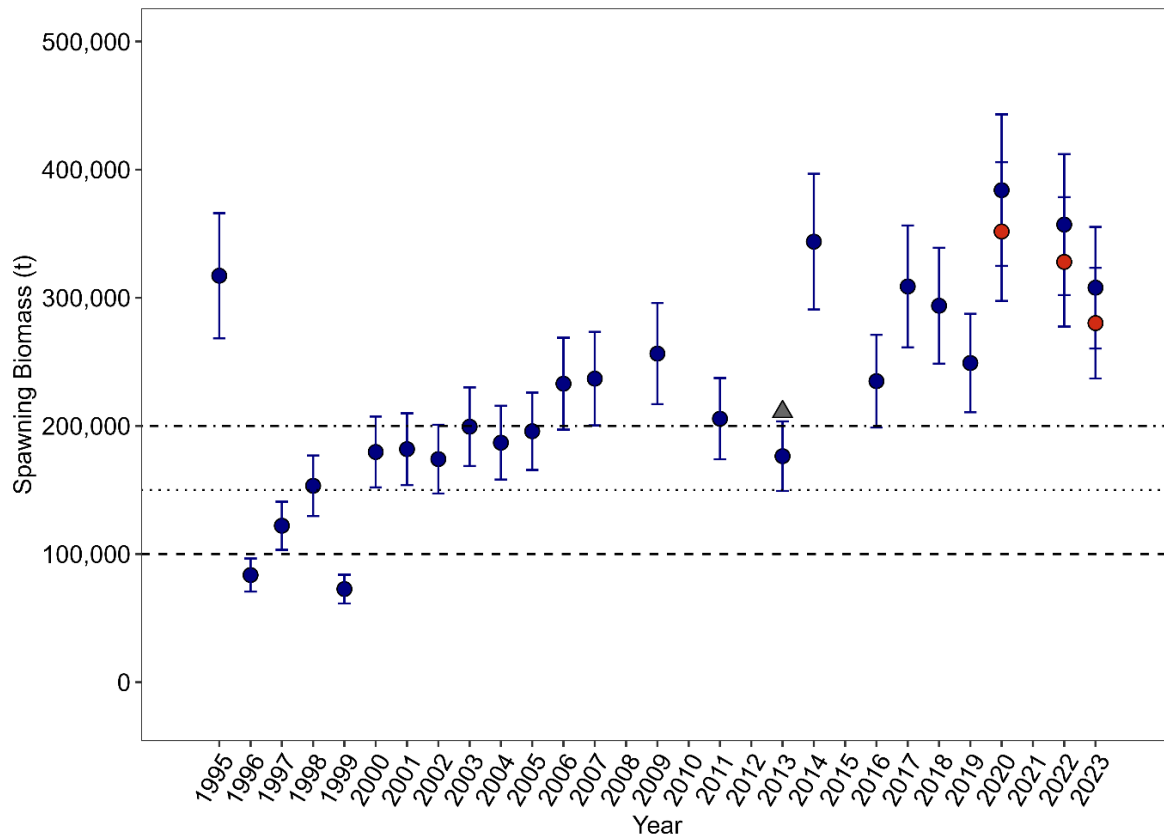
Figure 4-5. Estimates of spawning biomass (95% CI) for Sardine off South Australia from 1995 to 2023 using the Daily Egg Production Method (DEPM). Adult parameters were estimated from data obtained during 1998-2018 (Ward et al. 2021). Spawning area (*A*) was estimated annually. The log-linear model was used to estimate mean daily egg production (P_0) from data collected between 1998 and 2023. The red circles for 2020, 2022 and 2023 are the estimate of spawning biomass obtained using estimate of *A* without the additional stations added since 2020. The triangle for 2013 (when the survey did not cover the entire spawning area) is the estimate of spawning biomass using the mean *A* from 2002 to 2011 (45,406 km^2). The horizontal lines indicate the 100,000 t (dash), 150,000 t (dotted) and 200,000 t (dash/dot) reference points in the harvest strategy (PIRSA 2023).

4.4 Discussion

The DEPM has been integral to the rapid and sustainable development of the SASF. The information about the size of spawning stock of Sardine in waters off South Australia provided by the DEPM has underpinned the growth of the fishery. Estimates of spawning biomass obtained during the first few years when the method was applied off South Australia were uncertain, due to limited understanding of key parameters, especially mean daily egg production (P_0) and spawning fraction (S) (e.g. Ward et al. 2001a, 2011). Improved knowledge obtained over the last two decades provided a valuable opportunity to re-evaluate how the size of the population has fluctuated over time and develop recommendations about how the method should be applied (see Ward et al. 2021). Those recommendations have been implemented since 2020 to ensure that future estimates of spawning biomass are as accurate and precise as possible (e.g. Grammer et al. 2021, Grammer and Ivey 2022, 2023)

The revised estimate of spawning biomass for 1995 of approximately 320,000 t provides a useful proxy for unfished spawning biomass (see Chapter 5). Similarly, the estimates of spawning biomass of about 84,000 t in 1996 t and 73,000 t in 1999 provide useful insights into the likely impacts of the two mass mortality events on the adult population. The increase in the spawning biomass from about 180,000 t in 2000 to 260,000 t in 2009 shows how quickly the population recovered from the two mortality events. The low estimate of spawning biomass in 2013 largely reflects the failure of that year's survey to cover the entire spawning area. Since the adaptive approach to sampling was adopted in 2014, estimates of spawning biomass have been consistently above 230,000 t. Spawning biomass peaked in 2020 at approximately 380,000 t and estimates have been greater than 300,000 t since then. In 2023, spawning biomass was estimated to be 307,881 t (260,468–412,113 t), which is comparable to estimates since 2014.

Previous studies have shown that Sardine abundance is strongly correlated with spawning area (Mangel and Smith 1990, Gaughan et al. 2004). Spawning area has been confirmed as a good proxy for the abundance of adult Sardine off South Australia (Ward et al. 2021). Using historical data to estimate all DEPM parameters except spawning area means that fluctuations in estimates of spawning biomass are driven entirely by changes in the measure of spawning area. As a result, future surveys must cover as much of the spawning area as possible and should continue to involve the adaptive approach to sampling that has been in place from 2014 onwards. The total area surveyed in 2023 of 136,471 km^2 was the largest to date. The estimate of spawning area in 2020 of 82,627 km^2 was the highest on record. Spawning area has been consistently above 50,000 km^2 since the previous peak at 73,981 km^2 in 2014. The reduction in spawning area in

2023, compared to 2020 and 2022, is likely due to changes in environmental conditions in the region related to warmer sea surface temperatures, high densities of zooplankton, and the freshwater influence of the 2022/2023 River Murray flood event (Grammer and Ivey 2023). The spawning areas observed in both 2022 (76,841 km^2) and 2023 (66,248 km^2) provide strong evidence that Sardine continue to be widespread and abundant off South Australia in 2023.

Inter-annual variability in estimates of P_0 is low compared to statistical uncertainty (imprecision) for Sardine off South Australia (e.g. Ward et al. 2020b, 2021). The estimate of P_0 obtained by adding data from each additional DEPM survey (e.g. 2022, 2023) to all historical data was more precise (SD = 4.3) than the estimate obtained using data from a given year only (e.g. 2023: SD = 26.1). Using historical data to estimate of P_0 prevents large inter-annual fluctuations in estimates of spawning biomass driven by variations in the annual estimates of this parameter caused by statistical uncertainty. However, it is critical that P_0 continue to be monitored annually to look for changes in the parameter over time to reduce the risk of over- or under-estimating spawning biomass (e.g. the basin hypothesis of McCall 1990) (Ward et al. 2021). In future applications of the DEPM to Sardine off South Australia, P_0 should continue to be estimated using data obtained in all years since 1998, as well as within each year.

Re-analysis of adult samples of Sardine collected off South Australia since 1998 suggest that both individual parameters and mean daily fecundity are relatively stable among years, especially when inter-annual variability is evaluated within the context of potential sources of statistical uncertainty (i.e. precision and bias) (Ward et al. 2021). Large variations among years observed in the estimates of the adult parameters are more likely to reflect the limitations of the adult sampling program, rather than actual differences among years in the reproductive patterns of the population (Ward et al. 2021). Therefore, in the foreseeable future, adult parameters used to calculate the spawning biomass of Sardine off South Australia should be estimated from data obtained in all adult surveys conducted since 1998.

Adult reproductive parameters of Sardine off South Australia were not correlated with spawning area, and correlation would have suggested density dependent effects had occurred (Ward et al. 2021). Detecting changes in the adult population of Sardine over time due to environmental conditions or density dependent effects is important. Adult sampling is costly and logistically challenging, yet necessary. In recent years (since 2018), completing a successful ichthyoplankton survey that covers the entire spawning area has taken precedence over adult sampling. Detecting any changes in key adult parameters of Sardine, such as spawning fraction (*S*), is critical since

errors when estimating these parameters have major implications for estimates of spawning biomass (Ward et al. 2021). To mitigate this risk, an extensive adult sampling program will be conducted in 2024 and repeated periodically (e.g. every 3-5 years) to determine if changes in key adult parameters have occurred.

5.   STOCK ASSESSMENT MODEL

5.1 Introduction

This chapter describes the application of the stock assessment model, SardEst, developed specifically for the SASF (Ward et al. 2020b). In 2019, this model superseded the Stock Synthesis model (the SS model) used in previous assessments (Ward et al. 2015, 2017, 2020a).

SardEst is based on a single stock, single fleet and single area, and fits to commercial catch data (Chapter 2), fishery-dependent age-composition data (Chapter 3) and fishery-independent estimates of spawning biomass obtained using the DEPM (Chapter 4). Biological parameters (e.g. growth, maturity and weight-at-age) are estimated externally from fishery-dependent and fishery-independent data (Chapter 3). Model specifications are detailed in Appendix B.

The SardEst model presents three distinct features compared to other models previously used: 1) recruitment is estimated at age one, as deviations to an average value ($\bar{R}$) that are fit as random effects, 2) natural mortality (M) is freely estimated as a time and age invariant parameter rather than being assumed, and 3) the mass mortality events of 1995 and 1998 are explicitly estimated using increased natural mortality (M) in those years. SardEst is built in Template Model Builder (TMB), which is a contemporary, auto-differentiation program that incorporates random effects (Kristensen et al. 2016). This approach provides better estimates of recruitment deviations that are explicitly recognised as random processes that vary annually about $\bar{R}$ (Thorson et al. 2014). Improved estimates of recruitment are important as they ensure the model provides better estimates of annual fishing mortality (F) and natural mortality in 1995 and 1998, when the mass mortality events occurred (Ward et al. 2001b).

The 2019 SardEst model version (Ward et al. 2020b) was externally reviewed by CSIRO in 2020 (Hillary 2020). The review indicated that SardEst was a clear improvement on the previous SS model (Ward et al. 2015, 2017, 2020b), but made a series of recommendations to continue model improvement: 1) clarify whether selectivity is being fixed or estimated; 2) correct a misspecification of the catch-at-age likelihood; and 3) apply data weightings consistent with agreed best practice. Implementation of these recommendations began in 2021 and have been continued in the current stock assessment (Grammer et al. 2021, Appendices B and C). During implementation of these recommendations, a coding error was introduced, which was detected and corrected in the application of the SardEst model for this assessment. It occurred when sample size was being incorporated into the age-composition multinomial likelihood and has been corrected in the

current version of SardEst (see Appendix C for details). Thus, some model outputs from the previous assessment (Grammer et al. 2021), whilst not significant, will differ from those presented here.

5.2 Methods

5.2.1 Base-case model

Model structure

The SardEst model is age-structured and sex-independent and assumes a single area fleet and stock for the SASF. The 2022 model includes data from the commencement of the fishery to present (1992 to 2022 by calendar year). Age-composition data were available from 1995–2022 except for 2007. Therefore, predicted catch-at-age in 2007 are not fitted to data. Spawning biomass estimates are available from 1995–2022 but are not available in 2008, 2010, 2012, 2015 and 2021 when surveys were not undertaken. Therefore, spawning biomass is not fitted to data in those years. As SardEst is a single sex model, spawning biomass includes both males and females. The model time step is annual.

SardEst uses the Hybrid *F* method to determine fishing mortality (*F*) which is also implemented by SS (Methot 2000). It is called 'hybrid' as it combines the best features of the standard Pope-approximation catch-conditioned models and effort-conditioned Baranov models. It assumes exponential survival within each time step of Baranov, but rather than setting *F* proportional to fishing effort, it computes the Baranov *F* that is needed to remove the exact reported catch across each model time step. The survival of Sardine in each age class is then adjusted with these estimates of *F* and fitted to fishery age-composition data and DEPM estimates of spawning biomass. The advantage of this approach is that it reduces the number of parameters estimated by the model (no catchability is defined), while giving exact reported catch removals (Methot 2000).

Biological and fishery parameters

The biological parameters (i.e. growth and maturity) used in the models were based on information presented in previous chapters. Previous analyses have found no significant temporal changes to these parameters during the history of the fishery, or that there has been insufficient sampling to detect inter-annual variations (Ward et al. 2010, 2012, 2015, 2017, 2020a, Grammer

et al. 2021). Each parameter was fixed at historical values and held constant in the stock assessment model.

Growth was assumed to follow the von Bertalanffy growth function with sex-independent parameters (Table 5-1). Sex specific weight-length relationships were derived from both commercial and fishery-independent samples. An allometric relationship of the form $W = A * FL^B$ was applied, where *W* is weight in kg, *FL* is caudal fork length in mm and *A* and *B* are the scaling and power coefficients respectively.

Maturity-at-age was determined for females using a logistic regression fit with a binomial error structure and a logit-link function where the logistic function takes the form:

$$P(a) = \left(1 + e^{-\ln(19)(\frac{a-a_{50}}{a_{95}-a_{50}})}\right)^{-1}$$

Where *P(a)* is the proportion mature-at-age *a*, a_{50} is the age at 50% mature and a_{95} is the age at 95% mature. Female a_{50} and a_{95} were estimated as 2.63 years and 4.10 years, respectively (Table 5-1; Figure 5-1).

The SardEst model assumes that fishing occurs across a single stock and single area. In the Stock Synthesis model (prior to SardEst; Ward et al. 2015, 2017, 2020b), selectivity for the commercial fishing fleet was assumed to be a time-invariant, dome-shaped function of age, with the parameters of a double-normal selectivity curve being estimated in the model (Methot 2000). The estimation of parameters in the double-normal curve in SardEst was more difficult because of the lack of precision and consistency in length-, weight-, and age-frequency data. Consequently, the selectivity parameters estimated in Stock Synthesis have been used as fixed parameters in SardEst since 2019 (Figure 5-1) (Ward et al. 2020b, Grammer et al 2021). These parameters result in a selectivity curve with a descending right-side limb that mimics the expected reduced availability of older fish to the main components of the fishery, where younger (and smaller) fish dominate (Figure 5-1).
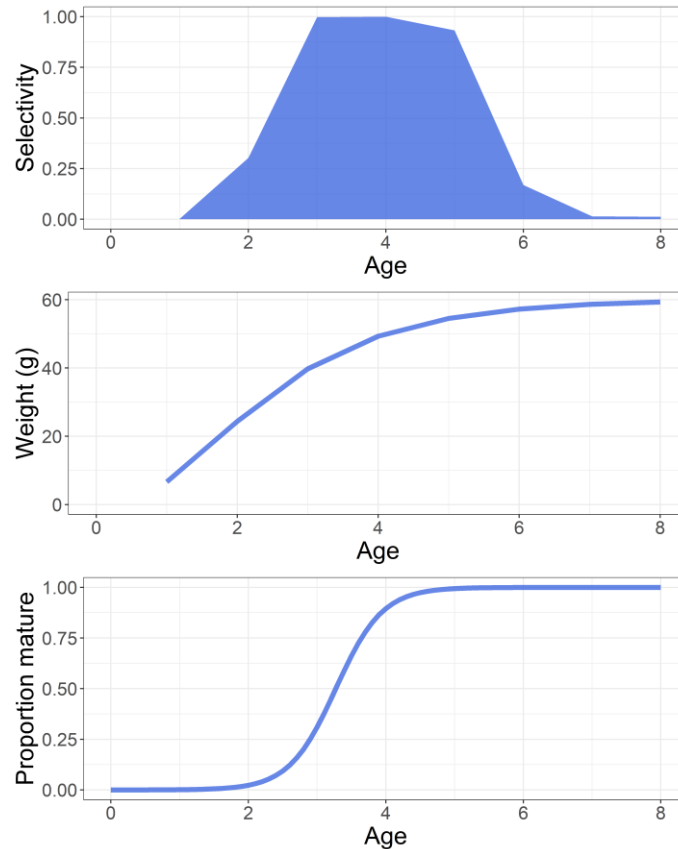
Figure 5-1. Age-based selectivity (expected proportion available to fishing by age), weight (g) and proportion of mature females used as inputs to SardEst.

Natural mortality and mass mortality events

Natural mortality (*M*) has been freely estimated in the current SardEst rather than being a fixed at 0.7yr⁻¹, as was done in previous assessments (Ward et al. 2015, 2017, 2020a). This was facilitated by increased precision in the inputs from the DEPM biomass data (Ward et al. 2021), that allowed natural mortality to be estimated rather than assumed. *M* was estimated as constant for all ages and across all years except for 1995 and 1998. In those years, two mass mortality events each killed an estimated 70% of the adult population (Ward et al. 2001b). Here, the SardEst model estimated the increased natural mortality for the adult population based on declines in spawning biomass as determined through DEPM surveys. Mass mortality was assumed to only affect the mature fish. This was performed by estimating the maximum level of additional mortality (M_t^{max}) in year *t* (where *t* = 1995 or 1998) and multiplying this value by the proportion mature at each age class.

For example, natural mortality-at-age *a* in 1995 (M_{1995}^{max}) was estimated as:

$$M_{1995,a} = M + M_{1995}^{max} * P(a)$$

Where *P(a)* is the proportion mature-at-age *a*. Total mortality-at-age ($Z_{t,\,a}$) is then the sum of total natural mortality-at-age and fishing mortality-at-age *a* ($F_{t,\,a}$) determined via the hybrid method:

$$Z_{1995,a} = M_{1995,a} + F_{1995,a}$$

Model parameters and likelihood weighting

The SardEst model fits to two data sources as likelihood components: 1) Annual age-compositions (1995–2006 and 2008–2022), and 2) DEPM spawning biomass estimates (1995–2007, 2009, 2011, 2013, 2014, 2016–2020, 2022, 2023). Additionally, annual total catches are used to condition estimates of *F* during the Hybrid *F* tuning method (Methot 2000). The likelihood components include the fits to age compositions and DEPM estimates, as well as the log-recruitment deviates, which are fitted as random effects. The estimated parameters of SardEst are:

1. $\bar{R}$ – mean number of recruits in log space.
2. $\tilde{R}_t$ – recruitment deviations for year *t* in log space
3. σ_R – the standard deviation of the recruitment deviates in log space
4. *M* – natural mortality as time and age invariant
5. M_t^{max} – the maximum level of additional mortality in year *t* (where *t* = 1995 or 1998).

Based on the recommendations of the SardEst review (Hillary 2020), the likelihood function used for the age-compositions was modified to incorporate annual sample sizes. In the 2021 stock assessment (Grammer et al. 2021), the total number of fish per catch sample per year (n) was used as the effective sample size. In the current assessment, this was changed to the number of catch samples (N) per year. The data weighting for the age-compositions also needed to be adjusted due to this modification (see below and Appendix C).

During model estimation, TMB first maximises the likelihood for the random effects (recruitment deviates) for a proposed set of fixed effects. Following this, TMB calculates the Hessian matrix for these random effects and uses this to compute the joint likelihood of both random and fixed effects (Thorson et al. 2015). Due to random effects being estimated prior to the fixed effects, it

was apparent that the model was initially maximising the joint likelihood at lower estimates of σ_R. Therefore, data weighting needed to be applied. The likelihood weightings were adjusted to account for the precision of the data sources. The precision of the DEPM biomass estimates have recently increased (Ward et al. 2021), and as a result, DEPM estimates are more reliable than age-composition data. Therefore, the likelihood weighting of the age-composition was reduced to 0.2, while the likelihood weighting of DEPM remained at one. This adjustment means that the importance of the age-composition likelihood was reduced by a factor of five relative to DEPM biomass likelihood.

5.2.2 Input data

Data from multiple sources were integrated for the purposes of the assessment, including age-composition data, spawning stock biomass estimates from DEPM surveys (Chapter 4), and catch data from the commercial fishery. Table 5–1 shows the data used in the model by type, year, and data source.

Commercial catch data

Commercial catch data were available for all years between 1992 and 2022. Data based on CDRs were used, as they are considered most accurate. Full details on the collection and analyses of commercial catch data are presented in Chapter 2. As no catch data was available for 2023, an assumption was made that the 2023 catch would match the allocated TACC for 2023 of 50,000 t.

Fishery-independent spawning biomass estimates

Spawning biomass estimates obtained from annual DEPM surveys from 1995–2007, 2009, 2011, 2013, 2014, 2016–2020, 2022 and 2023 were used as a measure of absolute abundance in the model. The methodology for estimating daily egg production was updated in Chapter 4 of this assessment so that consistent methodology was applied across the time series of surveys. These refined estimates of spawning biomass and their coefficients of variation were included in the SardEst model.

Table 5-1. Model specifications for the SardEst assessment model.

Specification	Value
Time-step	Yearly
Model years	1992–2023
Catch (t)	1992–2022
Spawning biomass (t, yearly, from DEPM)	1995–2007; 2009; 2011; 2013–14, 2016–20, 2022, 2023
CPUE index	Not included
Model age classes	Ages 1–8+
Age composition data	Ages 1–8, 1995–2022 (excluding 2007)
Growth parameters	Fixed, time-invariant von-Bertalanffy
K	0.71
L_∞	17.8
L_0	0.035
Length-weight relationship (both sexes)	Fixed power function (approx. cubic)
A (Scalar parameter)	$5.03*10^{-6}$
B (Power parameter)	3.26
Maturity (females only)	Fixed logistic function of age
A_{50}	2.63 years
A_{95}	4.10 years
Stock-recruitment	Estimated Average recruitment ($\bar{R}$)
Recruitment deviations	Estimated as random effects
Recruitment variance, σ_R	Estimated
Selectivity	
Commercial Fishery	Fixed, domed-shaped function of age

Age data

Age composition data from commercial catches were available for all years between 1995 and 2022, except for 2007. Ages were determined from an estimated otolith-weight-age relationship and applied to fish in commercial catch samples for which an otolith weight was available. Details on the collection of age-composition data and determination of age from otolith weights are presented in Chapter 3.

5.2.1   Sensitivity analyses and model diagnostics

The sensitivity of the assessment model changes in two quantities: 1) age-at-recruitment which is a fixed value, and 2) M which was previously fixed (Ward et al. 2020b) but is now estimated (see Grammer et al. 2021). This was achieved for age-at-recruitment by re-fitting the model across a greater range of values. The impact of different age-at-recruitment values on spawning biomass was also examined. The impact of a fixed M versus an estimated M was examined by re-fitting the model using multiple fixed M values and determining their impact on estimates of spawning biomass and harvest fraction.

5.3 Results

5.3.1   Model fits to data

The model fitted well to the DEPM estimates during the mass mortality years (1995 and 1998), which had been overestimated in previous models (Ward et al. 2017). During the 2000's, model estimates of spawning biomass fitted closely to DEPM estimates. In recent years (2013–2022), estimated biomass smoothed out DEPM estimates that were low and high in 2013 and 2014, respectively (Figure 5-2). In these years, SardEst determined that these DEPM estimates of spawning biomass were not supported by age-compositions, determined levels of F, nor estimated recruitment and were likely influenced by limitations in the DEPM surveys. The standard deviations of the SardEst estimates of spawning biomass were lower than the DEPM estimates, demonstrating good compatibility between data sources (i.e. catch, DEPM estimates and age compositions). SardEst provided good fits to age composition data in most years of the fishery (Figure 5–3). Poorer fits occurred in the years following the mass mortality events of 1995 and 1998. Overall, the fits to age composition data were satisfactory.
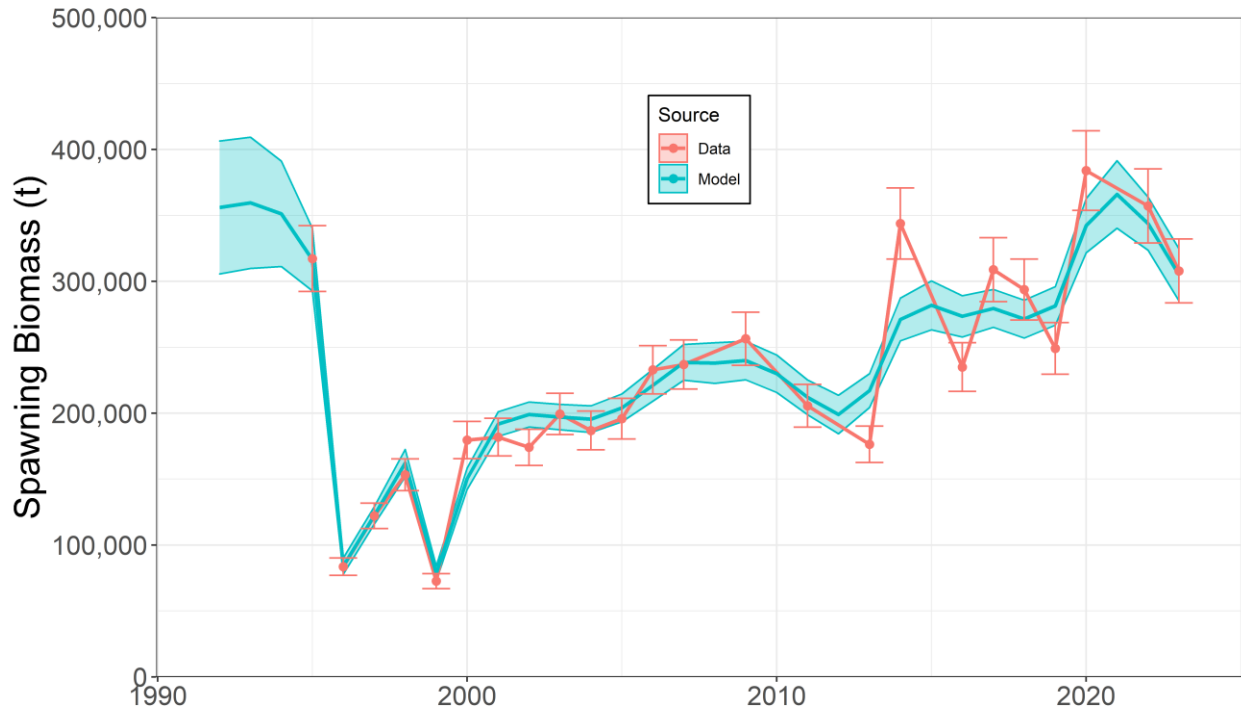
Figure 5-2. Estimated spawning biomass (total weight of mature fish) from the SardEst model. Blue line and shading represent the annual model estimates and respective standard deviations. Red points and lines show annual estimates of spawning biomass from DEPM surveys. Red error bars are the standard deviation of these survey estimates. Note that surveys did not occur in 2008, 2010, 2012, 2015 and 2021.
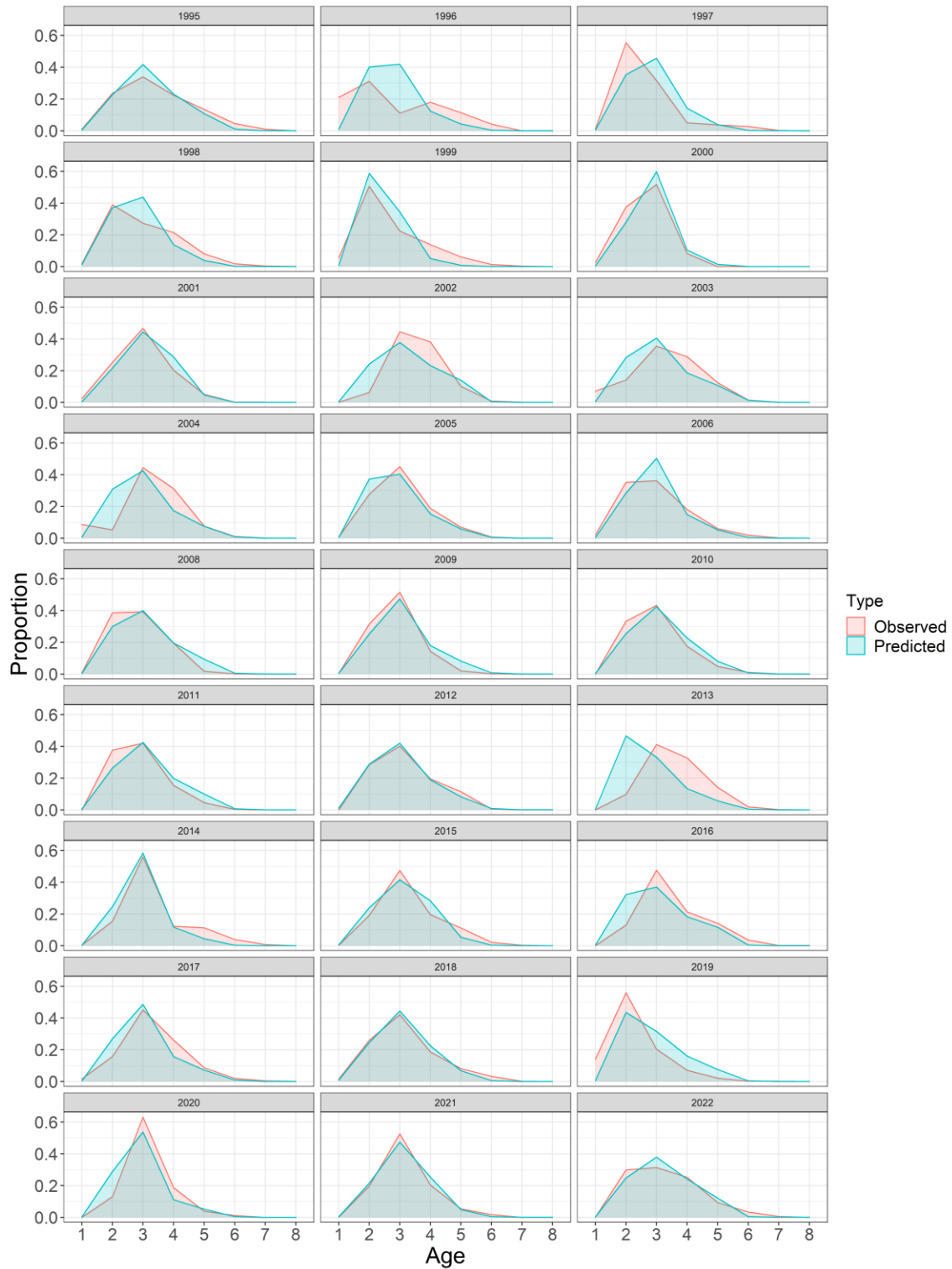
Figure 5-3. Comparison of annual observed (red shading) and model estimated (blue shading) age compositions. Note: no age compositions were available in 2007.

5.3.2 Parameter estimates

The two fixed effects recruitment parameters ($\log(\bar{R})$ and $log(\sigma_R)$) were estimated with high levels of precision (Table 5–2), while estimates of M_{1995}^{max} and M_{1998}^{max} were less precise. This was anticipated given that estimating natural mortality is a difficult undertaking in integrated stock assessment models (Sippel et al. 2017). The annual recruitment deviates (random effect parameters in log space) were estimated between -0.56 and 0.71.

Table 5-2. Fixed effects parameters with standard deviation estimated by SardEst.

Parameter	Estimate	Standard Deviation
$\log(\bar{R})$	16.24	0.19
$log(\sigma_R)$	-1.08	0.17
M_{1995}^{max}	2.20	0.36
M_{1998}^{max}	2.83	0.69
M	0.65	0.06

5.3.3 Biomass and relative depletion

The SardEst model estimated unfished total biomass (B_0) as 645,000 t (± 108,000 t) (Figure 5-4). The lowest level of total biomass in the history of the fishery was 229,000 t (± 20,000 t) in 1996, the year following the first mass mortality event. This represents the lowest level of depletion at 36% (± 5%) (Figure 5-4). Since 2000, the fishery has recovered and consistently remained above 50% depletion. The mean level of depletion over the history of the fishery has been 75% (± 10%) and in 2022, the estimated depletion was just under 95%. This corresponds to a total biomass of 612,000 t (± 51,000 t). In 2023, the estimated depletion was 85% for a total biomass of 545,000 t (± 63,000 t).

Model estimated spawning biomass in 2022 was 344,000 t (± 20,000 t) (Figure 5–2), which is more than twice the upper trigger reference point of 150,000 t set in the management plan (PIRSA 2023). The model estimate for 2023 was 305,000 t (± 20,000 t). The spawning biomass has only fallen below the upper trigger point of 150,000 t after the mass mortality events of 1995 and 1998 (Figure 5–2).
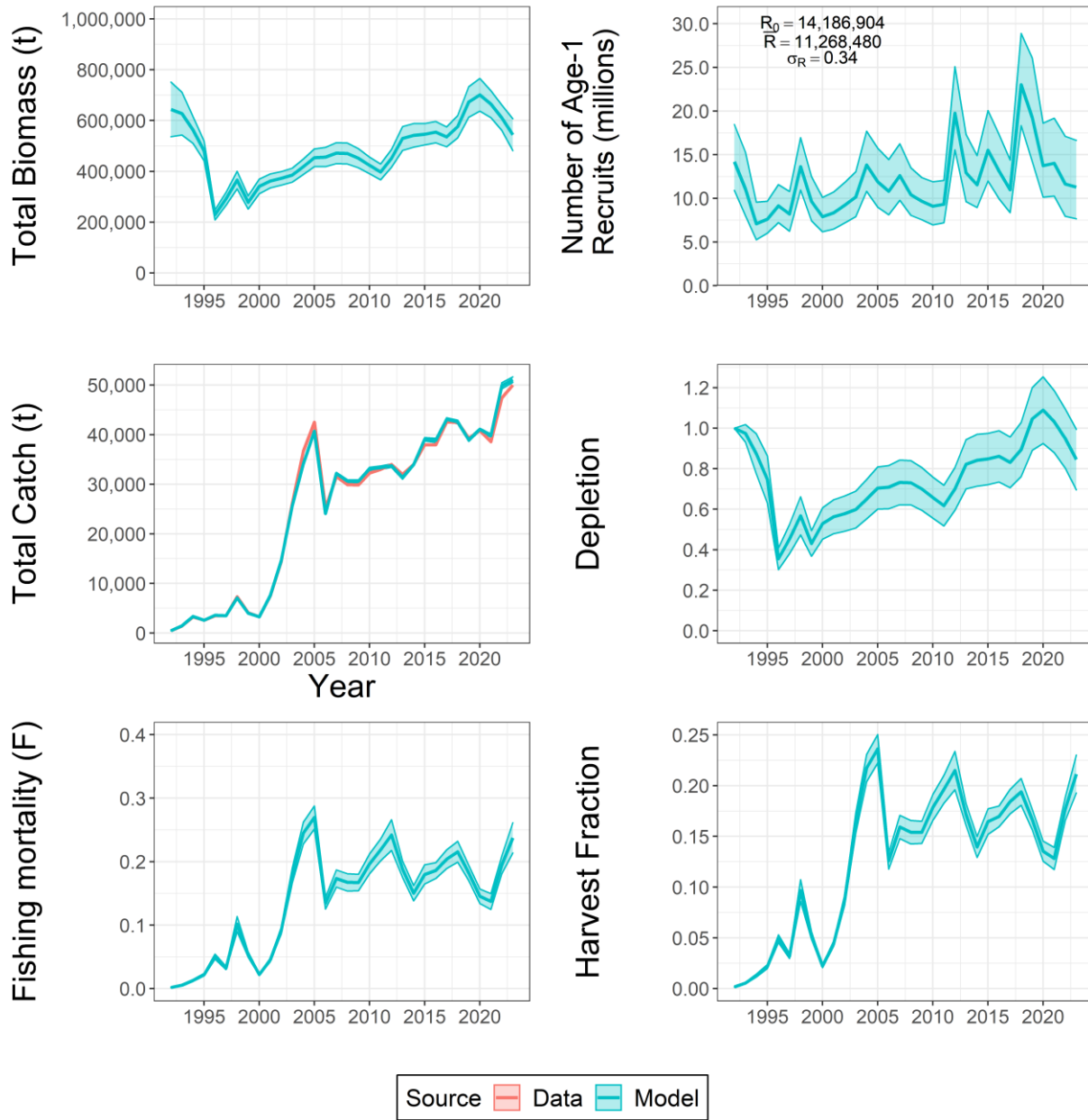
Figure 5-4. Estimates and standard deviation of time series derived quantities from SardEst. These include (left to right and top to bottom): 1) Total biomass (total weight of all age 1+ fish); 2) Annual recruitment (number of age 1 fish); 3) Annual total catch; 4) Level of depletion (Total biomass in 1992 [B_0] divided by annual total biomass); 5) Full, annual, instantaneous, fishing mortality (*F*); and 6) Harvest fraction (*H*). Blue lines denote model estimated values and blue shading represents the standard error around each estimate. Observed annual catches are represented by the red line.

5.3.4 Mass mortality events of 1995 and 1998

The SardEst model determined that ages 5 years and older had an *M* of 2.85 yr^{-1} in 1995 and 3.48 yr^{-1} in 1998. Mass mortality was assumed to be less for Sardine aged 4 and under (Figure 5–5), for which the maximum level of additional mortality (M_t^{max}) was assumed to be reduced by the independent estimates of proportion-mature-at-age. These estimates of mortality allowed SardEst to provide significantly closer fits to DEPM spawning biomass estimates in 1995 and 1998 than other stock assessment models (e.g. the Stock Synthesis Model) (Ward et al. 2020b). Earlier estimates of mortality rates in the mass mortality events of 1995 and 1998 were around 70% adult mortality across mature age classes (Ward et al. 2001b).
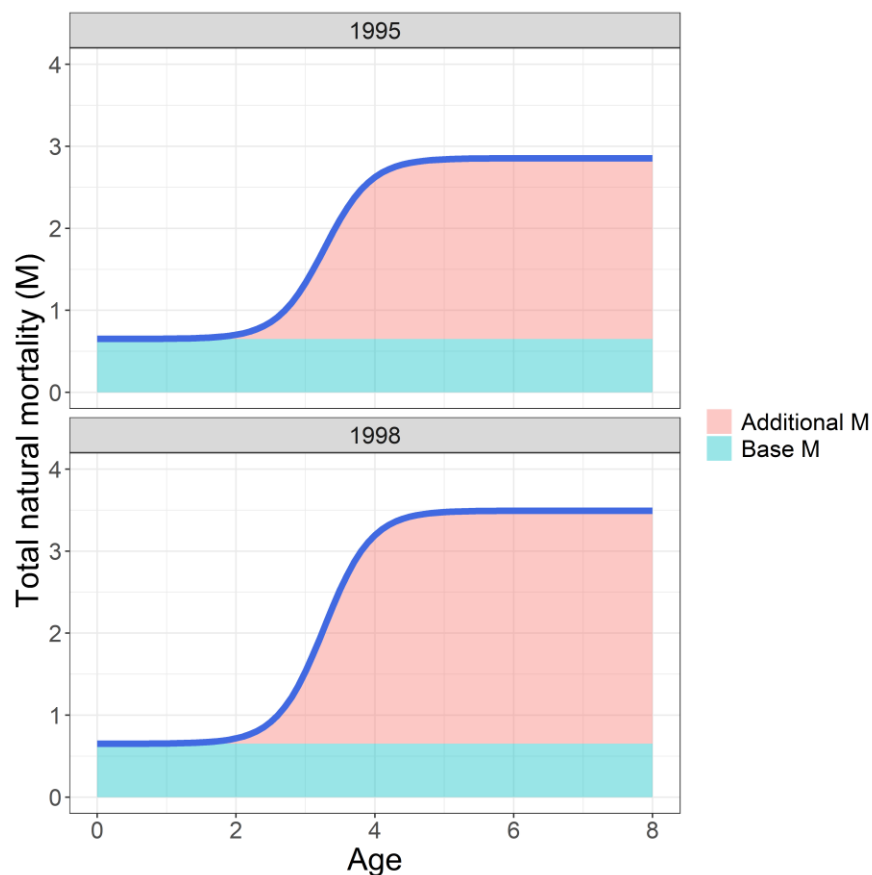
Figure 5-5. Natural mortality-at-age (*M$_a$*) during the 1995 and 1998 mass mortality events. The blue line indicates the total level of *M* for each age class. The blue shading shows the estimated and fixed level of *M* applied to all ages and years in the model. The red shading shows the additional *M$_a$* estimated by the SardEst model in 1995 and 1998.

5.3.5 Recruitment

Model estimated unfished equilibrium recruitment (R_0) was 14.2 million age-one fish (± 3.8-million). The model-estimated mean recruitment ($\bar{R}$) was 11.3 million which differed from R_0 by approximately 20%. Recruitment mostly remained between 10 and 25 million recruits (Figure 5-4) with two main peaks of 20 and 23 million recruits in 2012 and 2018, respectively. The model estimated 2012 and 2018 to be the years of high recruitment as 2014 and 2020 had a high biomass (Figure 5–4) and was composed mostly of age three fish (Figure 5–3).

5.3.6 Exploitation rates

The Hybrid F method provided nearly exact agreement with the yearly catch totals in weight, therefore yielding more accurate estimates of annual fishing mortality (F). Since 2010, the highest levels of F (0.24 yr^{-1}, ± 0.02) occurred in both 2012 and 2023. The increase in 2012 was due to a decline in model-estimated biomass, while the increase in 2023 was due to both a decline in model-estimated biomass and an increase in catch (Figure 5–4). Another high level of F (0.27 yr^{-1}, ± 0.02) occurred in 2005, although this increase in F was due to an increase in catch (Figure 5–4). Over the last 10 years, F has remained between 0.13 and 0.24 yr^{-1}, with a significant increase in the last 3 years due to an increase in catch. The level of F in 2022 was 0.19 yr^{-1} (± 0.01) which equates to a harvest fraction of 18.0% (± 1.2%). The level of F in 2023 was 0.24 yr^{-1} (± 0.02) with a harvest fraction of 21.0% (± 1.9%).

5.3.7 Model diagnostics

One key input is a fixed parameter in the SardEst model: the age-at-recruitment. Sensitivity analyses performed using different values of this parameter demonstrated that the age-at-recruitment could have an effect on model spawning biomass (Figure 5–6). However, an age-at-recruitment from zero to two years had little effect on the spawning biomass estimates, with the exception of years 1992–1994, where there are no estimates of spawning biomass to inform the model (Figure 5–6). The rest of the spawning biomass time series mainly differed when age-at-recruitment was three (Figure 5-6). This is an unrealistic age-at-recruitment as age one and two fish are regularly present in age samples (Figure 5–3; Chapter 3). Therefore, this difference can be disregarded.

Sensitivity analyses performed using different values of natural mortality demonstrated that estimating the value of natural mortality in the model had little effect on key outputs of the model, the spawning biomass and the harvest fraction (Figure 5–7).
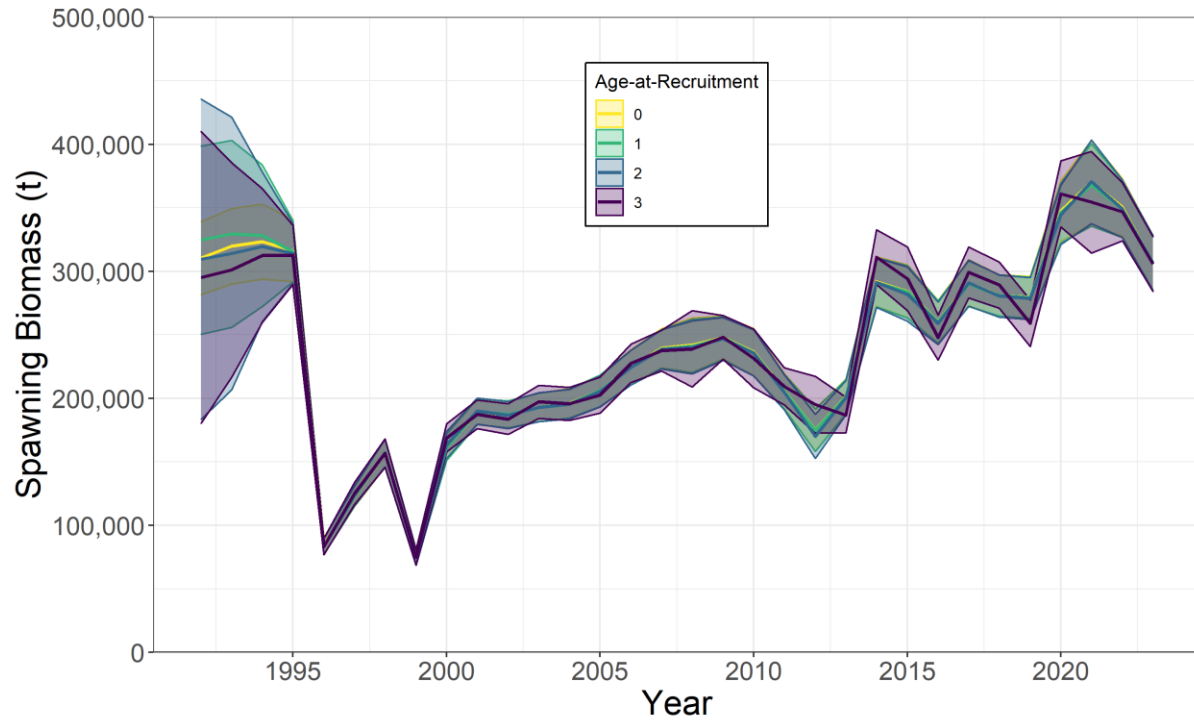
Figure 5-6. Model sensitivities to fixed values of age-at-recruitment. The figure shows different model estimates of spawning biomass using different values of the parameter in the model. Lines are the model estimates and shaded areas are the standard deviations.
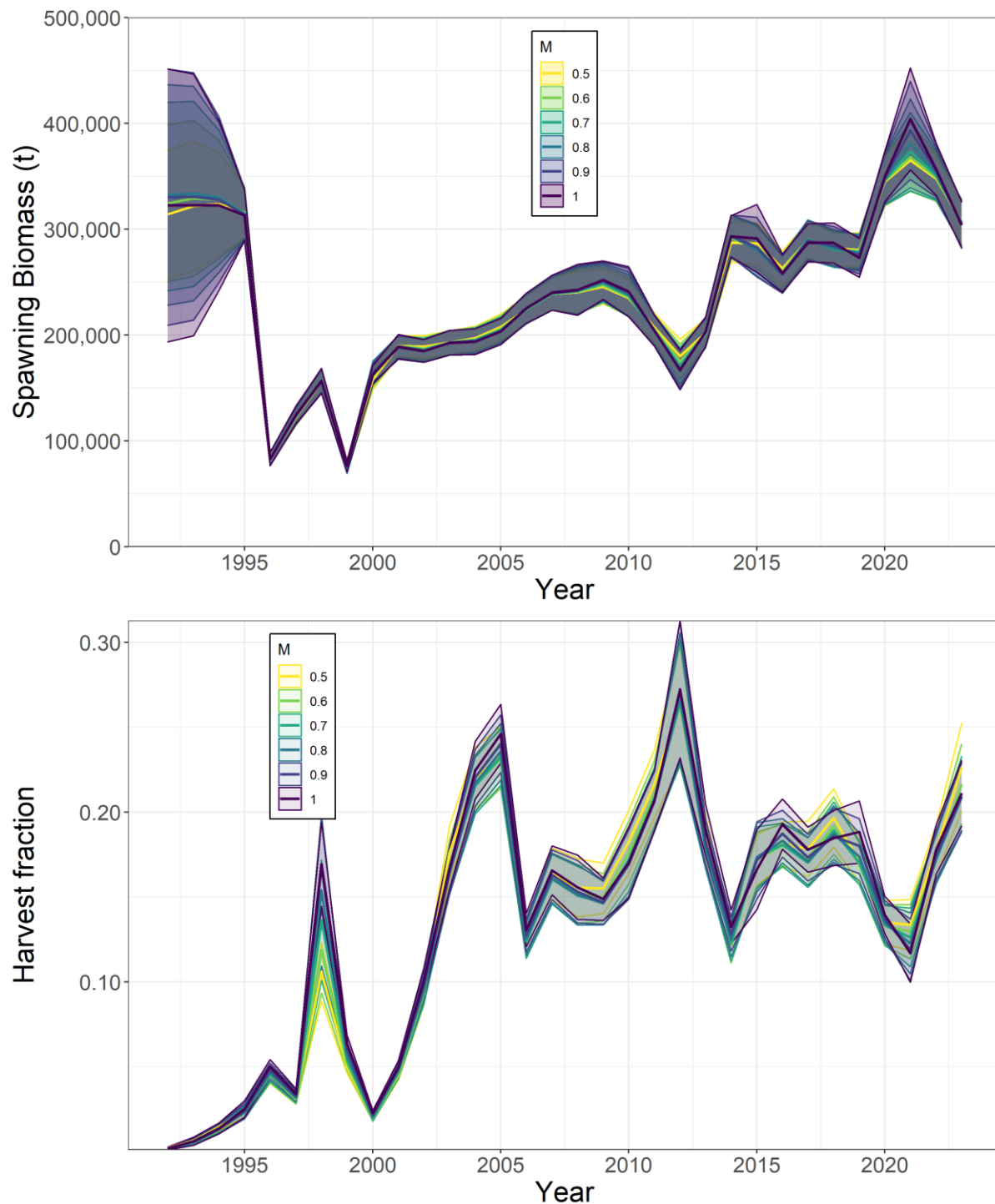
Figure 5-7. Model sensitivities to different values of natural mortality. Top panel shows different model estimates of spawning biomass using different values of natural mortality in the model. Bottom plot shows different model estimates of harvest fraction using different values of natural mortality in the model. Lines are the model estimates and shaded areas are standard deviations.

5.4 Discussion

The SardEst model was refined in 2021 after the DEPM spawning biomass was estimated with greater precision following methodological updates (Ward et al. 2021). The most important development in SardEst in the previous report was the estimation of natural mortality by the model (Grammer et al. 2021). Estimating M in integrated stock assessment models has long been discussed but has rarely been achieved with confidence (Brodziak et al 2011). Simulation studies have shown that estimating M is theoretically possible when a model is correctly specified (Lee et al. 2011, Sippel et al. 2017). However, it has also been highlighted that all stock assessment models have some degree of mis-specification, and therefore, estimating M is rarely achievable (Francis 2012). In the present report, SardEst also estimated an age and time invariant M. Sufficient information was available for the model to estimate M, since more precise estimates of spawning biomass were available (Ward et al. 2021, Grammer and Ivey 2023). These estimates of biomass provided a greater level of information about the population's survivorship, allowing M to be estimated rather than fixed at an assumed and somewhat arbitrary value. In many cases, attempts to estimate time variant M can be problematic, as it can influence results across the entire time series (Johnson et al. 2015). Therefore, estimating M in stock assessment models remains controversial (Francis 2012, Johnson et al. 2015). However, the estimate of M from SardEst was 0.65 yr^{-1}, which aligns with the fixed values of 0.6 yr^{-1} and 0.7 yr^{-1} used in previous assessments (Ward et al. 2017, 2020b). Additionally, the primary quantities of management interest—spawning biomass and harvest fraction—were not influenced by changes in M. Therefore, continuing to estimate M in this model is reasonable, as the outcomes and conclusions of the assessment are not impacted.

Data weighting can have substantial impact on the outcomes of integrated stock assessment modelling (Francis 2011, 2017). The data weightings applied to the DEPM biomass likelihood and the annual age-compositions likelihood were adjusted due to: 1) the modification of the likelihood function used for the age-compositions to incorporate the effective annual sample sizes (N rather than n) (Hillary 2020; Appendix B), and 2) correction of the coding error in found in the 2021 SardEst model (Appendix C). Following the weighting philosophy of Francis (2011), which suggests that the model should approximately fit the trends in the abundance indices and the variation implied by the residuals around the estimates should match the variation assigned to those data, the DEPM biomass likelihood was given more weight (i.e. weighting of 1) and age-compositions likelihood was down-weighted to 0.2. This weighting reflects the higher precision in DEPM data (Ward et al. 2021, Grammer and Ivey 2023) compared to age composition data.

Weighting values used in the present stock assessment produced a reasonable fit of the model and variance around estimates for spawning biomass.

In SardEst, recruitment is estimated for age-one fish without requiring a stock recruitment relationship. This allows the model to make better use of information on age compositions. Recruitment is also estimated as random effects about a mean recruitment value, which decreases the variability around their estimates (Thorson et al. 2014). This is important, as all stock assessment models must reconcile changes in biomass through changes in either mortality or recruitment. If biomass increases, a model could interpret this as a pulse in recruitment or a decline in mortality. When explicitly attempting to determine the effects of catches on a population, these aspects become increasingly significant. By better handling of recruitment, SardEst can more effectively model mortality, providing greater confidence in its estimates of exploitation rate and levels of catch. In addition, recruitment is less prone to variation because it is fitted with random effects, meaning that pulses or failures in recruitment will only occur when the model can find no other explanation in the data.

The total biomass estimated by SardEst in 2022 was 612,000 t (± 51,000 t) and was 545,000 t (± 63,000 t) for 2023, which is below the unfished total biomass (B_0) (645,000 t ± 108,000 t) estimated for 1992, representing an estimated depletion of 95% and 85%, respectively. Early (and initial) estimates of biomass are likely to be less reliable than more recent estimates, as DEPM surveys were not undertaken until 1995, and earlier surveys are considered less reliable since the assessment program was in its infancy. This may complicate estimating the exact level of depletion, but it remains apparent that current stock health is good, and biomass is at high levels on par with the commencement of the fishery.

The model-estimated spawning biomass in 2023 was 305,000 t (± 20,000 t), which is lower than the model estimates in 2021 and 2022 (344,000 ± 20,000 t). Although the model estimate for 2023 has decreased, it is twice the upper trigger reference point of 150,000 t (PIRSA 2023). The model estimated exploitation rate for spawning biomass in 2022 is 18%, which is below the maximum exploitation rate of 22.5% for Tier 3 identified in the management plan (PIRSA 2023). The model estimated exploitation rate for spawning biomass in 2023 is 21%, which is below the maximum exploitation rate of 25% for Tier 2 (PIRSA 2023).

SardEst is a recently developed model with scope for further development. Future improvements that should be considered for SardEst include:

1) SardEst does not currently provide projections. Development of a projection component would be beneficial and could possibly be expanded to include management strategy evaluation (MSE).

2) SardEst is currently a single sex model that uses the maturity data for females only. Therefore, there may be potential benefits in developing a two-sex model.

3) SardEst is a single area model that does not consider the different zones of the fishery. Developing a multi-zone model may be beneficial as catch proportions increase outside the SG Zone.

4) Selectivity is a key parameter that cannot be known *a priori*. Consequently, selectivity should be estimated in the model rather than defined as a fixed parameter.

5) Developing climate-enhanced stock assessment models represents a vital challenge for managing fish stocks in the context of climate change (Punt et al. 2021). Time series of environmental data (e.g., sea temperature) could be included into the model and linked to key parameters (e.g., recruitment, growth) to determine how these parameters are influenced by the environmental inputs.

6.   DISCUSSION

6.1 Stock status and uncertainty

Under the criteria outlined in the harvest strategy for the SASF (PIRSA 2023), the southern stock of Australian Sardine in 2022 is classified as **Sustainable**. The estimates of spawning biomass obtained using the DEPM in 2022 was 355,075 t (299,956–410,193 t), and in 2023 was 307,881 t (260,468–412,113 t), which are above the target reference point of 200,000 t (PIRSA 2023). The model estimate of spawning biomass for 2023 of 305,000 t (± 20,000 t) was similar and also above the target reference point. The exploitation rate for spawning biomass (DEPM) in 2022 was 13% and below the maximum rate at Tier 3 of 22.5% identified in the management plan (PIRSA 2023). Similarly, the exploitation in 2023 was 16% and below the maximum rate at Tier 2 of 25% (PIRSA 2023). These findings are consistent with other recent assessments of the status of the southern stock of Sardine which classified the stock as sustainable (e.g. Grammer et al. 2021, Piddocke et al. 2021).

The strongest piece of empirical evidence indicating that the southern stock of Sardine should be classified as sustainable is that the spawning area recorded during the 2023 survey was 66,200 km^2 (Grammer and Ivey 2023), which is the sixth highest on record. It is widely recognised that spawning area (A) is strongly correlated with the size of the spawning stock of Sardine (e.g. Mangel and Smith 1990, Gaughan et al. 2004, Ward et al. 2021). Under the refined approach used to apply the DEPM in this report, inter-annual variations in estimates of spawning biomass are driven primarily by fluctuations in the spawning area (Chapter 4). Currently, we do not know the uncertainty around the estimation of A.

In the current assessment, further developments were made to the SardEst model that continue to improve upon the population model outputs from previous assessments. Recommendations from an external review of SardEst in 2020 (Hillary 2020) have continued to be implemented. These included 1) the modification of the likelihood function used for the age-compositions to incorporate the effective annual sample sizes (N rather than n), and 2) adjustments to the data weightings applied to the DEPM biomass likelihood and the annual age-compositions likelihood. In addition, a coding error found in the 2021 SardEst model was corrected for this assessment. Natural mortality M continues to be estimated by the model, which was possible due to the greater precision in the revised estimates of spawning biomass obtained from the DEPM. These continued developments and improvements increased precision around the time series of

SardEst model estimates of total biomass, annual recruitment, total catch, relative depletion, fishing mortality, and harvest fraction.

The total biomass estimated by the model in 2022 was 612,000 t (± 51,000 t) and was 545,000 t (± 63,000 t) in 2023, which is below the unfished total biomass (B_0) (645,000 t ± 108,000 t) estimated in 1992, representing an estimated depletion of 95% and 85%, respectively. Early (and initial) estimates of biomass are likely to be less reliable than more recent estimates, as DEPM surveys were not undertaken until 1995, and earlier surveys were in an exploratory phase (Chapter 4). This may complicate estimating the exact level of depletion, but it is clear the current biomass of Sardine off South Australia is at high levels on par with the beginning of the fishery.

6.2 Future directions

Future applications of the DEPM to Sardine off South Australia should continue to adopt the revised methods (see Ward et al. 2021) that have been outlined in this report and are currently being applied (e.g. Grammer and Ivey 2022, 2023). Because future estimates of spawning biomass will be driven primarily by the estimate of spawning area, it will be critical for future surveys to utilise the adaptive sampling implemented in 2014 and cover other areas off South Australia where Sardine are likely to spawn, including waters east of Kangaroo Island. During 2019 and 2022 DEPM surveys, a second plankton sample was taken in each sampling grid (a random distance from original sampling site). These data have provided an opportunity to investigate uncertainty associated with the estimation of A. Preliminary results suggest that estimates of A for Sardine can be replicated with considerable precision if using comparable sampling gear (SARDI unpublished data). The application of geostatistical methods around estimates of A and P_0 is a priority to be investigated in the future.

Further to this, an extensive adult sampling program will be conducted in 2024 and repeated periodically (e.g. every 3-5 years) to determine if changes in key adult parameters, particularly spawning fraction, have occurred. Consideration should also be given to further developing SardEst as a two-sex, multi-zone population model with capability to undertake projections, incorporate climate-related data, estimate size/age selectivity and conduct management strategy evaluations.

The driver(s) of the declining trend in size-at-maturity (L_{50}) of the Sardine in the Gulf Zones is unclear. Initial investigation suggests it is not caused by insufficient sampling and no long-term shift has been detected in the size- or age-structure from the Gulf Zones. Changes in L_{50} over time may be a result of a genetic change to the population due to selectively targeting fish above

the size at maturity; a physiological response to a change in environmental conditions (e.g. size at maturity declines with increasing water temperatures, or a combination of the two). Both scenarios warrant further investigation and consideration.

Under the current harvest strategy, an ecosystem assessment is required every four years (PIRSA 2023) with the first one projected to occur in 2025. The assessment should be based on the recommendations and outcomes from Goldsworthy et al. (2011, 2013) and should collect data on key ecological indicator species, update the ecosystem model with new data, and estimate ecological performance indicators.

7.   REFERENCES

Barnes, J. T., and T. J. Foreman. 1994. Recent-Evidence for the Formation of Annual Growth Increments in the Otoliths of Young Pacific Sardines (*Sardinops-Sagax*). California Fish and Game **80**:29-35.

Blackburn, M. 1950. Studies on the age, growth, and life history of the sardine *Sardinops neopilchardus* (Steindachner), in Southern and Western Australia. Australian Journal of Marine and Freshwater Research **1**:221-258.

Brodziak, J. K. T., J. N. Ianelli, K. Lorenzen, and R. D. Methot. 2011. Estimating natural mortality in stock assessment applications August 11-13, 2009, Alaska Fisheries Science Center, Seattle, WA.

Brooks, M. E., K. Kristensen, K. J. v. Benthem, A. Magnusson, C. W. Berg, A. Nielsen, and B. M. Bolker. 2017. glmmTMB Balances Speed and Flexibility Among Packages for Zero-inflated Generalized Linear Mixed Modeling. The R Journal **9**:378-400.

Bulman, C. M., S. A. Condie, F. J. Neira, S. D. Goldsworthy, and E. A. Fulton. 2011. The trophodynamics of small pelagic fishes in the southern Australian ecosystem and the implications for ecosystem modelling of southern temperate fisheries. Final report for FRDC project 2008/023., CSIRO Marine and Atmospheric Research. Hobart. 101 pp.

Butler, J. L., M. L. Granados, J. T. Barnes, M. Yaremko, and B. J. Macewicz. 1996. Age composition, growth, and maturation of the Pacific sardine (*Sardinops sagax*) during 1994. California Cooperative Oceanic Fisheries Investigations Reports **37**:152-159.

Checkley, D. M. J., and R. G. R. Asch, R. R. . 2017. Climate, Anchovy, and Sardine. Annual Review of Marine Science **9**:469-493.

Cury, P., A. Bakun, R. J. M. Crawford, A. Jarre, R. A. Quiñones, L. J. Shannon, and H. M. Verheye. 2000. Small pelagics in upwelling systems: patterns of interaction and structural changes in "wasp-waist" ecosystems. ICES Journal of Marine Science **57**:603-618.

Daly, K. 2007. The diet and guild structure of the small pelagic fish community in the eastern Great Australian Bight, South Australia. Honours thesis, University of Adelaide.

Dimmlich, W. F., W. G. Breed, M. Geddes, and T. M. Ward. 2004. Relative importance of gulf and shelf waters for spawning and recruitment of Australian anchovy, *Engraulis australis*, in South Australia. Fisheries Oceanography **13**:310-323.

Dimmlich, W. F., and T. M. Ward. 2006. Ontogenetic shifts in the distribution and reproductive patterns ofAustralian anchovy (*Engraulis australis*) by otolith microstructure analysis. Marine and Freshwater Research **57**:373-381.

Dimmlich, W. F., T. M. Ward, and B. W.G. 2009. Spawning dynamics and biomass estimates of Australian anchovy (*Engraulis australis*) in gulf and shelf waters of South Australia. Journal of Fish Biology **75**:1560-1576.

Espinoza, P., A. Bertrand, C. D. van der Lingen, S. Garrido, and B. Rojas de Mendiola. 2009. Diet of sardine (*Sardinops sagax*) in the northern Humboldt Current system and comparison with the diets of clupeoids in this and other eastern boundary upwelling systems. Progress In Oceanography **83**:242-250.

Fletcher, W., and R. Tregonning. 1992. Distribution and timing of spawning by the Australian pilchard (*Sardinops sagax neopilchardus*) off Albany, Western Australia. Marine and Freshwater Research **43**:1437-1449.

Fletcher, W. J. 1995. Application of the otolith weight-age relationship for the pilchard, *Sardinops sagax neopilchardus*. . Canadian Journal of Fisheries and Aquatic Science. **52**:657-664.

Fletcher, W. J., and S. J. Blight. 1996. Validity of using translucent zones of otoliths to age the pilchard *Sardinops sagax neopilchardus* from Albany, western Australia. Marine and Freshwater Research **47**:617-624.

Fletcher, W. J., N. C. H. Lo, E. A. Hayes, R. J. Tregonning, and S. J. Blight. 1996. Use of the daily egg production method to estimate the stock size of western Australian sardines (*Sardinops sagax*). Marine and Freshwater Research **47**:819-825.

Fletcher, W. J., R. J. Tregonning, and G. J. Sant. 1994. Interseasonal variation in the transport of pilchard eggs and larvae off southern Western Australia. Marine Ecology Progress Series **111**:209-224.

Francis, R. I. C. C. 2011. Data weighting in statistical fisheries stock assessment models. Canadian Journal of Fisheries and Aquatic Sciences **68**:1124-1138.

Francis, R. I. C. C. 2012. The reliability of estimates of natural mortality from stock assessment models. Fisheries Research 119-120:133-134.

Francis, R. I. C. C. 2017. Revisiting data weighting in fisheries stock assessment models. Fisheries Research **192**:5-15.

Ganias, K. 2012. Thirty years of using the postovulatory follicles method: Overview, problems and alternatives. Fisheries Research **117–118**:63-74.

Gaughan, D. J., W. J. Fletcher, and J. P. McKinlay. 2002. Functionally distinct adult assemblages within a single breeding stock of the sardine, *Sardinops sagax*: management units within a management unit. Fisheries Research **59**:217-231.

Gaughan, D. J., T. I. Leary, R. W. Mitchell, and I. W. Wright. 2004. A sudden collapse in distribution of Pacific sardine (*Sardinops sagax*) off southwestern Australia enables an objective re-assessment of biomass estimates. Fishery Bulletin **102**:617-633.

Goldsworthy, S. D., B. Page, P. J. Rogers, C. Bulman, A. Wiebkin, L. J. McLeay, L. Einoder, A. M. M. Baylis, M. Braley, R. Caines, K. Daly, C. Huveneers, K. Peters, A. D. Lowther, and T. M. Ward. 2013. Trophodynamics of the eastern Great Australia Bight ecosystem: ecological change associated with the growth of Australia's largest fishery. Ecological Monitoring **255**.

Goldsworthy, S. D., B. Page, P. J. Rogers, and T. M. Ward. 2011. Establishing ecosystem based management for the South Austalian Sardine Fishery: developing ecological performance indicators and reference points to assess the need for ecological allocations. Fisheries Research and Development Corporation, SARDI Publication Number F2010/000863-1.

Grammer, G., F. Bailleul, A. Ivey, and J. Smart. 2021. Stock assessment of Australian Sardine (*Sardinops sagax*) off South Australia 2021. Report to PIRSA Fisheries and Aquaculture. South Australian Research and Development Institute (Aquatic Sciences), Adelaide. SARDI Publication No. F2007/000765-8. SARDI Research Report Series No. 1120. 96pp.

Grammer, G. L., and A. R. Ivey. 2022. Spawning biomass of Sardine, *Sardinops sagax*, in waters off South Australia in 2022. Report to PIRSA Fisheries and Aquaculture. Institution: South Australian Research and Development Institute (Aquatic Sciences), Adelaide. SARDI Publication No. F2007/000566-12. SARDI Research Report Series No.1152. 27pp.

Grammer, G. L., and A. R. Ivey. 2023. Spawning biomass of Sardine, *Sardinops sagax*, in waters off South Australia in 2023. Report to PIRSA Fisheries and Aquaculture. Institution: South Australian Research and Development Institute (Aquatic Sciences), Adelaide. SARDI Publication No. F2007/000566-13. SARDI Research Report Series No.1194. 32pp.

Grammer, G. L., T. M. Ward, and L. M. Durante. 2022. Commonwealth Small Pelagic Fishery: Fishery Assessment Report 2019-2021. Report to the Australian Fisheries Management Authority. South Australian Research and Development Institute (Aquatic Sciences), Adelaide. SARDI Publication No. F2010/000270-11. SARDI Research Report Series No. 1133. 101pp.

Grant, W. S., A. M. Clark, and B. W. Bowen. 1998. Why restriction fragment length polymorphism analysis of mitochondrial DNA failed to resolve sardine (*Sardinops*) biogeography: Insights from mitochondrial DNA cytochrome b sequences. Canadian Journal of Fisheries and Aquatic Sciences **55**:2539-2547.

Grant, W. S., and R. W. Leslie. 1996. Late Pleistocene dispersal of Indian-Pacific sardine populations in an ancient lineage of the genus Sardinops. Marine Biology **120**:133-142.

Grift, R. E., A. D. Rijnsdorp, S. Barot, M. Heino, and U. Dieckmann. 2003. Fisheries-induced trends n reaction norms for maturation in North Sea plaice. Marine Ecology Progress Series **257**:247-257.

Hayashi, A., Y. Yamashita, K. Kawaguchi, and T. Ishii. 1989. Rearing method and daily otolith ring of Japanese sardine larvae. Nippon Suisan Gakkaishi **55**:997-1000.

Hilborn, R., R. O. Amoroso, E. Bogazzi, O. P. Jensen, A. M. Parma, C. Szuwalski, and C. J. Walters. 2017. When does fishing forage species affect their predators? Fisheries Research **191**:211-221.

Hillary, R. 2020. Review of Australian sardine stock assessment. July 2020. CSIRO Oceans & Atmosphere. Hobart. 10p.

Hunter, J. R., and S. R. Goldberg. 1980. Spawning incidence and batch fecundity in northern anchovy, *Engraulis mordax*. Fisheries Bulletin **77**:641-652.

Hunter, J. R., and B. J. Macewicz. 1985. Measurement of spawning frequency in multiple spawning fishes. National Marine Fisheries Services. National Oceanic and Atmospheric Administration Technical Report.

Izzo, C., T. M. Ward, A. R. Ivey, I. M. Suthers, J. Stewart, S. C. Sexton, and B. M. Gillanders. 2017. Integrated approach to determining stock structure: implications for fisheries management of sardine, *Sardinops sagax*, in Australian waters. Reviews in Fish Biology and Fisheries **27**:267-284.

Johnson, K. F., C. C. Monnahan, C. R. McGilliard, K. A. Vert-pre, S. C. Anderson, C. J. Cunningham, F. Hurtado-Ferro, R. R. Licandeo, M. L. Muradian, K. Ono, C. S. Szuwalski, J. L. Valero, A. R. Whitten, and A. E. Punt. 2015. Time-varying natural mortality in fisheries stock assessment models: identifying a default approach. ICES Journal of Marine Science **72**:137-150.

Jones, J. B., A. D. Hyatt, P. M. Hine, R. J. Whittington, D. A. Griffin, and N. J. Bax. 1997. Australasian pilchard mortalities. World Journal of Microbiology & Biotechnology **13**:383-392.

Kailola, P. J., M. J. Williams, P. C. Stewart, A. M. Reichelt, and C. Grieve. 1993. Australian Fisheries Resourses. Bureau of Resource Sciences, Department of Primary Industries and Energy and the Fisheries Research and Development Corporation, Canberra.

Kerstan, M. 2000. Estimation of precise ages from the marginal increment widths of differently growing sardine (*Sardinops sagax*) otoliths. Fisheries Research **46**:207-225.

Kristensen, K., A. Nielsen, C. W. Berg, H. Skaug, and B. M. Bell. 2016. TMB: Automatic Differentiation and Laplace Approximation. 70:21.

Kuriyama, P. T., K. T. Hill, and J. P. Zwolinski. 2022. Update assessment of the Pacific sardine resource in 2022 for U.S. management in 2022-2023. U.S. Department of Commerce, NOAA Technical Memorandum NMFS-SWFSC-662. 30 pp.

Lasker, R. 1985. An egg production method for estimating spawning biomass of pelagic fish: Application to the Northern Anchovy, *Engraulis mordax*. National Marine Fisheries Services. National Oceanic and Atmospheric Administration Technical Report.

Le Clus, F., and P. Malan. 1995. Models of temperature-dependent rate of development of pilchard *Sardinops sagax* eggs, to be used in routine procedures for estimating daily egg production. South African Journal of Marine Science **16**:1-8.

Lee, H.-H., M. N. Maunder, K. R. Piner, and R. D. Methot. 2011. Estimating natural mortality within a fisheries stock assessment model: An evaluation using simulation analysis based on twelve stock assessments. Fisheries Research 109:89-94.

Louw, G. G., C. D. Van der Lingen, and M. J. Gibbons. 1998. Differential feeding by sardine *Sardinops sagax* and anchovy *Engraulis capensis* recruits in mixed shoals. South African Journal of Marine Science **19**:227-232.

Mangel, M., and P. E. Smith. 1990. Presence-absence sampling for fisheries management. Canadian Journal of Fisheries and Aquatic Sciences **47**:1875-1887.

McCall, A. D. 1990. Dynamic Geography of Marine Fish Populations. University of Washington Press, Seattle, WA.

McLeay, L. J., B. Page, S. D. Goldsworthy, T. M. Ward, and D. C. Paton. 2009a. Size matters: variation in the diet of chick and adult crested terns. Marine Biology **156**:1765-1780.

McLeay, L. J., B. Page, S. D. Goldsworthy, T. M. Ward, D. C. Paton, M. Waterman, and M. D. Murray. 2009b. Demographic and morphological responses to prey depletion in a crested tern (Sterna bergii) population: can fish mortality events highlight performance indicators for fisheries management? ICES Journal of Marine Science **66**:237-247.

Methot, R. D. 2000. Technical description of the stock synthesis assessment program. NOAA Technical Memorandum. Seattle, Washington.

Neira, F. J., J. M. Lyle, and J. P. Keane. 2009. Shelf spawning habitat of *Emmelichthys nitidus* in south-east Australia - Implications and suitability for egg-based biomass estimation. Estuarine Coastal and Shelf Science **81**:521-532.

Neira, F. J., A. Miskiewicz, and T. Trnski. 1998. Larvae of temperate Australian fishes: laboratory guide for larval fish identification. University of Western Australia Press, Nedlands, W.A.

Newman, S. J., B. S. Wise, K. G. Santoro, and D. J. e. Gaughan. 2023. Status Reports of the Fisheries and Aquatic Resources of Western Australia 2021/22: The State of the Fisheries. Department of Primary Industries and Regional Development, Western Australia. 310pp.

Parker, K. 1985. Biomass model for the egg production method. Pages 5-6 *in* R. Lasker, editor. An egg production method for estimating spawning biomass of pelagic fish: Application to the Northern Anchovy, *Engraulis mordax*. National Marine Fisheries Services. National Oceanic and Atmospheric Administration Technical Report.

Parrish, R. H., R. Serra, and W. S. Grant. 1989. The Monotypic Sardines, Sardina and Sardinops - Their Taxonomy, Distribution, Stock Structure, and Zoogeography. Canadian Journal of Fisheries and Aquatic Sciences **46**:2019-2036.

Pauly, D., and R. S. V. Pullin. 1988. Hatching time in spherical, pelagic, marine fish eggs in response to temperature and egg size. Environmental biology of fishes **22**:261-271.

Picquelle, S., and G. Stauffer. 1985. Parameter estimation for an egg production method of anchovy biomass assessment. National Marine Fisheries Services. National Oceanic and Atmospheric Administration Technical Report.

Piddocke, T., C. Ashby, K. Hartmann, A. Hesp, P. Hone, J. Klemke, S. Mayfield, A. Roelofs, T. Saunders, J. Stewart, B. Wise, and J. Woodhams (eds). 2021. Status of Australian fish stocks reports 2020, Fisheries Research and Development Corporation, Canberra.

Pikitch, E., P. D. Boersma, I. L. Boyd, D. O. Conover, P. Cury, T. Essington, S. S. Heppell, E. D. Houde, M. Mangel, D. Pauly, É. Plagányi, K. Sainsbury, and R. S. Steneck. 2012. Little Fish, Big Impact: Managing a Crucial Link in Ocean Food Webs. Lenfest Ocean Program. Washington, DC. 108 pp. http://www.oceanconservationscience.org/foragefish/.

PIRSA. 2007. Addendum to the management plan for the South Australian pilchard fishery. South Australian fisheries management series, Paper No. 47.

PIRSA. 2014. Management plan for the South Australian commercial marine scalefish fishery. Part B–Management arrangements for the taking of Sardines. Paper number 68.

PIRSA. 2020. Sardine Fishery Operator User Guide January 2021.

PIRSA. 2021. Policy Paper - Managing of under-catch and over-catch in South Australian fisheries. Government of South Australia 2021. 10pp.

PIRSA. 2023. Management Plan for the South Australian Commercial Sardine Fishery. Fisheries Management Series paper number 87. The South Australian Fisheries Management Series. Department of Primary Industries and Regions. Government of South Australia. 49 pp.

Punt, A. E., M. G. Dalton, W. Cheng, A. J. Hermann, K. K. Holsman, T. P. Hurst, J. N. Ianelli, K. A. Kearney, C. R. McGilliard, D. J. Pilcher, and M. Véron. 2021. Evaluating the impact of climate and demographic variation on future prospects for fish stocks: An application for northern rock sole in Alaska. Deep Sea Research Part II: Topical Studies in Oceanography **189-190**:104951.

Quinonez-Velazquez, C., M. O. Nevarez-Martinez, and M. G. Gluyas-Millan. 2000. Growth and hatching dates of juvenile pacific sardine *Sardinops caeruleus* in the Gulf of California. Fisheries Research **48**:99-106.

R Core Team. 2023. R: A language and environment for statistical computing. R Foundation for Statistical Computing, Vienna, Austria. URL http://www.R-project.org/.

Rice, J. A. 1995. Mathematical Statistics and Data Analysis. Duxbury Press, Belmont, California.

Rijnsdorp, A. D. 1993. Fisheries as a large-scale experiment on life-history evolution: disentangling phenotypic and genetic effects in changes in maturation and reproduction of North Sea plaice, *Pleuronectes platessa* L. Oecologia **96**:391-401.

Rogers, P. J., M. Geddes, and T. M. Ward. 2003. Blue sprat *Spratelloides robustus* (Clupeidae: Dussumieriinae): A temperate clupeoid with a tropical life history strategy? Marine Biology **142**:809-824.

Rogers, P. J., P. Stephenson, L. J. McLeay, W. F. Dimmlich, and T. M. Ward. 2004. Sardine (*Sardinops sagax*). South Australian Research and Development Institute Aquatic Sciences.

Rogers, P. J., and T. M. Ward. 2007. Application of a 'case-building approach' to investigate the age distributions and growth dynamics of Australian sardine (*Sardinops sagax*) off South Australia. Marine and Freshwater Research **58**:461-474.

SAFS. 2023. Status of Australian fish stocks reports 2023, Fisheries Research and Development Corporation, Canberra.

Schwartzlose, R. A., J. Alheit, A. Bakun, T. R. Baumgartner, R. Cloete, R. J. M. Crawford, W. J. Fletcher, Y. Green-Ruiz, E. Hagen, T. Kawasaki, D. Lluch-Belda, S. E. Lluch-Cota, A. D. MacCall, Y. Matsuura, M. O. Nevárez-Martínez, R. H. Parrish, C. Roy, R. Serra, K. V. Shust, M. N. Ward, and J. Z. Zuzunaga. 1999. Worldwide large-scale fluctuations of sardine and anchovy populations. South African Journal of Marine Science **21**:289-347.

Sexton, S. C., T. M. Ward, and C. Huveneers. 2017. Characterising the spawning patterns of Jack Mackerel (*Trachurus declivis*) off eastern Australia to optimise future survey design. Fisheries Research **186**:223-236.

Sexton, S. C., T. M. Ward, J. Stewart, K. M. Swadling, and C. Huveneers. 2019. Spawning patterns provide further evidence for multiple stocks of sardine (Sardinops sagax) off eastern Australia. Fisheries Oceanography **28**:18-32.

Sippel, T., H. H. Lee, K. Piner, and S. L. H. Teo. 2017. Searching for M: Is there more information about natural mortality in stock assessments than we realize? Fisheries Research 192:135-140.

Smith, A. D. M., C. J. Brown, C. M. Bulman, E. A. Fulton, P. Johnson, I. C. Kaplan, H. Lozano-Montes, S. Mackinson, M. Marzloff, L. J. Shannon, Y.-J. Shin, and J. Tam. 2011. Impacts of fishing low–trophic level species on marine ecosystems. Science **333**:1147-1150.

Smith, A. D. M., T. M. Ward, F. Hurtado, N. Klaer, E. Fulton, and A. E. Punt. 2015. Review and update of harvest strategy settings for the Commonwealth Small Pelagic Fishery: Single species and ecosystem considerations. Final Report of FRDC Project No. 2013/028. CSIRO Oceans and Atmosphere Flagship, Hobart. 74 pp.

Smith, P. E., and S. L. Richardson. 1977. Standard techniques for pelagic fish egg and larva surveys. Food and Agriculture Organisation. Fisheries Technical Paper No. 175. 100 pp.

Somarakis, S., I. Palomera, A. Garcia, L. Quintanilla, C. Koutsikopoulos, A. Uriarte, and L. Motos. 2004. Daily Egg Production of anchovy in European waters. ICES Journal of Marine Science **61**:944-958.

Thomas, R. M. 1984. A method of age determination for the South West African pilchard *Sardinops ocellata*. South African Journal of Marine Science **2**:63-70.

Thorson, J. T., A. C. Hicks, and R. D. Methot. 2014. Random effect estimation of time-varying factors in Stock Synthesis. ICES Journal of Marine Science 72:178-185.

Thorson, J. T., J. N. Ianelli, S. B. Munch, K. Ono, and P. D. Spencer. 2015. Spatial delay-difference models for estimating spatiotemporal variation in juvenile production and population abundance. Canadian Journal of Fisheries and Aquatic Sciences 72:1897-1915.

Tourre, Y. M., S. E. Lluch-Cota, and W. B. White. 2007. Global multidecadal ocean climate and small-pelagic fish population. Environmental Research Letters, 2: 9pp.

Turner, R. 2023. deldir: Delaunay Triangulation and Dirichlet (Voronoi) Tessellation. R package version 0.1-9. https://cran.r-project.org/web/packages/deldir/index.html.

van der Lingen, C. D. 1994. Effect of Particle-Size and Concentration on the Feeding-Behavior of Adult Pilchard *Sardinops sagax*. Marine Ecology-Progress Series **109**:1-13.

Van Der Lingen, C. D. 2002. Diet of sardine *Sardinops sagax* in the southern Benguela upwelling ecosystem. South African Journal of Marine Science **24**:301-316.

Venables, W. N., and B. D. Ripley. 2002. Modern Applied Statistics with S. Fourth Edition. Springer, New York.

Véron, M., E. Duhamel, M. Bertignac, L. Pawlowski, M. Huret, and L. Baulier. 2020. Determinism of temporal variability in size at maturation of srdine *Sardina pilchardus* in the Bay of Biscay. Frontiers in Marine Science **7**.

Waldron, M. 1998. Annual ring validation of the South African sardine *Sardinops sagax* using daily growth increments. South African Journal of Marine Science **19**:425-430.

Ward, T. M., P. Burch, and A. R. Ivey. 2010. South Australian Sardine (*Sardinops sagax*) Fishery: Stock Assessment Report 2010: Report to PIRSA Fisheries. SARDI Aquatic Sciences (Adelaide).

Ward, T. M., P. Burch, and A. R. Ivey. 2012. South Australian Sardine (Sardinops sagax) Fishery: Stock Assessment Report 2012. South Australian Research and Development Institute (Aquatic Sciences), Adelaide.

Ward, T. M., P. Burch, L. J. McLeay, and A. R. Ivey. 2011. Use of the Daily Egg Production Method for stock assessment of sardine, *Sardinops sagax*; lessons learned over a decade of application off southern Australia Reviews in Fisheries Science **19**:1-20.

Ward, T. M., J. Carroll, G. L. Grammer, C. James, R. McGarvey, J. Smart, and A. R. Ivey. 2018. Improving the precision of estimates of egg production and spawning biomass obtained using the Daily Egg Production Method. South Australian Research and Development Institute (Aquatic Sciences), Adelaide. FRDC project No. 2014/026. 90 pp.

Ward, T. M., G. L. Grammer, A. R. Ivey, J. J. Smart, and R. McGarvey. 2021. Increasing the precision of the daily egg production method; 2020's remix of a 1980's classic. ICES Journal of Marine Science **78**:1177-1195.

Ward, T. M., F. Hoedt, L. McLeay, W. F. Dimmlich, G. Jackson, P. J. Rogers, and K. Jones. 2001a. Have recent mass mortalities of the sardine *Sardinops sagax* facilitated an expansion in the distribution and abundance of the anchovy *Engraulis australis* in South Australia? Marine Ecology-Progress Series **220**:241-251.

Ward, T. M., F. Hoedt, L. McLeay, W. F. Dimmlich, M. Kinloch, G. Jackson, R. McGarvey, P. J. Rogers, and K. Jones. 2001b. Effects of the 1995 and 1998 mass mortality events on the spawning biomass of *Sardinops sagax* in South Australian waters. ICES Journal of Marine Science **58**:830-841.

Ward, T. M., A. R. Ivey, and G. L. Grammer. 2020a. Spawning biomass of Sardine, *Sardinops sagax*, in waters off South Australia in 2020. Report to PIRSA Fisheries and Aquaculture., South Australian Research and Development Institute (Aquatic Sciences), Adelaide.

SARDI Publication No. F2007/000566-11. SARDI Research Report Series No.1074. 27pp.

Ward, T. M., M. Kinloch, J. G.K., and F. J. Neira. 1998. A Collaborative Investigation of the Usage and Stock Assessment of Baitfish in Southern and Eastern Australian Waters, with Special Reference to Pilchards (*Sardinops sagax*). South Australian Research and Development Institute (Aquatic Sciences). Final Report to Fisheries Research and Development Corporation.

Ward, T. M., and L. J. McLeay. 1998. Use of the Daily Egg Production Method to Estimate the Spawning Biomass of Pilchards (*Sardinops sagax*) in Shelf Waters of Central and Western South Australia in 1998. Report to the South Australian Sardine Working Group. South Australian Research and Development Institute Report.

Ward, T. M., and L. J. McLeay. 1999. Spawning biomass of Pilchards (*Sardinops sagax*) in shelf waters of central and western South Australia in 1999 Report to the South Australian Pilchard Working Group.

Ward, T. M., L. J. McLeay, W. F. Dimmlich, P. J. Rogers, S. McClatchie, R. Matthews, J. Kampf, and P. D. Van Ruth. 2006. Pelagic ecology of a northern boundary current system: effects of upwelling on the production and distribution of sardine (*Sardinops sagax*), anchovy (*Engraulis australis*) and southern bluefin tuna (*Thunnus maccoyii*) in the Great Australian Bight. Fisheries Oceanography **15**:191-207.

Ward, T. M., P. J. Rogers, P. Stephenson, D. K. Schmarr, N. Strong, and L. J. McLeay. 2005. Implementation of an Age Structured Stock Assessment Model for Sardine (*Sardinops sagax*) in South Australia. Final report to Fisheries Research and Development Corporation.

Ward, T. M., J. Smart, G. L. Grammer, A. Ivey, and R. McGarvey. 2020b. Stock assessment of Australian Sardine (*Sardinops sagax*) off South Australia 2019. Report to PIRSA Fisheries and Aquaculture. South Australian Research and Development Institute (Aquatic Sciences), Adelaide. SARDI Publication No. F2007/000765-7. SARDI Research Report Series No. 1048. 107 pp.

Ward, T. M., J. Smart, and A. Ivey. 2017. Stock assessment of Australian Sardine (*Sardinops sagax*) off South Australia 2017. Report to PIRSA Fisheries and Aquaculture. South Australian Research and Development Institute (Aquatic Sciences), Adelaide. SARDI Publication No. F2007/000765-6. SARDI Research Report Series No. 971.:107.

Ward, T. M., and J. Staunton-Smith. 2002. Comparison of the spawning patterns and fisheries biology of the sardine, *Sardinops sagax*, in temperate South Australia and sub-tropical southern Queensland. Fisheries Research **56**:37-49.

Ward, T. M., A. R. Whitten, and A. R. Ivey. 2015. South Australian Sardine (*Sardinops sagax*) Fishery: Stock Assessment Report 2015. Report to PIRSA Fisheries and Aquaculture. South Australian Research and Development Institute (Aquatic Sciences), Adelaide.

Ward, T. M., B. W. Wolfe, G. L. Grammer, A. R. Ivey, E. King, A. Schiller, K. S. McDonald, and J. M. Dambacher. 2023. Large sardine resource discovered off south-eastern Australia: Potential risks, challenges and benefits of establishing a new fishery. Marine Policy **155**:105739.

Watson, D. F. 1981. Computing the n-dimensional Delaunay tessellation with application to Voronoi polytopes. The Computer Journal. pp167-172.

White, K. V., and W. J. Fletcher. 1998. Identifying the developmental stages for eggs of the Australian pilchard, *Sardinops sagax*. Fisheries Western Australia. Fisheries Research Report No.103.

Whittington, I. D., M. Crockford, D. Jordan, and B. Jones. 2008. Herpesvirus that caused epizootic mortality in 1995 and 1998 in pilchard, *Sardinops sagax* (Steindachner), in Australia is now endemic. Journal of Fish Diseases **31**:97-105.

Wood, S. N. 2006. Generalized Additive Models An Introduction with R. Chapman and Hall/CRC.

APPENDIX A: ANNUAL ESTIMATES OF SELECTED BIOLOGIAL PARAMETERS

Table A1. Annual sex ratio of Sardine for commercial catch samples from all regions between 1995 and 2022. Data were unavailable for 2007 and limited for 2019. Sex ratio was calculated as number of females divided by total number of fish collected per sample.

Year	Females	Males	Sex Ratio
1995	1248	728	0.63
1996	1501	1049	0.59
1997	317	251	0.56
1998	1088	928	0.54
1999	1117	779	0.59
2000	358	398	0.47
2001	1461	929	0.61
2002	1662	1412	0.54
2003	2020	1715	0.54
2004	1827	1477	0.55
2005	1601	959	0.63
2006	608	585	0.51
2007	NA	NA	NA
2008	1168	797	0.59
2009	3088	2317	0.57
2010	4078	4152	0.50
2011	923	929	0.50
2012	1003	1063	0.49
2013	682	760	0.47
2014	828	843	0.50
2015	1445	1540	0.48
2016	1793	1515	0.54
2017	1751	1319	0.57
2018	1047	878	0.54
2019	59	53	0.53
2020	625	543	0.54
2021	898	923	0.49
2022	984	761	0.56

Table A2. Summary of otolith readability index scores for otoliths collected between 1995 and 2022 from commercial and fishery-independent samples.

	Readability					
Year	**1**	**2**	**3**	**4**	**5**	**Total**
1995	0	87	411	159	2	659
1996	1	145	366	109	10	632
1997	0	154	275	54	3	486
1998	18	200	800	262	11	1,291
1999	0	50	546	389	18	1,003
2000	2	82	490	65	2	641
2001	0	59	1,431	689	113	2,292
2002	0	53	1,527	895	133	2,608
2003	0	39	1,057	229	18	1,343
2004	10	121	690	465	265	1,551
2005	1	13	301	235	368	918
2006	0	9	180	135	469	793
2008	0	9	144	183	303	639
2009	0	27	314	370	784	1,495
2010	4	64	469	577	73	1,187
2011	1	7	111	138	91	348
2012	0	0	9	14	13	36
2013	0	15	222	146	143	526
2014	0	9	253	150	110	522
2015	0	6	297	184	310	797
2016	0	33	389	224	127	773
2017	0	0	0	0	0	0
2018	0	0	0	0	0	0
2019	0	2	20	22	10	54
2020	0	18	230	266	90	604
2021	0	11	220	270	120	621
2022	0	31	297	264	136	728
All Years	**37**	**1,244**	**11,049**	**6,494**	**3,722**	**22,546**

Table A3: Annual and all-years parameters used to calculate estimates of Spawning Biomass. Total A: total area sampled (km^2), A: spawning area (km^2); P_0: mean daily egg production (egg·m^{-2}·day^{-1}); S: spawning fraction; R: sex ratio; W: mean female weight (g); $\hat{F}$: batch fecundity (oocytes·batch^{-1}); F': Fecundity / Female Weight. Errors around the estimates are standard deviation (SD). N: number of samples; n: number of individuals. F' was calculated using the all-years $\hat{F}$ relationship with W from that year. Data sources for table: Ward et al. (2021), Grammer and Ivey (2023).

Time	Total A	A	P_0	P_0 SD	N.P_0	S	S SD	N.S	n.S	R	R SD	N.R	n.R	W	W SD	N.W	n.W	$\hat{F}$	$\hat{F}$ SD	N. $\hat{F}$	n. $\hat{F}$	F'	F' SD
All Years	-	-	84.1	4.3	6835	0.108	0.006	247	16334	0.55	0.01	210	27931	58.4	18.0	255	16995	17835	7166	255	16995	305.4	0.6
1998	48379	32980	99.0	30.8	164	0.139	0.015	12	530	-	-	-	-	46.5	11.2	12	554	14070	5295	12	554	302.3	3.8
1999	65956	15637	50.0	14.9	213	0.169	0.021	15	763	-	-	-	-	52.4	13.0	16	785	15743	5616	16	785	300.7	3.0
2000	102198	38658	52.9	12.7	290	0.158	0.012	15	1012	0.52	0.05	15	2179	49.2	12.2	16	1071	14543	5416	16	1071	295.9	2.5
2001	132382	39131	59.7	15.6	316	0.179	0.014	10	743	0.56	0.04	10	1397	50.7	9.1	11	1002	15614	5069	11	1002	307.7	2.7
2002	131574	37462	97.4	29.1	319	0.077	0.014	22	1631	0.60	0.04	22	2932	61.8	19.5	22	1841	19093	7664	22	1841	309.0	1.8
2003	133058	42905	113.5	27.4	320	0.103	0.008	7	435	0.48	0.03	7	986	52.4	8.5	7	435	16179	4720	7	435	308.9	3.9
2004	105621	40219	145.3	41.3	284	0.166	0.016	10	412	0.52	0.04	10	879	78.7	16.2	10	413	23995	7607	10	413	304.8	3.7
2005	122831	42142	59.5	14.3	334	0.100	0.019	32	2223	0.51	0.04	32	4827	73.9	16.0	33	2234	22426	7367	33	2234	303.5	1.6
2006	119038	50121	102.4	26.5	341	0.095	0.018	20	1332	0.59	0.05	20	2445	63.1	21.8	21	1337	19163	8194	21	1337	303.6	2.2
2007	119036	50972	104.9	27.1	341	0.130	0.019	20	1084	0.54	0.07	20	2244	71.1	16.8	21	1086	21723	7266	21	1086	305.7	2.3
2009	119031	55179	66.3	14.1	340	0.156	0.022	19	1537	0.36	0.04	9	2425	59.9	13.3	19	1537	17886	6183	19	1537	298.7	2.0
2011	119449	44245	51.5	15.4	340	0.044	0.006	14	1169	0.65	0.05	13	1798	46.8	12.3	15	1181	14640	5487	15	1181	312.9	2.5
2013	119297	37953	39.0	8.7	340	0.072	0.016	9	703	0.69	0.03	9	1089	51.3	12.3	9	723	15842	5761	9	723	309.1	3.2
2014	125249	73981	92.7	20.0	355	0.041	0.006	16	886	0.57	0.02	16	1574	47.9	13.9	16	886	14896	5983	16	886	311.1	3.0
2016	122598	50551	47.7	9.9	350	0.088	0.012	9	656	0.65	0.03	9	1088	49.7	17.3	9	681	15399	6774	9	681	309.6	3.3
2017	119661	66453	136.3	25.8	343	0.120	0.019	8	504	0.52	0.05	9	1042	59.6	12.3	9	511	18331	6250	9	511	307.8	3.7
2018	120043	63215	112.4	24.6	343	0.054	0.009	9	714	0.70	0.03	9	1026	46.5	7.2	9	718	14466	4430	9	718	311.0	3.0
2019	119369	53600	68.1	16.3	339	-	-	-	-	-	-	-	-	-	-	-	-	-	-	-	-	-	-
2020	129700	82627	94.0	18.4	379	-	-	-	-	-	-	-	-	-	-	-	-	-	-	-	-	-	-
2022	129982	76842	97.6	19.0	381																		
2023	136471	66248	93.8	26.1	403																		

APPENDIX B: MODEL SPECIFICATIONS

This section describes the components of the SardEst model fitted in TMB. The likelihood function includes three components: 1) Estimates of spawning biomass from DEPM surveys, 2) age-compositions, and 3) deviations around mean annual recruitment ($\bar{R}$).

The model is age-structured with recruitment occurring at age one. The age index (*a*) therefore extends from 1 to 8+ with the final age-class forming a plus group (a_{max}).

Biological Parameters

$$P_a = 1 * (1 + e^{-\log(19)*(a-a_{50})/(a_{95}-a_{50})})^{-1}$$

where P_a is the proportion mature at age *a*, a_{50} is the age where 50% of the population is mature and a_{95} is the age where 95% of the population is mature

$$W_a = A * (l_a)^B$$

where *A* and *B* are the scalar and power parameters of the length-weight relationship for both sexes, respectively.

Growth, as (caudal fork) length l_a versus age, was assumed to follow a von Bertalanffy curve calculated as:

$$l_a = l_\infty - (l_\infty - l_0) * e^{(-k*a)}$$

where l_∞ is the asymptotic length, l_0 is the length at age zero, and *k* is the growth coefficient.

Selectivity

The selectivity-at-age was determined as a double normal function, which describes dome-shaped selectivity and was originally fitted in Stock Synthesis (Ward et al. 2015, 2017, 2020b). There are three components to the function: an ascending limb, a descending limb and a plateau, which are connected by steep logistic joiners that provide differentiability.

Selectivity-at-age *a* is calculated as

$$S_a = asc_a \left(1 - j_{1,a}\right) + j_{1,a} \left(\left(1 - j_{2,a}\right) + j_{2,a} dsc_a\right)$$

where the joiner functions are:

$$j_{1,a} = 1 / \left(1 + e^{\left(-20 \frac{a - \beta_1}{1 + (a - \beta_1)} \right)} \right)$$

and

$$j_{2,a} = 1 / \left(1 + e^{\left(-20 \frac{a - peak_2}{1 + (a - peak_2)} \right)} \right)$$

and the ascending and descending limbs are:

$$asc_a = \left(1 + e^{-\beta_5} \right)^{-1} + \left(1 - \left(1 + e^{-\beta_5} \right)^{-1} \right) \frac{e^{\left(\frac{-(a - \beta_1)^2}{e^{\beta_3}} \right)^2} - t1_{\min}}{1 - t1_{\min}}$$

$$dsc_a = 1 + \left(\left(1 + e^{-\beta_6} \right)^{-1} - 1 \right) \frac{e^{\left(\frac{-(a - peak_2)^2}{e^{\beta_4}} \right)}}{t2_{\min} - 1}.$$

$ß_1$ is the age where selectivity = 1.0 begins, $ß_2$ is age where selectivity = 1.0 ends, $ß_3$ determines the slope of the ascending limb (this is the width of the top, *peak₂* is the endpoint), $ß_4$ determines the slope of the descending limb, $ß_5$ is the selectivity at age-at-recruitment and $ß_6$ is the selectivity at a_{max}. $t1_{min}$ and $t2_{min}$ are defined as:

$$t1_{\min} = e^{\left(\frac{-(a_{\min} - \beta_1)^2}{e^{\beta_3}} \right)}$$

$$t2_{\min} = e^{\left(\frac{-(a_{\max} - peak_2)^2}{e^{\beta_3}} \right)}.$$

peak₂ is the endpoint where selectivity = 1.0, while

$$peak_2 = \beta_1 + 1 + \left(\frac{0.99 a_{\max} - \beta_1 - 1}{1 + e^{-\beta_2}} \right).$$

Recruitment

Annual recruitment is fit using a lognormal distributed recruitment deviates around a mean number of recruits:

$$R_t = \bar{R} * \exp\left(\log(\tilde{R}_t)\right)$$

where $\tilde{R}_t$ are fitted as random effects with σ_R as the standard deviation among recruitment deviations.

$$\log(\tilde{R}_t) = N(0; \sigma_R^2)$$

Population dynamics

Starting numbers-at-age

Because exploitation was nearly zero prior to the first year of data, initial numbers-at-age are determined from the estimated recruitment at time zero (R_0) and the estimated rate of natural mortality (M):

$$N_{0,a} = \begin{cases} R_0 & \text{for } a = 1 \\ N_{0,a-1} * e^{-M} & \text{for } a > 1 \end{cases}.$$

Population with fishing mortality

Sardine population numbers $N_{t+1,a}$ at age a having recruited that year or undergone survival from start of year t to start of year $t+1$ are written

$$N_{t+1,a} = \begin{cases} R_{t+1} & \text{for } a = 1 \\ N_{t,a-1} * e^{-Z_{t,a-1}} & 2 \leq a \leq a_{max} - 1 \\ N_{t,a-1} * e^{-Z_{t,a-1}} + N_{t,a} * e^{-Z_{t,a}} & \text{for } a = a_{max} \end{cases}$$

where survival to the plus group occurs from both the plus group and the age below, and where $Z_{t,a}$ is the total instantaneous mortality rate at age a over year t,

$$Z_{t,a} = M + (F_t * S_a),$$

and where F_t is the fishing mortality rate over year t, determined using the hybrid fishing mortality method.

The hybrid fishing method allows the full F (F_t) to be tuning coefficients to match predicted catch ($\hat{C}_t$) to observed catch (C_t^{obs}), rather than full estimated parameters. Pope's approximation is used to determine the initial (first iteration) harvest rate, which is used as the initial Baranov continuous F. These values of F are then tuned over a series of iterations (approximately five) until the resulting predicted catch matches observed catch for each corresponding F:

$$temp_{1,t} = \frac{C_t^{obs}}{B_t + 0.1 C_t^{obs}}$$

$$j_{1,t} = \left(1 + e^{\left(30\left(temp_{1,t} - 0.95\right)\right)}\right)^{-1}$$

$$F_{1,t} = \frac{-\ln\left(1 - \left(j_{1,t} temp_{1,t} + 0.95\left(1 - j_{1,t}\right)\right)\right)}{\delta}$$

where $\delta = 1.0$ for the duration of the season, B_t is the estimated biomass in year t, and $j_{1,t}$ is a logistic joiner that prevents the initial values of F from exceeding 0.95yr^{-1}.

Catch in numbers for year t at age a is:

$$C_{t,a} = \frac{F_t}{Z'_{t,a}}\left(S_a N_{t,a}\right)\lambda_{t,a}$$

where $\lambda_{t,a}$ is survivorship in year t at age a:

$$\lambda_{t,a} = 1 - e^{\left(-\delta Z_{t,a}\right)} / Z_{t,a}.$$

Estimated catch in weight in year t is estimated as:

$$\hat{C}_t = \sum_a \frac{F_{1,t,}}{Z_{t,a}}\left(W_a N_{t,a} S_{,a}\right)\lambda_{t,a}.$$

An adjustment is made to yearly Z_t^{adj} in each iteration based on how closely predicted catch matches observed catch:

$$Z_t^{adj} = \frac{C_t^{obs}}{\hat{C}_t + 0.0001}$$

This adjustment is then applied to all *F*'s and $Z_{t,a}$ and $\lambda_{t,a}$ are tuned.

$$Z_{t,a} = M + Z_{t,a}^{adj}\left(Z_{t,a} - M\right)$$

$$\lambda_{t,a} = \left(1 - e^{\left(-\delta Z_{t,a}\right)}\right)/\left(Z_{t,a}\right).$$

This adjusted mortality rate is then used to calculate a new value for total catch and the new *F* estimate is the ratio of this value to observed catch:

$$temp_{2,t} = \sum_a \left(W_a N_{t,a} S_a\right)\lambda_{t,a}$$

$$F_{2,t} = \frac{C_t^{obs}}{temp_{2,t} + 0.0001}.$$

A second joining function prevents any *F* from exceeding a maximum value *Fmax*:

$$j_{2,t} = \left(1 + \exp^{30\left(F_{2,t} - 0.95 * F_{max}\right)}\right)^{-1}.$$

The final updated F_t are calculated as:

$$F_t = j_{2,t} F_{2,t} + \left(1 - j_{2,t}\right)F_{max}.$$

Spawning stock biomass was calculated as the proportion of the population that was mature:

$$\hat{G}_t = \sum_a W_a P_a N_{t,a}.$$

Total biomass was calculated as the total weight of the population:

$$B_t = \sum_a W_a N_{t,a}.$$

Proportional age-composition was calculated as:

$$\hat{p}_{t,a} = \hat{C}^{W}_{t,a} \sum_{a} \hat{C}^{W}_{t,a} \ .$$

Likelihoods

The probability of the recruitment deviates were estimated as lognormal random effects around mean recruitment ($\bar{R}$) as:

$$L_{\tilde{R}} = \sum_{t} \log(\sigma_{R}) + 0.5 * (\log(R_{t}) - \log(\bar{R}))^{2} / \sigma_{R}^{2} \ .$$

The proportional age-compositions were fit using a multinomial likelihood:

$$L_{p} = -\sum_{t,a} n_{t} p_{t,a} * \log(\hat{p}_{t,a})$$

where $p_{t,a}$ is the proportional age composition data in year *t* for age *a* and n_{t} was the sample size in year *t*.

Estimated spawning stock biomass was fit to the DEPM estimates as:

$$L_{I} = \sum_{t} 0.5 \cdot \log(\sigma_{t}^{2}) + \frac{\left[\log(I_{t}) - \left(\log(\hat{G}_{t}) - \sigma_{t}^{2}/2 \right) \right]^{2}}{2\sigma_{t}^{2}}$$

where I_{t} is the DEPM estimate of spawning stock biomass in year t, and where the lognormal likelihood σ_{t}^{2} parameter for each year can be written in terms of the coefficient of variation, Cv_{t}^{2}, obtained for each yearly spawning biomass estimate from the DEPM survey analysis as $\sigma_{t}^{2} = \log(Cv_{t}^{2} + 1)$.

The catch likelihood was estimated as:

$$L_{c} = \frac{1}{2\sigma_{C}^{2}} \sum_{y} \left(\log \hat{C}_{t} - \log C_{t}^{\text{obs}} \right)^{2}$$

where σ_c is the standard deviation of the logs of the catches in weight, assumed to be 0.05 so as penalise any substantial difference between $\hat{C}_t$ and C_t^{obs}.

The joint likelihood function was the sum of the four likelihood components with weightings of 1 (λ_I) and 0.2 (λ_p) applied to the DEPM and age-composition data, respectively:

$$L(\theta \mid D) = L_I * \lambda_I + L_p * \lambda_p + L_{\tilde{R}} + L_c.$$

APPENDIX C: CORRECTIONS TO 2021 SARDEST MODEL AND COMPARISON OF OUTPUTS

A coding error in the 2021 SardEst model (Grammer et al. 2021) was detected and corrected in SardEst for the current assessment. This error was not present in the 2019 SardEst model (Ward et al. 2020b). Following an external review of the 2019 SardEst model (Hillary 2020), a coding error was introduced in the 2021 SardEst model when recommendations from the review were being implemented. The consequences of the coding error are analysed and presented here.

What was the error and its potential implication on the outputs from the SardEst model?

SardEst is an age-structured model and age compositions from fishery data are fitted for every year. The coding error was introduced into the age-composition multinomial likelihood when sample size was being incorporated into the likelihood function as recommended in the review (Hillary 2020). It is important to note that the coding error was not a result of the review but occurred during the implementation of a recommendation. The likelihood was redefined as follow:

$$L_p = -\sum_{t,a} n_t p_{t,a} * \log(\hat{p}_{t,a})$$ Equation 1

where $p_{t,a}$ is the proportional age composition data in year *t* for age *a*, n_t was the sample size in year *t and* $\hat{p}_{t,a}$ was the proportion of predicted catch at age. Here, sample size is the total number of fish (n) rather than the total number of samples (N).

In the programming language (C++) used for SardEst, Equation 1 was coded in 2021 as follows:

LikeCAA = N_samples(Year)* PropN(Year,Age)*log(PropnPred(Year,Age))/-1

The C++ programming equates to the components of Equation 1 as below:

C++	Equation 1
LikeCAA	L_p
N_samples(Year)	n_t
PropN(Year,Age)	$p_{t,a}$
PropnPred(Year,Age)	$\hat{p}_{t,a}$
-1	Negative sign

The error was found as the symbol ∑ from the Equation 1 (meaning sum of the following components) was absent from the code. Consequently, when the likelihood values were supposed to be calculated for each age class for each year and then summed to have one final likelihood value, only one likelihood value for the last age class of the last year of the dataset (2020) was calculated and one sample size incorporated. This caused the model to incorrectly fit age-composition data and to misrepresent the number of samples integrated into the total likelihood. Consequently, the data weightings applied to age-composition and DEPM biomass likelihoods were also incorrect.

In the present stock assessment, the code has been corrected as follows (addition of **+**) to translate ∑ from the equation into the code:

        LikeCAA **+**= N_samples(Year)* PropN(Year,Age)*log(PropnPred(Year,Age))/-1

How did the error impact the outputs of SardEst in the 2021 stock assessment?

Comparisons between the outputs of SardEst in the 2021 stock assessment and the same outputs after the coding error was corrected are presented in Table C1 and Figure C1. Correction of the coding error allowed the model to calculate the total likelihood for all age-compositions data for all of the years, and the correct total number of samples to be incorporated.

The original data weightings were applied to the likelihoods for the DEPM biomass and age-compositions and were kept at 0.5 and 1, respectively. As expected, the integration of the entire dataset for age-composition (i.e. correct age distribution and sample sizes (n) for every year), after correction of the error, significantly affected the parameter estimates from the model. The model did not fit the DEPM biomass, which affected the calculation of spawning biomass, total biomass and recruitment. The variance around the estimates was also significantly reduced (green curves in Figure C1).

To obtain valid outputs from the corrected model, a readjustment of the data weighting was required. Because the quality of the DEPM biomass was better and the weight of age composition data highly increased, the data weighting for age compositions data was down-weighted to 0.01 relative to the DEPM biomass, for which the weighting was fixed to 1. Outputs are presented in Figure C1 (blue curves). Values of estimates from the model with the coding error, after correction of the error, and adjustment of the data weightings are detailed in Table C1. Note that the effective

sample size used in 2021 in the age composition likelihood calculation was the total number of fish per catch sample per year (n) (see *Chapter 5: Model parameters and likelihood weighting* above). This (very high number of fish) explains why the weight for age composition data was downscaled substantially compared to the DEPM biomass. For SardEst in the current stock assessment, we used the total number of catch samples per year (N) as the effective sample size and readjusted the data weighting for age-compositions accordingly (from 0.01 to 0.2).

We observe that although the estimates from the model with the coding error are slightly different from the estimates from the correct model (Table C1), the trends of the different curves are very similar, and the estimated values are still within the margin of error of the two versions of the model (Figure C1). This implies that the consequences of the coding error on the previous stock assessment in 2021 are minimal, and the conclusions presented would have remained the same when using the corrected model, i.e. the unfished, total and spawning biomasses are at high levels, and the stock is sustainable.

Table C1: Comparison between the estimates from the model with coding error and the model after the error has been corrected and the data weightings adjusted.

Parameter	2021 with error		2021 corrected & weights adjusted	
	Estimate	Standard Error	Estimate	Standard Error
Unfished equilibrium recruitment (R0)	21,119,220	17,230,695	14,515,524	3,966,944
Mean recruitment $(\log(\bar{R}))$	16.70	0.75	16.24	0.19
$\text{Log}(\sigma_R)$	-1.07	0.27	-1.08	0.20
M^{max}_{1995}	3.84	2.05	2.33	0.42
M^{max}_{1998}	4.71	3.21	2.69	0.65
M	0.83	0.30	0.66	0.07
Unfished total biomass_B0 (t)	679,000	257,000	639,000	113,000
Total biomass 2020 (t)	693,000	232,000	640,000	81,000
Spawning biomass 2020 (t)	310,000	32,000	332,000	25,000

Figure C1: Comparison between outputs from the model with coding error (red), the model corrected with data weightings unchanged (green), and model corrected with data weightings adjusted (blue).